Lecture notes for the Condensed Matter Physics course 2021/22

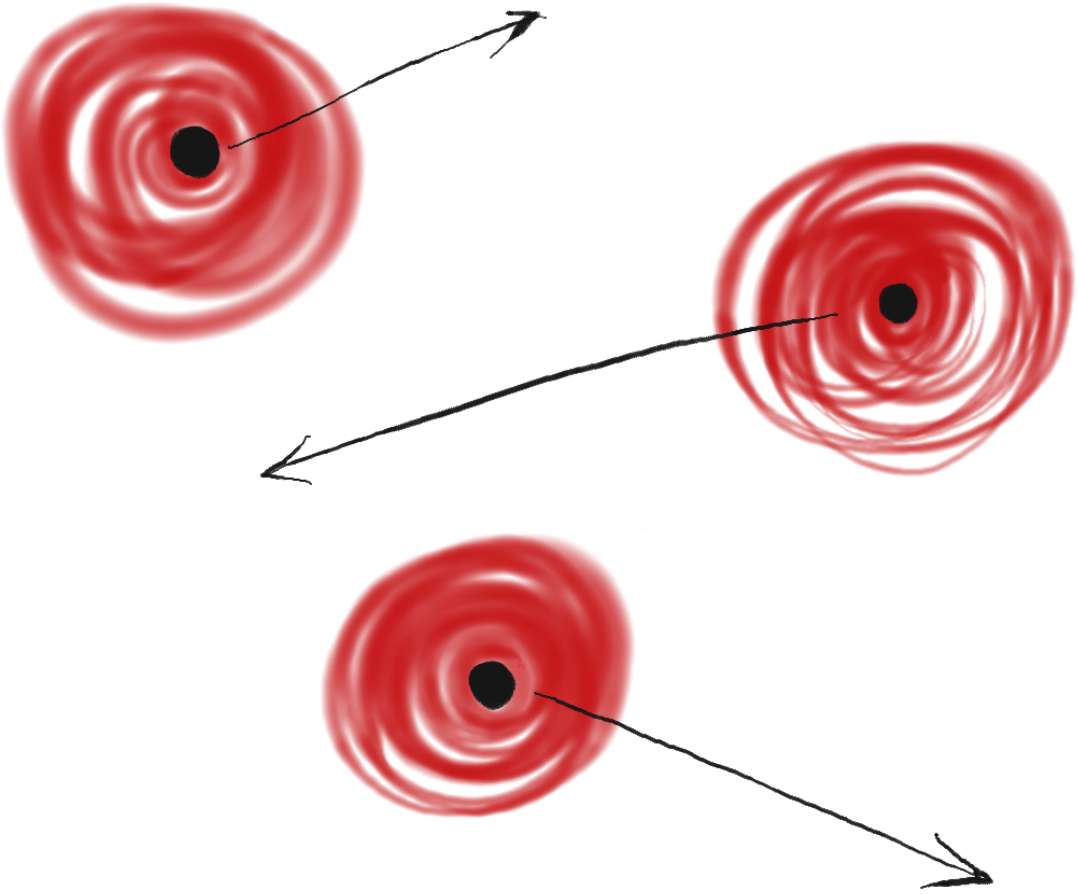

Rafael Sánchez Rodrigo

Departamento de Física Teórica de la Materia Condensada
Facultad de Ciencias. Universidad Autónoma de Madrid

Contents

Part I.

Many electron systems

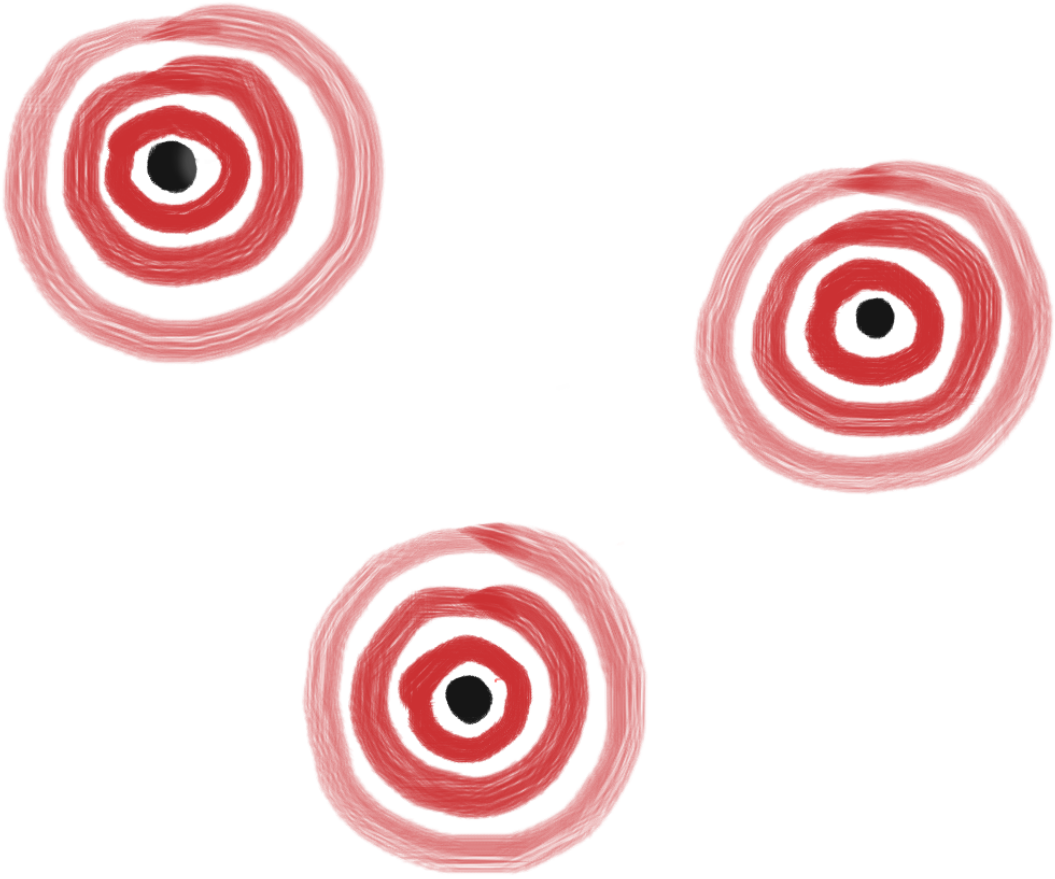

1. Second quantization

Let us start with an obvious statement. Condensed matter is composed of many particles. Indeed, the relevance of the field was argued by Anderson using his famous statement *more is different* [1.1] and the concept of *emergence* of new properties upon quantitative changes.[1] From the technical point of view, one soon encounters difficulties when trying to write the state of a system with many particles from the individual wavefunctions. To do this required a conceptual jump whose importance is emphasized by the name of *second quantization*. Historically, it was introduced by Dirac for bosons [1.2] (see also Ref. [1.3]) and one year later by Jordan and Wigner for fermions [1.4] by writing operators in terms of creation and anihilation of particles.

Detailed chapters on second quantization can be found almost every book on many particle physics or on relativistic quantum theory (it is an essential ingredient in that case, as particles are not conserved), also in some quantum mechanics or quantum optics ones. In this chapter we introduce this approach with a focus on its practical uses.

1.1. Many particle states

When we talk about many particle physics, we may mean that we want to describe systems with really a lot of particles[2]. In principle, the state of such a system with say N indistinguishable particles can be described once the state of each particle. Let us assume we have this information: each particle $i = 1, \ldots, N$ occupies a given state $|\phi_j\rangle_i$, where ϕ_j labels a set of quantum numbers characteristic of our system (e.g., momentum, spin....). The state of the system will be given by linear combinations of products of the single particle states of the form:

$$|p_1\rangle = |\phi_1\rangle_1 |\phi_2\rangle_2 \ldots |\phi_N\rangle_N \tag{1.1}$$

and all the possible permutations, e.g. $|p_2\rangle = |\phi_2\rangle_1 |\phi_1\rangle_2 \ldots |\phi_N\rangle_N$. It is important to fix a convention in the order of the states, so $\phi_1 < \phi_2 < \cdots < \phi_N$, especially when it comes to fermions[3]. If the distribution of particles is such that we have N_j particles in state $|\phi_j\rangle$, we will have

$$\mathcal{N} = \frac{N!}{\prod_j N_j!} \tag{1.2}$$

different terms, as illustrated in Fig. 1.1. You can readily see in Fig. 1.2 that things are worse when dealing with fermions, as two fermions cannot occupy the same state[4]. Then, one *only* has to be careful with the proper symmetrization of the wave function of the total state: the combination must be symmetric or antisymmetric under the exchange of two particles, if they are bosons or fermions, respectively[5]. You need to be patient if N is large!

[1] The motivation was to fight the reductionist strategy to understand the properties of a system by looking at the behaviour of its constituents.

[2] Think on the number of atoms in any piece of material.

[3] For bosons, it does not really matter, though it is always better to keep things in proper order.

[4] What is the number of possible combinations in that case?

[5] Remember your favourite book on quantum mechanics.

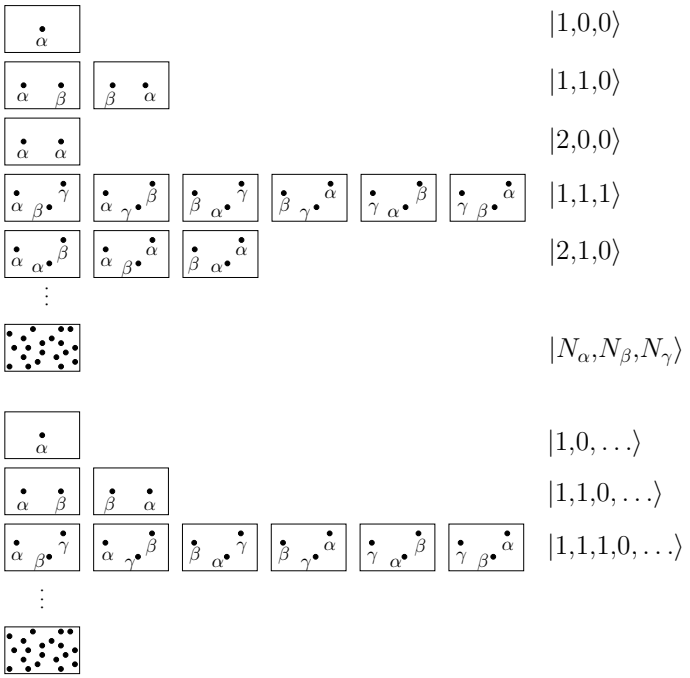

Figure 1.1.:
Fock states for systems of different number of particles (bosons) in a three-state system. States are labelled as $|\alpha\rangle$, $|\beta\rangle$ and $|\gamma\rangle$. Diagrams show all possible combinations for each particle distribution. Extending to an infinite-dimension Hilbert space is straightforward.

Figure 1.2.:
Fock states for fermions. A large number of particles require a large number of states to be allocated.

The fact that the particles are indistinguishable helps us, because we do not care about which but rather how many particles occupy each state. With that, we can construct the state of the system

$$|\vec{N}\rangle = |N_1, N_2, N_3, \dots\rangle. \tag{1.3}$$

These are known as Fock states [1.5]. Putting all together, we get:

$$|\vec{N}\rangle = \frac{1}{\sqrt{N}} \sum_{i=1}^{N} \pm^{\zeta_i} |p_i\rangle, \tag{1.4}$$

where the sum runs over all possible permutations and the sign ± accounts for bosons and fermions. Remember that the fermionic statistics imposes that $|\vec{N}\rangle$ is antisymmetric under the exchange of two particles The signature ζ_i is the minimal number of permutations that we need to do on $|p_i\rangle$ to recover $|p_1\rangle$.

1.1.1. Operators

In the paragraphs above, we learned how to write the wavefunction of particular realizations of a system with a fixed number of particles, N. We now need to know how these states are modified when an operator acts on them. Also, in some cases, the number of particles is not fixed: think for example on a system that emits particles, or the question of the energy cost to add an electron to a system. We will hence consider three types of operators: (i) single particle operators, that act on a single particle[6], (ii) two particle operators, that describe interactions between two particles, and (iii) particle creation and annihilation operators, you can imagine what they do.

Consider first a single particle operator, $\hat{o}_i$, that acts on particle i in the form

$$\hat{o}^{(i)}|\phi_j\rangle_i = \sum_k o_{kj}|\phi_k\rangle_i, \quad \text{with} \quad o_{kj} = {}_i\langle\phi_k|\hat{o}_i|\phi_j\rangle_i = \int d^3\mathbf{r}_i \phi_k^*(\mathbf{r}_i)\hat{o}^{(i)}\phi_j(\mathbf{r}_i). \tag{1.5}$$

[6] surprise!

It changes the state of particle i into a superposition of other states. On the many particle state, this means that the operator $\hat{O} = \sum_i \hat{o}_i$ (acting on all particles in the system) acts on the Fock states as:

$$|N_1, \ldots, N_j, \ldots, N_k, \ldots\rangle \longrightarrow |N_1, \ldots, N_j{-}1, \ldots, N_k{+}1, \ldots\rangle, \tag{1.6}$$

i.e., it *annihilates* particles in state $|\phi_j\rangle$ and *creates* them in other states $|\phi_k\rangle$. Let us see in detail the matrix elements of $\langle\vec{N}_\mathrm{f}|\hat{O}|\vec{N}_\mathrm{i}\rangle$. In *first quantization*, the initial and final states are written as

$$|\vec{N}_\mathrm{i}\rangle = |N_1, \ldots, N_j, \ldots, N_k, \ldots\rangle = \frac{1}{\sqrt{\mathcal{N}_\mathrm{i}}} \sum_{i=1}^{\mathcal{N}_\mathrm{i}} \pm^{\zeta_i} |p_i\rangle \tag{1.7}$$

$$|\vec{N}_\mathrm{f}\rangle = |N_1, \ldots, N_j{-}1, \ldots, N_k{+}1, \ldots\rangle = \frac{1}{\sqrt{\mathcal{N}_\mathrm{f}}} \sum_{i=1}^{\mathcal{N}_\mathrm{f}} \pm^{\zeta_i} |p'_i\rangle, \tag{1.8}$$

where

$$\mathcal{N}_\mathrm{i} = \frac{N!}{N_1! \ldots N_j! \ldots N_k! \ldots} \qquad \text{and} \qquad \mathcal{N}_\mathrm{i} = \frac{N!}{N_1! \ldots (N_j{-}1)! \ldots (N_k{+}1)! \ldots}. \tag{1.9}$$

All the $\mathcal{N}_\mathrm{i}$ permutations in $|\vec{N}_\mathrm{i}\rangle$ contain N_j particles in state $|\phi_j\rangle$. The operator acts on each of them separately, hence generating a combination of $N_j\mathcal{N}_\mathrm{i}$ states of the form $|p'_i\rangle$,[7] repeating the sum in Eq. (1.8) $\mathcal{N}_\mathrm{f}$ times, so we write it as $\mathcal{N}_\mathrm{f}^{-1/2}|\vec{N}_\mathrm{f}\rangle$ once we multiply by the normalization factor $\sqrt{\mathcal{N}_\mathrm{f}}$. We also need to make the necessary permutations f_{jk} to recover the form of $|\vec{N}_\mathrm{f}\rangle$, which will result in a sign $\pm^{f_{jk}}$. In the case $j < k$, this is $f_{jk} = \sum_{n=j+1}^{k} N_n$.[8] In other words:

$$\begin{aligned}\langle\vec{N}_\mathrm{f}|\hat{O}|\vec{N}_\mathrm{i}\rangle &= \langle\vec{N}_\mathrm{f}|\hat{O}\frac{1}{\sqrt{\mathcal{N}_\mathrm{i}}}\sum_{i=1}^{\mathcal{N}_\mathrm{i}}\pm^{\zeta_i}|p_i\rangle = \langle\vec{N}_\mathrm{f}|\frac{1}{\sqrt{\mathcal{N}_\mathrm{i}}}\mathcal{N}_\mathrm{i}N_j o_{kj}\frac{1}{\mathcal{N}_\mathrm{f}}\sum_{i=1}^{\mathcal{N}_\mathrm{f}}\pm^{\zeta_i}|p'_i\rangle \\ &= \langle\vec{N}_\mathrm{f}|\frac{1}{\sqrt{\mathcal{N}_\mathrm{i}}}\mathcal{N}_\mathrm{i}N_j o_{kj}\frac{\pm^{f_{jk}}}{\mathcal{N}_\mathrm{f}}\sqrt{\mathcal{N}_\mathrm{f}}|\vec{N}_\mathrm{f}\rangle = \pm^{f_{jk}}\sqrt{(N_k{+}1)N_j}\,o_{kj}.\end{aligned} \tag{1.10}$$

The diagonal elements:

$$\langle\vec{N}_\mathrm{i}|\hat{O}|\vec{N}_\mathrm{i}\rangle = \sum_j N_j o_{jj} = \left\langle\hat{O}\right\rangle, \tag{1.11}$$

give the expected value of the operator.[9]

☞ The action of an operator on a many particle states depends on how many particles occupy the different states, and can be interpreted as particles changing their state.

It is hence essential to introduce number operators that count the particles in each state, as well as operators that create and annihilate particles in the different states.

[7] ...and others that will be cancelled out when projecting on $\langle\vec{N}_\mathrm{f}|$.

[8] For bosons, this is obviously not a problem. For fermions, it may help to think on the many-fermion states as Slater determinants: the operator $\hat{O}$ replaces the $|\phi_j\rangle$ elements on row j of $|\vec{N}_\mathrm{i}\rangle$ by $|\phi_k\rangle$. This row needs now to be taken to its proper position k of the determinant giving $|\vec{N}_\mathrm{f}\rangle$. Unoccupied states (with $N_n = 0$) do not enter the determinant, so they are not counted.

[9] You can convince yourself of all this more easily by considering simple cases with two or three particles occupying two orbitals (left as exercises)

1.2. Creation and annihilation operators

We have seen in the previous section that the matrix elements of an operator in a many-body Fock space depend on the number of particles occupying the different microscopic states. The change of a system between two Fock states can hence be described in terms of operators that create or annihilate particles in the different states.

A way to obtain a many-particle Fock state $|N_1,\dots,N_k,\dots,N_j,\dots\rangle$ is to take an empty state with no particles:

$$|0\rangle \equiv |0,0,\dots,0,\dots\rangle \tag{1.12}$$

and add particles to it. This is done by introducing operators $\hat{a}_j^\dagger$ that create particles in a given state $|\phi_j\rangle$:[10]

$$|N_1,\dots,N_j,\dots,N_k,\dots\rangle \sim \underbrace{\hat{a}_1^\dagger\dots\hat{a}_1^\dagger}_{N_1\text{ times}}\dots\underbrace{\hat{a}_j^\dagger\dots\hat{a}_j^\dagger}_{N_j\text{ times}}\dots\underbrace{\hat{a}_k^\dagger\dots\hat{a}_k^\dagger}_{N_k\text{ times}}\dots|0\rangle. \tag{1.13}$$

Similarly to the previous section, the ordering of the states is important. Note that exchanging the position of two operators $\hat{a}_j^\dagger$ and $\hat{a}_k^\dagger$ is equivalent to exchanging two particles. Hence, such operation needs to respect the symmetry of the wavefunction. In other words:

☞ The bosonic/fermionic statistics of the many particle state will be enclosed in the properties of the creation operators.

Let us see how the creation operator it acts on the many-particle state. For this, we need to relate two Fock states which differ on one particle in a given state $|\phi_k\rangle$. Take the state with one particle more:

$$|N_1,\dots,N_j,\dots,N_k{+}1,\dots\rangle \sim \underbrace{\hat{a}_1^\dagger\dots\hat{a}_1^\dagger}_{N_1\text{ times}}\dots\underbrace{\hat{a}_j^\dagger\dots\hat{a}_j^\dagger}_{N_j\text{ times}}\dots\underbrace{\hat{a}_k^\dagger\dots\hat{a}_k^\dagger}_{N_k+1\text{ times}}\dots|0\rangle. \tag{1.14}$$

By exchanging the leftmost $\hat{a}_k^\dagger$ with all the operators with small index $j<k$, we recover something of the form $\hat{a}_k|N_1,\dots,N_j,\dots,N_k,\dots\rangle$. We only need to be careful once more with the sign acquired in a total of $s_k=\sum_{n=1}^{j-1}N_n$ particle-exchange operations.

Knowing this, we are ready to define the creation operator as:

$$\hat{a}_j^\dagger|\dots,N_j,\dots\rangle = \pm^{s_j}\alpha_{N_j}\sqrt{N_j{+}1}|\dots,N_j{+}1,\dots\rangle, \tag{1.15}$$

where $\alpha_N=1$ for bosons, and $\alpha_N=\delta_{N0}$, for fermions[11]. The chose of the squared-rooted prefactor is not arbitrary, as will be clear in a few lines. The sign again accounts for bosons (+) and fermions (−). Projecting on the state in the right hand side of Eq. (1.17) and conjugating:

$$\left(\langle\dots,N_j{+}1,\dots|\hat{a}_j^\dagger|\dots,N_j,\dots\rangle\right)^* = \langle\dots,N_j,\dots|\hat{a}_j|\dots,N_j{+}1,\dots\rangle = \pm^{s_j}\alpha_{N_j}\sqrt{N_j{+}1}, \tag{1.16}$$

we get the definition of the annihilation operator:

$$\hat{a}_j|\dots,N_j,\dots\rangle = \pm^{s_j}\alpha_{N_j-1}\sqrt{N_j}|\dots,N_j{-}1,\dots\rangle, \tag{1.17}$$

[10] The reason of having a dagger in the definition will be obvious soon.
[11] The Kronecker delta takes care of the Pauli exclusion principle.

The prefactor ensures that one can not annihilate particles in an empty state, neither for bosons nor for fermions[12]. The product of the two operators leaves the Fock state unchanged:

$$\hat{a}_j^\dagger \hat{a}_j |\dots, N_j, \dots\rangle = N_j |\dots, N_j, \dots\rangle \tag{1.18}$$

and counts how many particles are there in $|\phi_j\rangle$. This way, we can define the number operator as:

$$\hat{n}_j = \hat{a}_j^\dagger \hat{a}_j. \tag{1.19}$$

The final goal is to be able to write any kind of operator in terms of products of the form $\hat{a}_k^\dagger \hat{a}_j$. Comparing Eqs. (1.5), (1.10), (1.17) and (1.15), we see we are not far from there. For instance, the number operator could clearly be introduced in the diagonal elements in Eq. (1.11) with no harm. However, one needs to be careful with the signs when creating and annihilating particles in different states. It becomes clearer if we consider bosons and fermions separately.

1.2.1. Bosons

With bosons, we do not need to take care of signs. This way, it is straightforward to find:

$$|N_1, \dots, N_j, \dots, N_k, \dots\rangle = \frac{1}{\sqrt{N_1! \dots N_j! \dots N_k! \dots}} \left(\hat{a}_1^\dagger\right)^{N_1} \dots \left(\hat{a}_j^\dagger\right)^{N_j} \dots \left(\hat{a}_k^\dagger\right)^{N_k} \dots |0\rangle. \tag{1.20}$$

This shows the advantage of second quantization: there is no need to do any permutation to construct the many-particle wavefunction!

Symmetry introduces no restriction to the number of particles that can occupy each state. Hence, similarly to how we obtained Eq. (1.18), we get:

$$\hat{a}_j \hat{a}_j^\dagger |\dots, N_j, \dots\rangle = (N_j + 1) |\dots, N_j, \dots\rangle, \tag{1.21}$$

rendering the commutation relation

$$[\hat{a}_j, \hat{a}_j^\dagger] = 1. \tag{1.22}$$

For particles in different states, $j \neq k$, the order in which two creation/annihilation operators act on the state does not change the result:

$$\begin{aligned} \hat{a}_j \hat{a}_k |\dots, N_j, \dots, N_k, \dots\rangle &= \hat{a}_j \hat{a}_k |\dots, N_j, \dots, N_k, \dots\rangle \\ &= \sqrt{N_j N_k}\, \hat{a}_j \hat{a}_k |\dots, N_j{-}1, \dots, N_k{-}1, \dots\rangle \end{aligned} \tag{1.23}$$

$$\begin{aligned} \hat{a}_j^\dagger \hat{a}_k |\dots, N_j, \dots, N_k, \dots\rangle &= \hat{a}_k \hat{a}_j^\dagger |\dots, N_j, \dots, N_k, \dots\rangle \\ &= \sqrt{(N_j{+}1) N_k}\, \hat{a}_j \hat{a}_k |\dots, N_j{+}1, \dots, N_k{-}1, \dots\rangle. \end{aligned} \tag{1.24}$$

These relations can be expressed in a more general way as the commutation relations:

$$\begin{aligned} [\hat{a}_j, \hat{a}_k^\dagger] &= \delta_{jk} \\ [\hat{a}_j, \hat{a}_k] &= [\hat{a}_j^\dagger, \hat{a}_k^\dagger] = 0. \end{aligned} \tag{1.25}$$

You must have seen these before (remember the excitations of the harmonic oscillator [1.6]). However, they apply to any kind of bosonic particles: photons, phonons, magnons, Higgs...

[12] Nothing to do with the Pauli exclusion principle, this time!

1.2.2. Fermions

We know that two fermions cannot be in the same state. This is a consequence of the antisymmetry of the wavefunction under the exchange of two particles. Consider for simplicity a system with only two particles. If they were to be in the same state, the wavefunction would fulfil

$$\hat{a}_j^\dagger \hat{a}_j^\dagger |0\rangle = -\hat{a}_j^\dagger \hat{a}_j^\dagger |0\rangle. \tag{1.26}$$

The only way is:

$$\hat{a}_j^\dagger \hat{a}_j^\dagger = 0, \tag{1.27}$$

which expresses the Pauli exclusion principle. Hence, the wavefunction in Eq. (1.13) cannot contain one creation operator repeated, reading:

$$|\dots,1_j,\dots,1_k,\dots\rangle = \dots \hat{a}_j^\dagger \dots \hat{a}_k^\dagger \dots |0\rangle, \tag{1.28}$$

where he have made explicit that for every state, $N_j = 0, 1$.[13] Then, it is obvious that we cannot annihilate two particles from the same state, so

$$\hat{a}_j \hat{a}_j = 0. \tag{1.29}$$

This way, the definitions of the creation and annihilation operators in Eqs. (1.15) and (1.17) are restricted to the cases:

$$\hat{a}_j^\dagger |\dots,0_j,\dots\rangle = \pm^{s_j} |\dots,1_j,\dots\rangle \tag{1.30}$$

$$\hat{a}_j |\dots,1_j,\dots\rangle = \pm^{s_j} |\dots,0_j,\dots\rangle. \tag{1.31}$$

Otherwise, they are zero.

Changing the order on which the creation operators act on any many particle state is also important, as it affects the sign of the resulting operation. Consider the creation of two particles, $\hat{a}_j^\dagger$ and $\hat{a}_k^\dagger$, with $j < k$. Then:

$$\hat{a}_j^\dagger \hat{a}_k^\dagger |\dots,0_j,\dots,0_k,\dots\rangle = (-1)^{s_j^0} (-1)^{s_k^0} |\dots,1_j,\dots,1_k,\dots\rangle \tag{1.32}$$

$$\hat{a}_k^\dagger \hat{a}_j^\dagger |\dots,0_j,\dots,0_k,\dots\rangle = (-1)^{s_k^0+1} (-1)^{s_j^0} |\dots,1_j,\dots,1_k,\dots\rangle, \tag{1.33}$$

where $s_j^0 = \sum_{n=1}^{j-1} \langle \dots,0_j,\dots,0_k,\dots | \hat{n}_n | \dots,0_j,\dots,0_k,\dots \rangle$ counts the particles in the original state. Therefore:

$$\hat{a}_j^\dagger \hat{a}_k^\dagger = -\hat{a}_k^\dagger \hat{a}_j^\dagger. \tag{1.34}$$

Using a similar argument with $\hat{a}_j \hat{a}_k$, and taking into account Eqs. (1.27) and (1.29), we arrive to the *anticommutation* relations:

$$\{\hat{a}_j, \hat{a}_k\} = \{\hat{a}_j^\dagger, \hat{a}_k^\dagger\} = 0. \tag{1.35}$$

For creation and annihilation operators, we follow a similar procedure:

$$\hat{a}_j^\dagger \hat{a}_k |\dots,0_j,\dots,1_k,\dots\rangle = (-1)^{s_j^1} (-1)^{s_k^1} |\dots,1_j,\dots,0_k,\dots\rangle = (-1)^{f_{jk}} |\dots,1_j,\dots,0_k,\dots\rangle \tag{1.36}$$

$$\hat{a}_k \hat{a}_j^\dagger |\dots,0_j,\dots,1_k,\dots\rangle = (-1)^{s_k^1+1} (-1)^{s_j^1} |\dots,1_j,\dots,0_k,\dots\rangle, \tag{1.37}$$

[13] Note that, respecting the order in the successive creation of particles onto the vacuum state (those with the highest index first), we do not need to worry about sign.

where in this case $s_j^1 = \sum_{n=1}^{j-1}\langle \dots,0_j,\dots,1_k,\dots|\hat{n}_n|\dots,0_j,\dots,1_k,\dots\rangle$. We then have, for $j \neq k$:

$$\hat{a}_j^\dagger \hat{a}_k = -\hat{a}_k \hat{a}_j^\dagger. \tag{1.38}$$

In the case $j = k$:

$$\begin{aligned} \hat{a}_j^\dagger \hat{a}_j|\dots,0_j,\dots\rangle &= 0, & \hat{a}_j^\dagger \hat{a}_j|\dots,1_j,\dots\rangle &= 1, \\ \hat{a}_j \hat{a}_j^\dagger|\dots,0_j,\dots\rangle &= 1, & \hat{a}_j \hat{a}_j^\dagger|\dots,1_j,\dots\rangle &= 0. \end{aligned} \tag{1.39}$$

Joining Eqs. (1.38) and (1.39), we get:

$$\{\hat{a}_j^\dagger, \hat{a}_k\} = \delta_{jk}. \tag{1.40}$$

- ☞ In second quantization, we do not need to care about doing huge numbers of permutations in order to write the many particle wavefunctions.
- ☞ The definition of the vacuum state, $|0\rangle$, together with the (anti)commutation relations —Eq. (1.25), for bosons, and Eqs. (1.35) and (1.40), for fermions— contain all the statistical properties.

1.2.3. Change of basis

From the beginning of the chapter, we assumed a description of the many particle state in terms of the different particles occupying states $|\phi_j\rangle$ being elements of a particular basis. Of course, this description is not unique, and different basis may be most convenient for different configurations. As any operator, the creation and annihilation operators will then also be different,

Consider two complete and ordered basis, $\{|\xi\rangle\}$ and $\{|\zeta\rangle\}$, of the single-particle states. We want to find the operators $\hat{a}_\mu^\dagger$ out of the $\hat{a}_\nu^\dagger$. In both cases, the states are defined from the vacuum: $|\zeta\rangle = \hat{a}_\zeta^\dagger|0\rangle$ and $|\xi\rangle = \hat{a}_\xi^\dagger|0\rangle$. Then, by simply projecting:

$$|\zeta\rangle = \sum_\xi |\xi\rangle\langle\xi|\zeta\rangle \tag{1.41}$$

we get

$$\hat{a}_\zeta^\dagger = \sum_\xi \langle\zeta|\xi\rangle^* \, \hat{a}_\xi^\dagger \quad \text{and} \quad \hat{a}_\zeta = \sum_\xi \langle\zeta|\xi\rangle \, \hat{a}_\xi. \tag{1.42}$$

Quantum field operators

A particular case of the above is when we change to the position basis, $\{|\mathbf{r}\rangle\}$. The coefficients are then the single-particle wavefunctions in position space, $\langle\mathbf{r}|\xi\rangle = \psi_\xi(\mathbf{r})$, hence:

$$\hat{\Psi}^\dagger(\mathbf{r}) = \sum_\xi \psi_\xi^*(\mathbf{r}) \, \hat{a}_\xi^\dagger \tag{1.43}$$

is a field operator that describes the creation of a particle, not in a particular state $|\xi\rangle$ but in a given position, $\mathbf{r}$. We can also annihilate it:

$$\hat{\Psi}(\mathbf{r}) = \sum_\xi \psi_\xi(\mathbf{r}) \, \hat{a}_\xi. \tag{1.44}$$

1.3. Single and two particle operators

We need now to see how to operators are written in terms of creation and annihilation operators. In Sec. 1.1.1, we found how a single particle operator, $\hat{O} = \sum_i \hat{o}^{(i)}$, acts on a many particle state, cf. Eq. (1.10)

$$\langle \dots, N_j - 1, \dots, N_k + 1, \dots | \hat{O} | \dots, N_j, \dots, N_k, \dots \rangle = \pm^{f_{jk}} \sqrt{(N_k+1)N_j} o_{kj}. \tag{1.45}$$

It is straightforward now to check that

$$\hat{O} = \sum_{jk} o_{jk} \hat{a}_j^\dagger \hat{a}_k \tag{1.46}$$

has the same matrix elements[14].

One also finds frequently operators that act on two particles,

$$\hat{O}^{(2)} = \frac{1}{2} \sum_{i \neq i'} \hat{o}^{(ii')} \tag{1.47}$$

Think on any type of particle interactions, e.g. the Coulomb interaction, spin exchange... These are written as

$$\hat{o}^{(ii')} |\phi_j\rangle_i |\phi_k\rangle_{i'} = \frac{1}{2} \sum_{lm} o_{lm,jk} |\phi_l\rangle_i |\phi_m\rangle_{i'}, \tag{1.48}$$

with

$$o_{lm,jk} = {}_i\langle \phi_l |_{i'} \langle \phi_m | \hat{o}^{(ii')} | \phi_j \rangle_i | \phi_k \rangle_{i'} = \int d^3\mathbf{r}_i d^3\mathbf{r}_{i'} \phi_l^*(\mathbf{r}_i) \phi_m^*(\mathbf{r}_{i'}) \hat{o}^{(i)} \phi_j(\mathbf{r}_i) \phi_k(\mathbf{r}_{i'}). \tag{1.49}$$

i.e., changing the state of one particle from $|\phi_j\rangle_i$ to $|\phi_l\rangle_i$, and of another one from $|\phi_k\rangle_{i'}$ to $|\phi_m\rangle_{i'}$. This is the same as the action of annihilating two particles $\hat{a}_j \hat{a}_k$ and creating other two $(\hat{a}_l \hat{a}_m)^\dagger = \hat{a}_m^\dagger \hat{a}_l^\dagger$, so we can write

$$\hat{O}^{(2)} = \frac{1}{2} \sum_{jklm} o_{lm,jk} \hat{a}_m^\dagger \hat{a}_l^\dagger \hat{a}_j \hat{a}_k. \tag{1.50}$$

Note that this ordering verifies that if the operator does not change the state of the particles, i.e., $l = j$ and $m = k$, no spurious sign is generated, $\hat{a}_k^\dagger \hat{a}_j^\dagger \hat{a}_j \hat{a}_k = (\hat{a}_k^\dagger \hat{a}_k)(\hat{a}_j^\dagger \hat{a}_j)$. In the opposite case, $l = k$ and $m = j$, the operator corresponds to the exchange of the two particles. Then, fermions get the correct sign: $\hat{a}_j^\dagger \hat{a}_k^\dagger \hat{a}_j \hat{a}_k = -\hat{a}_k^\dagger \hat{a}_j^\dagger \hat{a}_j \hat{a}_k = -(\hat{a}_k^\dagger \hat{a}_k)(\hat{a}_j^\dagger \hat{a}_j)$.

Other operators involving three or more particles, or even different types of particles (e.g., the electron-photon interaction essential in quantum electrodynamics and quantum optics, electron-phonon interaction...), but we are not treating them in this course.

1.3.1. Expectation values

Given a many-body state, we can now calculate the expectation values of any operator

$$\langle \hat{O} \rangle = \langle \vec{N} | \hat{O} | \vec{N} \rangle. \tag{1.51}$$

For single and two-particle operators, this can be calculated by noticing:

$$\langle \hat{a}_m^\dagger \hat{a}_l \rangle = \langle \hat{n}_m \rangle \delta_{ml}, \tag{1.52}$$

[14] If it is less obvious for fermions, go back to Eq. (1.36)

because the same particle needs to be re-created once it has been annihilated if one needs to recover the same many-particle state. With similar arguments one finds:

$$\left\langle \hat{a}_m^\dagger \hat{a}_n^\dagger \hat{a}_l \hat{a}_p \right\rangle = \left\langle \hat{a}_m^\dagger \hat{a}_p \right\rangle \left\langle \hat{a}_n^\dagger \hat{a}_l \right\rangle \pm \left\langle \hat{a}_m^\dagger \hat{a}_l \right\rangle \left\langle \hat{a}_n^\dagger \hat{a}_p \right\rangle = \langle \hat{n}_m \rangle \langle \hat{n}_n \rangle (\delta_{mp}\delta_{nl} \pm \delta_{np}\delta_{ml}). \tag{1.53}$$

An elegant and systematic way to obtain such expressions (quite convenient when the product of operators is long) is Wick's theorem, which expresses the expectation value of normal-ordered[15] products of creation and annihilation operators as combinations of pairs (called *contractions* in this context).

1.3.2. Second-quantizing special operators

Let us see some particular cases that will be useful during the course. For the sake of concreteness, we consider the case of electrons with momentum $\hbar\mathbf{k}$ and spin σ. The corresponding creation and annihilation operators are written as $\hat{c}^\dagger_{\mathbf{k}\sigma}$ and $\hat{c}_{\mathbf{k}\sigma}$, respectively. In most cases, it will be useful to consider the planewave basis, with

$$\psi_{\mathbf{k}\sigma}(\mathbf{r}) = \frac{1}{\sqrt{\mathcal{V}}} e^{i\mathbf{k}\mathbf{r}} \chi_\sigma, \tag{1.54}$$

where $\mathcal{V}$ is the system volume, and χ_σ is the spinor function.

Hamiltonian of a free particle

For a system of free electrons, the hamiltonian is given by the kinetic energy:

$$\hat{T} = -\frac{\hbar^2}{2m} \sum_i \nabla^2_{\mathbf{r}_i} \tag{1.55}$$

which we want to write in the form:

$$\hat{T} = \sum_{\mathbf{k}_1\mathbf{k}_2} \sum_{\sigma_1\sigma_2} T_{\mathbf{k}_1\sigma_1,\mathbf{k}_2\sigma_2} \hat{c}^\dagger_{\mathbf{k}_1\sigma_1} \hat{c}_{\mathbf{k}_2\sigma_2}, \tag{1.56}$$

with the matrix elements

$$T_{\mathbf{k}_1\sigma_1,\mathbf{k}_2\sigma_2} = \int d^3\mathbf{r} \psi^*_{\mathbf{k}_1\sigma_1}(\mathbf{r}) \left(-\frac{\hbar^2}{2m} \nabla^2_{\mathbf{r}} \right) \psi_{\mathbf{k}_2\sigma_2}(\mathbf{r}). \tag{1.57}$$

For free electrons, it is natural to consider planewaves, such that the kinetic energy coefficients become:

$$T_{\mathbf{k}_1\sigma_1,\mathbf{k}_2\sigma_2} = \frac{\hbar^2\mathbf{k}^2}{2m\mathcal{V}} \int d^3\mathbf{r} e^{i(\mathbf{k}_2-\mathbf{k}_1)\mathbf{r}} \delta_{\sigma_1\sigma_2} = \frac{\hbar^2\mathbf{k}_2^2}{2m} \delta_{\mathbf{k}_1,\mathbf{k}_2} \delta_{\sigma_1\sigma_2}. \tag{1.58}$$

Including this in Eq. (1.56), we finally get:

$$\hat{T} = \sum_{\mathbf{k},\sigma} \frac{\hbar^2\mathbf{k}^2}{2m} \hat{c}^\dagger_{\mathbf{k}\sigma} \hat{c}_{\mathbf{k}\sigma}. \tag{1.59}$$

The interpretation is clear: $\hat{c}^\dagger_{\mathbf{k}\sigma}\hat{c}_{\mathbf{k}\sigma}$ counts how many particles have a given momentum $\hbar\mathbf{k}$.

[15] When all creation operators are to the left and all annhilation ones to the right.

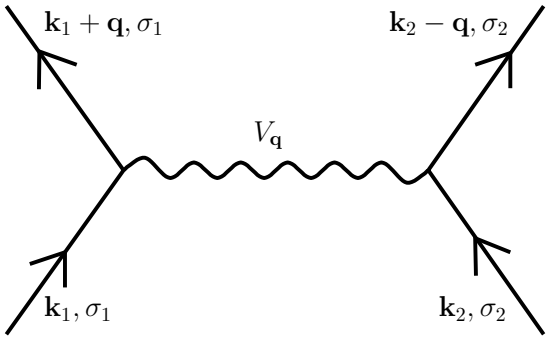

Figure 1.3.:
Feynman diagram of the Coulomb interaction of two electrons with initial states $|\mathbf{k}_1,\sigma_1\rangle$ and $|\mathbf{k}_2,\sigma_2\rangle$, according to Eq. (1.66).

Coulomb interaction of two electrons

The Coulomb interaction is:

$$\hat{V}_{\text{e-e}} = \frac{1}{2}\sum_{i\neq j}\frac{e^2}{|\mathbf{r}_i - \mathbf{r}_j|} \tag{1.60}$$

which, being a two-particle operator is written as

$$\hat{V}_{\text{e-e}} = \frac{1}{2}\sum_{\mathbf{k}_1\mathbf{k}_2\mathbf{k}_3\mathbf{k}_4}\sum_{\sigma_1\sigma_2} V_{\mathbf{k}_3\sigma_1\mathbf{k}_4\sigma_2,\mathbf{k}_1\sigma_1\mathbf{k}_2\sigma_2}\hat{c}^\dagger_{\mathbf{k}_3\sigma_1}\hat{c}^\dagger_{\mathbf{k}_4\sigma_2}\hat{c}_{\mathbf{k}_2\sigma_2}\hat{c}_{\mathbf{k}_1\sigma_1}. \tag{1.61}$$

in second quantized form. Note that we have taken into account (for simplicity in the later calculation) that the Coulomb interaction does not change the spin of the electrons. For planewaves:

$$V_{\mathbf{k}_3\sigma_1\mathbf{k}_4\sigma_2,\mathbf{k}_1\sigma_1\mathbf{k}_2\sigma_2} = \frac{e^2}{\mathcal{V}^2}\int d^3\mathbf{r}_1 d^3\mathbf{r}_2 \frac{1}{|\mathbf{r}_1 - \mathbf{r}_2|}\mathrm{e}^{i(\mathbf{k}_1-\mathbf{k}_3)\mathbf{r}_1 + i(\mathbf{k}_2-\mathbf{k}_4)\mathbf{r}_2}. \tag{1.62}$$

Defining $\mathbf{q} \equiv \mathbf{k}_2 - \mathbf{k}_4$ and $\mathbf{r} \equiv \mathbf{r}_2 - \mathbf{r}_1$, the exponent reads:

$$(\mathbf{k}_1 - \mathbf{k}_3)\mathbf{r}_1 + (\mathbf{k}_2 - \mathbf{k}_4)\mathbf{r}_2 = (\mathbf{k}_1 - \mathbf{k}_3 + \mathbf{k}_2 - \mathbf{k}_4)\mathbf{r}_1 + \mathbf{q}\mathbf{r}, \tag{1.63}$$

such that:

$$V_{\mathbf{k}_3\sigma_1\mathbf{k}_4\sigma_2,\mathbf{k}_1\sigma_1\mathbf{k}_2\sigma_2} = \frac{1}{\mathcal{V}^2}V_\mathbf{q}\int d^3\mathbf{r}_1 \mathrm{e}^{i(\mathbf{k}_1-\mathbf{k}_3+\mathbf{q})\mathbf{r}_1} = \frac{1}{\mathcal{V}}V_\mathbf{q}\delta_{\mathbf{k}_1,\mathbf{k}_3-\mathbf{q}}, \tag{1.64}$$

where we have also defined:

$$V_\mathbf{q} = e^2\int d^3\mathbf{r}\frac{1}{|\mathbf{r}|}\mathrm{e}^{i\mathbf{q}\mathbf{r}} = \frac{4\pi e^2}{|\mathbf{q}|^2}. \tag{1.65}$$

The calculation of the integral in Eq. (1.65) is left as an exercise. Finally, replacing Eq. (1.64) in Eq. (1.61), the Coulomb interaction hamiltonian then reads:

$$\hat{V}_{\text{e-e}} = \frac{1}{2\mathcal{V}}\sum_{\sigma_1\sigma_2}\sum_{\mathbf{k}_1\mathbf{k}_2}\sum_{\mathbf{q}} V_\mathbf{q}\hat{c}^\dagger_{\mathbf{k}_1+\mathbf{q},\sigma_1}\hat{c}^\dagger_{\mathbf{k}_2-\mathbf{q},\sigma_2}\hat{c}_{\mathbf{k}_2,\sigma_2}\hat{c}_{\mathbf{k}_1,\sigma_1}. \tag{1.66}$$

This can be easily interpreted as two electrons, initially with wavenumber $\mathbf{k}_1$ and $\mathbf{k}_2$, which exchange a momentum $\hbar\mathbf{q}$. See Fig. 1.3 for a diagrammatic representation of this interaction.

The density operator

The density operator is $\hat{\rho}(\mathbf{r}) = \sum_i \delta(\mathbf{r} - \mathbf{r}_i)$, which becomes (that may include spin):

$$\hat{\rho}(\mathbf{r}) = \sum_{\mathbf{k}\mathbf{k}'\sigma} \rho_{\mathbf{k}\sigma,\mathbf{k}'\sigma'}(\mathbf{r}) \hat{c}^\dagger_{\mathbf{k}\sigma} \hat{c}_{\mathbf{k}'\sigma}, \quad \text{with} \quad \rho_{\mathbf{k}\sigma,\mathbf{k}'\sigma'}(\mathbf{r}) = \int d^3\mathbf{r}_i \psi^*_{\mathbf{k}\sigma}(\mathbf{r}_i) \delta(\mathbf{r} - \mathbf{r}_i) \psi_{\mathbf{k}'\sigma}(\mathbf{r}_i). \tag{1.67}$$

The coefficients $\rho_{\mathbf{k}\sigma,\mathbf{k}'\sigma'}(\mathbf{r})$ define what is known as the density matrix[16]. Once more, in the planewave basis, the integral leads to

$$\hat{\rho}(\mathbf{r}) = \frac{1}{\mathcal{V}} \sum_{\mathbf{k}\mathbf{k}'\sigma} \mathrm{e}^{i(\mathbf{k}'-\mathbf{k})\mathbf{r}} \hat{c}^\dagger_{\mathbf{k}\sigma} \hat{c}_{\mathbf{k}'\sigma} = \frac{1}{\mathcal{V}} \sum_{\mathbf{q}} \sum_{\mathbf{k}\sigma} \mathrm{e}^{i\mathbf{q}\mathbf{r}} \hat{c}^\dagger_{\mathbf{k}\sigma} \hat{c}_{\mathbf{k}+\mathbf{q},\sigma}, \tag{1.68}$$

so we get, in the reciprocal space:

$$\hat{\rho}(\mathbf{q}) = \sum_{\mathbf{k}\sigma} \hat{c}^\dagger_{\mathbf{k}\sigma} \hat{c}_{\mathbf{k}+\mathbf{q},\sigma}. \tag{1.69}$$

Bibliography

[1.1] P. W. Anderson. More is different. *Science*, 177(4047):393–396, 1972.

[1.2] P. A. M. Dirac. The quantum theory of the emission and absorption of radiation. *Proc. R. Soc. London A*, 114(767):243–265, Mar 1927.

[1.3] P. Jordan and O. Klein. Zum Mehrkörperproblem der Quantentheorie. *Z. Phys.*, 45(11):751–765, Nov 1927.

[1.4] P. Jordan and E. Wigner. Über das Paulische Äquivalenzverbot. *Z. Phys.*, 47(9):631–651, Sep 1928.

[1.5] V. Fock. Konfigurationsraum und zweite Quantelung. *Z. Phys.*, 75(9):622–647, Sep 1932.

[1.6] C. Cohen-Tannoudji, B. Diu, and F. Laloë. *Quantum Mechanics, Volume 1: Basic Concepts, Tools, and Applications, 2nd Edition*. Wiley, Weinheim, Germany, Jun 2020.

Further reading

- ☞ H. Bruus and K. Flensberg, *Many-Body Quantum Theory in Condensed Matter Physics* (Oxford Univ. Press, Oxford, 2004)
- ☞ L. D. Landau and E. M. Lifshitz, *Quantum Mechanics (Non-relativistic theory)* (Pergamon, Oxford, 1977)
- ☞ A. Altland and B. Simmons, *Condensed Matter Field Theory* (Cambridge Univ. Press, Cambridge, 2006)
- ☞ G. F. Giuliani and G. Vignale, *Quantum Theory of the Electron Liquid* (Cambridge Univ. Press, Cambridge, 2008)
- ☞ A. L. Fetter and J. D. Walecka, *Quantum Theory of Many-Particle Systems* (McGraw-Hill, New York, 1971)

[16] The diagonal elements are the probability densities $\rho_{\mathbf{k}\sigma,\mathbf{k}\sigma}(\mathbf{r}) = |\psi_{\mathbf{k}\sigma}(\mathbf{r})|^2$.

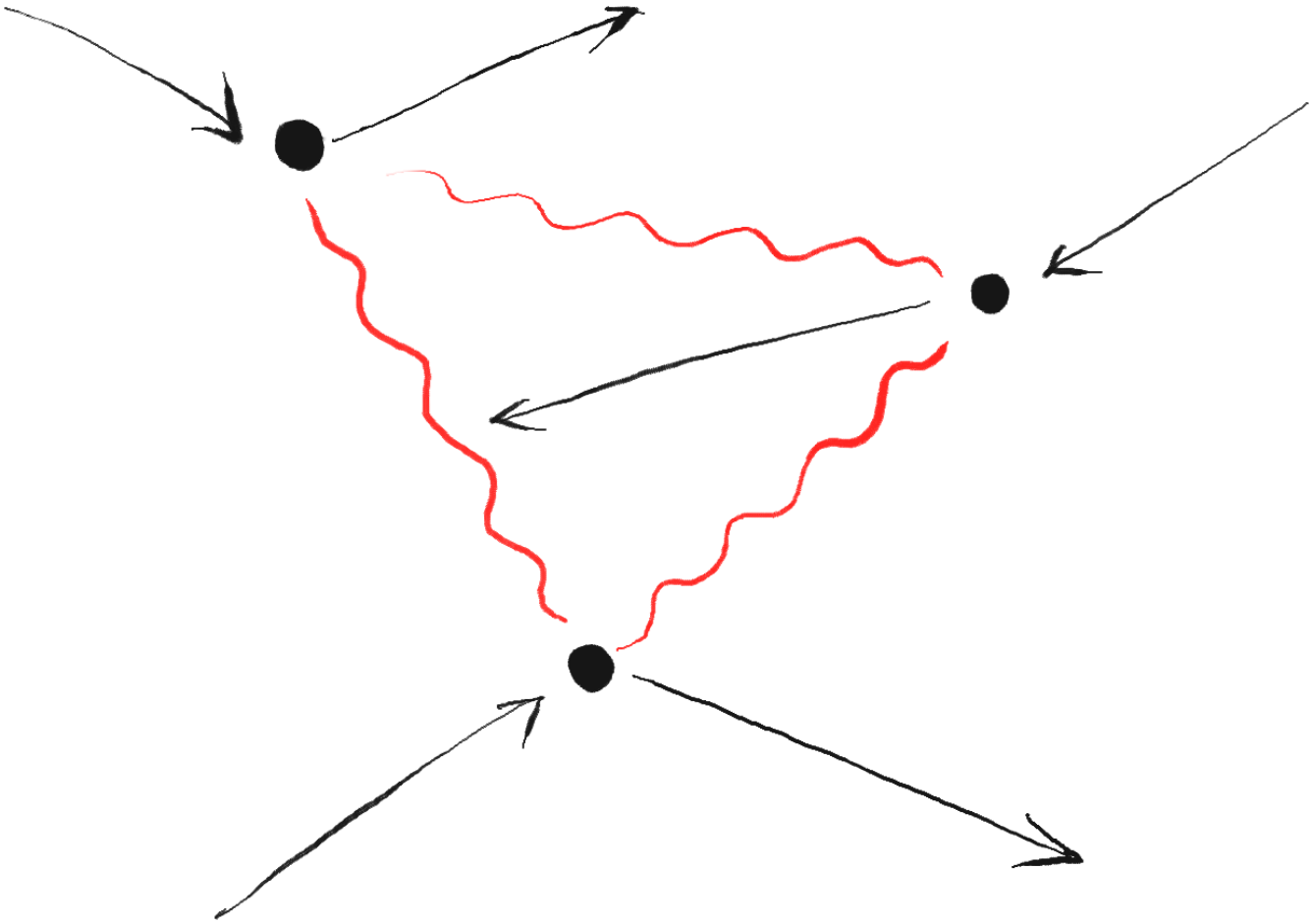

The low temperature properties of metals were described by Sommerfeld based on the treatment of conduction electrons as a noninteracting fermionic gas[17]. The initial success of this theory to reproduce experimental evidences contains at least two surprises: (i) it gives a quantum mechanical description of macroscopic objects, what indeed helped the physics community at that time to take quantum mechanics seriously; and (ii) the Coulomb interaction is neglected and nevertheless it works! However we know since our school years that electrons interact, and their interaction extends over long ranges.

In the chapters forming this part, we will try to understand what is the role of interactions in many electron systems. We will start from the noninteracting description, identify the difficulties in the theoretical treatment of electron-electron interactions, and introduce different approaches and models to address them.

[17] A. Sommerfeld. Zur Elektronentheorie der Metalle auf Grund der Fermischen Statistik. Z. Phys., 47(1):43–60, Jan 1928.

2. Interactions in the electron gas

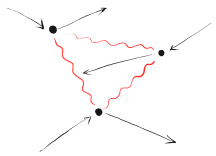

In this chapter, we will start by reviewing the Sommerfeld model for electrons in a metal based on purely statistical considerations for non-interacting fermions. We will then try to justify its rather crude assumptions with the description of electrons moving in a constant potential (what is known as the *jellium* model). A perturbative approach is introduced in the last section for the case of weak electron-electron interactions which introduces the first notion of emergence, but also very soon emphasizes its own limitations.

2.1. The free electron gas. Sommerfeld model

In essence, the model introduced by Sommerfeld explores the impact of Pauli-exclusion principle in the statistics of an ideal gas of particles [2.1]. As such, it can be seen as the minimal approach including quantum effects. Let us hence start with a brief reminder of statistical mechanics, see e.g., Ref. [2.2] for more details.

The outcome of a measurement is not given by the expected value of an operator: we need to know the occupation of each state:

$$\left\langle \hat{O} \right\rangle = \sum_{ik} \rho_{ki} \left\langle i \left| \hat{O} \right| k \right\rangle = \mathrm{tr}\left(\hat{\rho}\hat{O}\right),$$

where the coefficients $\rho_{ki} = \langle k|\hat{\rho}|i\rangle$ are the elements of the density matrix, $\hat{\rho}$, with ρ_{ii} being the probability to find the system in state $|i\rangle$.The density matrix hence satisfies $\mathrm{tr}\,(\hat{\rho}) = 1$.

2.1.1. Thermodynamic quantities

Consider a gas of N electrons of wave vector $\mathbf{k}$ and spin σ. We write their states as $|k\rangle = |\mathbf{k}\sigma\rangle$. Each electron has an energy ε_k (we do not need to specify the dispersion relation here). In the grand canonical ensemble, its state is given by

$$\hat{\rho}_{\mathrm{G}} = \mathcal{Z}_{\mathrm{G}}^{-1} \mathrm{e}^{-\beta\left(\hat{H}-\mu\hat{N}\right)}, \tag{2.1}$$

where $\hat{H} = \sum_k \varepsilon_k \hat{n}_k$ is the hamiltonian, $\hat{N} = \sum_k \hat{n}_k$ is the number operator, $\beta = 1/k_{\mathrm{B}}T$ is the inverse temperature, and μ is the chemical potential. The normalization condition $\mathrm{tr}\,(\hat{\rho}_{\mathrm{G}}) = 1$ gives the partition function:

$$\mathcal{Z}_{\mathrm{G}} = \sum_{n_k} \mathrm{e}^{-\beta\sum_k \hat{n}_k(\varepsilon_k-\mu)} = \prod_k \left(1 + \mathrm{e}^{-\beta(\varepsilon_k-\mu)}\right), \tag{2.2}$$

where one uses that the Pauli exclusion principle only allows $n_k = 0, 1$. The particle occupation is then:

$$\langle n_k \rangle = \mathrm{tr}\,(\hat{\rho}_{\mathrm{G}}\hat{n}_k) = \frac{1}{\mathcal{Z}_{\mathrm{G}}} \sum_{n_k=0,1} n_k \mathrm{e}^{-\beta n_k(\varepsilon_k-\mu)} = \frac{\mathrm{e}^{-\beta(\varepsilon_k-\mu)}}{1+\mathrm{e}^{-\beta(\varepsilon_k-\mu)}} = \frac{1}{1+\mathrm{e}^{\beta(\varepsilon_k-\mu)}} = f(\varepsilon_k), \tag{2.3}$$

which is of course the Fermi-Dirac distribution function.

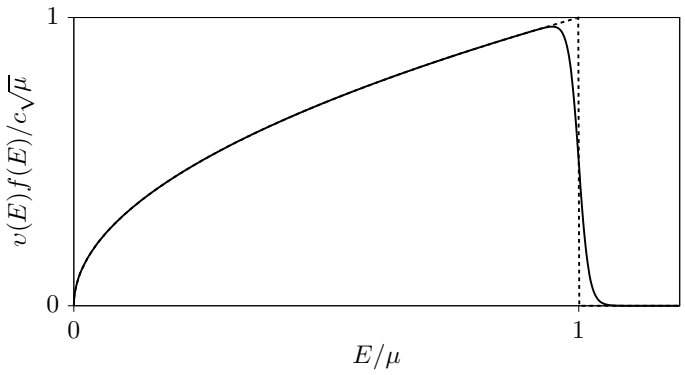

Figure 2.1.:
Density of states. Plot of $\upsilon(E)f(E)$ (normalized by $c = 2(2m)^{3/2}/(2\pi\hbar)^3$) for $T = 0$ (dashed line) and $T = 10^{-2}\mu/k_B$ (solid line).

With this, we can evaluate the thermodynamic quantities. The number of particles and the energy are obviously[1]:

$$N = \left\langle \hat{N} \right\rangle = \sum_k \langle n_k \rangle \quad \text{and} \quad U = \left\langle \hat{H} \right\rangle = \sum_k \langle n_k \rangle \varepsilon_k. \tag{2.4}$$

2.1.2. Density of states

As we are leading with really many particles (thermodynamic limit), it is convenient to transform sums into integrals:

$$\sum_{\mathbf{k},\sigma} \bullet \quad \longrightarrow \quad \int dE \upsilon(E) \bullet,$$

where $\upsilon(E) = g(E)/\mathcal{V}$ is the density of states per unit volume (of course, $g(E)$ is the density of states). Assuming free electrons with $|\mathbf{k}| = \sqrt{2mE}/\hbar$, and that $\bullet$ is homogeneous and does not depend on spin, we can simply calculate the number of states, $\Sigma = \int dE g(E)$:

$$\Sigma = 2 \int d^3\mathbf{r} \int \frac{d^3\mathbf{k}}{(2\pi)^3} = \mathcal{V} \int dE \upsilon(E), \tag{2.5}$$

where the factor 2 accounts for spin, and:

$$\upsilon(E) = 2\frac{(2m)^{3/2}}{4\pi^2\hbar^3}\sqrt{E}. \tag{2.6}$$

Using this result, the number of particles and energy from Eqs. (2.4) read:

$$N = \mathcal{V} \int dE \upsilon(E) f(E) \quad \text{and} \quad U = \mathcal{V} \int dE E \upsilon(E) f(E). \tag{2.7}$$

The integrand $\upsilon(E)f(E)$ is plotted in Fig. 2.1.

Sometimes it will also be convenient to consider densities: $\mathfrak{n} = N/\mathcal{V}$ and $u = U/\mathcal{V}$. In general, integrals of this kind are difficult to evaluate, specially at finite temperature. However, one notices that in metals, the chemical potential is typically two orders of magnitude larger than ambient temperature (e.g., for Cu: μ/k_B=8.16×10^3 K). Hence we can in most cases invoke a low temperature limit, $\mu \gg k_B T$.

[1] The same quantities can be obtained by using

$$N = k_B T \frac{\partial}{\partial \mu} \ln \mathcal{Z}_G \qquad \text{and} \qquad U = -\frac{\partial}{\partial \beta} \ln \mathcal{Z}_G$$

or, more generally, from derivatives of the grand-potential $\Phi = -k_B T \ln \mathcal{Z}_G$.

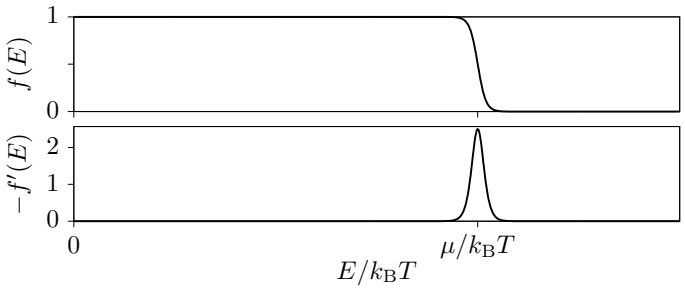

Figure 2.2.:
Fermi distribution and its derivative for $\mu = 100k_BT$.

2.1.3. Low temperature limit: the Sommerfeld expansion

We are left with calculating integrals of the form:

$$\mathcal{I} = \int_0^\infty dE f(E) \frac{d}{dE}\mathcal{G}(E). \tag{2.8}$$

Why we introduce the derivative in the integral will become clear in a second. In the cases we are interested in, the integrand happens to satisfy $\mathcal{G}(E{=}0) = 0$. We can then integrate by parts:

$$\mathcal{I} = -\int_0^\infty dE f'(E)\mathcal{G}(E). \tag{2.9}$$

The derivative of the Fermi function,

$$f'(E) = -\frac{1}{k_BT}\cosh^{-2}\left(\frac{E-\mu}{2k_BT}\right), \tag{2.10}$$

is a peak of width k_BT centered at μ, and vanishes everywhere else, see Fig. 2.2. At low temperatures, $\mu \gg k_BT$, the integral will be strongly dominated by how $\mathcal{G}(E)$ behaves close to μ. Expanding $\mathcal{G}(E)$ around μ:

$$\mathcal{G}(E) = \mathcal{G}(\mu) + \mathcal{G}'(\mu)(E-\mu) + \frac{1}{2}\mathcal{G}''(\mu)(E-\mu)^2 + \ldots, \tag{2.11}$$

the integral in Eq. (2.9) becomes:

$$\mathcal{I} = L_0\mathcal{G}(\mu) + L_1\mathcal{G}'(\mu) + L_2\mathcal{G}''(\mu) + \ldots, \qquad \text{with} \qquad L_n = -\frac{1}{n!}\int_0^\infty dE(E-\mu)^n f'(E). \tag{2.12}$$

Sticking to the low temperature limit, we can safely extend the range of integrals L_n: $\int_0^\infty \longrightarrow \int_{-\infty}^\infty$. We can then integrate:

$$L_0 \approx -\int_{-\infty}^\infty dE f'(E) = 1 \tag{2.13}$$

$$L_1 \approx -\int_{-\infty}^\infty dE(E-\mu)f'(E) = 0 \tag{2.14}$$

$$L_2 \approx -\frac{1}{2}\int_{-\infty}^\infty dE(E-\mu)^2 f'(E) = \frac{\pi^2}{6}(k_BT)^2. \tag{2.15}$$

For the same reason that Eq. (2.14), we find $L_{2n+1} \approx 0$. We are then left with what is known as the *Sommerfeld expansion* [2.1]:

$$\mathcal{I} \approx \mathcal{G}(\mu) + \frac{\pi^2}{6}(k_BT)^2\mathcal{G}''(\mu) + \ldots \tag{2.16}$$

At low temperatures, we obtain $\mathcal{I}$ by evaluating $\mathcal{G}(E)$ and its even derivatives at μ, where all electronic excitations occur.

2.1.4. Thermodynamic properties

We are ready now to evaluate the integrals of Eqs. (2.7), in particular their temperature dependence. Let us start with the number of particles ($\mathcal{V}$ plays no role, so we consider densities, for simplicity). It is clear that $\mathfrak{n}$ does not depend on temperature, i.e., $\mathfrak{n}(T) = \mathfrak{n}(0)$. The chemical potential will then change to absorb the temperature dependence. To show this, we compare the $T = 0$ expression

$$\mathfrak{n}(0) \approx \int_0^{\mu_0} dE \upsilon(E), \tag{2.17}$$

where $\mu_0 = \mu(T{=}0)$, with the one obtained by performing a Sommerfeld expansion [2]:

$$\mathfrak{n}(T) \approx \int_{-\infty}^{\mu} dE \upsilon(E) + \frac{(\pi k_B T)^2}{6} \upsilon'(\mu). \tag{2.18}$$

The remaining integrals in Eq. (2.17) and (2.18) can be calculated by using $\upsilon(E) \propto \sqrt{E}$, cf. Eq. (2.6). Making $\mathfrak{n}(T) = \mathfrak{n}(0)$, we get the relation between $\mu(T)$ and μ_0:

$$[\mu - \mu_0]\mu^{1/2} + \frac{\pi^2}{12}(k_B T)^2 \mu^{-1/2} = 0. \tag{2.19}$$

Keeping the leading order in temperature, we finally arrive to

$$\mu(T) \approx \mu_0 \left[1 - \frac{\pi^2}{12}\left(\frac{k_B T}{\mu_0}\right)^2\right]. \tag{2.20}$$

For the energy density, we get:

$$u \approx u_0 + \frac{\pi^2}{6}(k_B T)^2 \upsilon(\mu_0), \tag{2.21}$$

where $u_0 = (3/5)\mathfrak{n}\mu_0$ is the kinetic energy per unit volume at $T = 0$. With this, we can calculate the heat capacity.

$$c_V = \frac{\partial u}{\partial T} = \frac{\pi^2}{3} \upsilon(\mu_0) k_B^2 T, \tag{2.22}$$

reproducing the linear c_V observed in most metals at low temperatures. This is in contrast with the classical Drude model (assuming Maxwell-Boltzmann statistics), which predicts a temperature independent $c_V^{\text{Drude}} = (3/2)\mathfrak{n}k_B$[3].

> For the heat capacity, one also needs to take phonons into account, which results in $c_V \sim \alpha T^3 + \gamma T$. However, at low temperatures they do not contribute, so one measures only the electronic part.

The success of the Sommerfeld model was confirmed by the reproduction of the temperature behaviour of the magnetic susceptibility, χ. If we write the magnetization as

$$M = \frac{\mu_B}{2} \int dE[g(E + \mu_B H) - g(E - \mu_B H]f(E), \tag{2.23}$$

where μ_B is the Bohr magneton, one arrives for low fields H to $M = \mu_B^2 H g(\mu_0)$. Therefore,

$$\chi = \frac{\partial M}{\partial H} = \mu_B^2 g(\mu_0), \tag{2.24}$$

[2] What is $\mathcal{G}(E)$ in this case?

[3] This was the first measured evidence of what important principle of quantum mechanics?

which is left as an exercise.

Unfortunately, the model is not able to describe other phenomena such as the Hall or the thermoelectric effects. Nobody's prefect!

§

Recapping, we can extract two main messages from the Sommerfeld model, one that sounds obvious but is of fundamental importance, and one that sounds at least surprising:

- In metals,
  - ☞ carriers are fermions, and
  - ⚠ electron-electron interaction can be neglected.

2.2. The hamiltonian

In the previous section, not only the electron-electron interaction, but also the presence of the atoms is ignored. We present here all contributions by defining the hamiltonian of the system

$$\hat{H} = \hat{H}_{\text{ion}} + \hat{H}_{\text{el}} + \hat{H}_{\text{ion-el}}. \tag{2.25}$$

It is composed of a lattice of positive ions (formed by the nuclei and the bounded electrons) sitting at positions $\mathbf{R}_i$,

$$\hat{H}_{\text{ion}} = -\frac{\hbar^2}{2M}\sum_i \nabla^2_{\mathbf{R}_i} + \frac{1}{2}\sum_{i\neq j}\frac{Z^2e^2}{|\mathbf{R}_i - \mathbf{R}_j|}, \tag{2.26}$$

a cloud of electrons,

$$\hat{H}_{\text{el}} = -\frac{\hbar^2}{2m}\sum_i \nabla^2_{\mathbf{r}_i} + \frac{1}{2}\sum_{i\neq j}\frac{e^2}{|\mathbf{r}_i - \mathbf{r}_j|}, \tag{2.27}$$

and their interaction,

$$\hat{H}_{\text{ion-el}} = -\sum_{i,j}\frac{Ze^2}{|\mathbf{R}_i - \mathbf{r}_j|}. \tag{2.28}$$

(Spoiler alert): In most part of the course, the particular form of the lattice will play no role. For the moment, it will be enough to concentrate on the electronic part. We need to write it in second quantization, see chapter 1.

2.2.1. Second-quantizing the electronic hamiltonian

Let us consider a more general hamiltonian $\hat{H}_{\text{el}} = \hat{T} + \hat{U}_{\text{ext}} + \hat{V}_{\text{e-e}}$ by additionally including the contribution of a potential, $\hat{U}_{\text{ext}}$. We will work with its second quantization form, which we found in Sec. 1.3.2 in the planewave basis:

$$\hat{T} = -\frac{\hbar^2}{2m}\sum_i \nabla^2_{\mathbf{r}_i} \longrightarrow \frac{\hbar^2\mathbf{k}^2}{2m}\hat{c}^\dagger_{\mathbf{k}\sigma}\hat{c}_{\mathbf{k}\sigma} \tag{2.29}$$

$$\hat{U}_{\text{ext}} = \sum_i U(\mathbf{r}_i) \longrightarrow \sum_{\mathbf{k}_1\mathbf{k}_2}\sum_{\sigma_1\sigma_2} U_{\mathbf{k}_1\sigma_1,\mathbf{k}_2\sigma_2}\hat{c}^\dagger_{\mathbf{k}_1\sigma_1}\hat{c}_{\mathbf{k}_2\sigma_2} \tag{2.30}$$

$$\hat{V}_{\text{e-e}} = \frac{1}{2}\sum_{i\neq j}\frac{e^2}{|\mathbf{r}_i - \mathbf{r}_j|} \longrightarrow \frac{1}{2\mathcal{V}}\sum_{\sigma_1\sigma_2}\sum_{\mathbf{k}_1\mathbf{k}_2}\sum_{\mathbf{q}} V_{\mathbf{q}}\hat{c}^\dagger_{\mathbf{k}_1+\mathbf{q},\sigma_1}\hat{c}^\dagger_{\mathbf{k}_2-\mathbf{q},\sigma_2}\hat{c}_{\mathbf{k}_2,\sigma_2}\hat{c}_{\mathbf{k}_1,\sigma_1}. \tag{2.31}$$

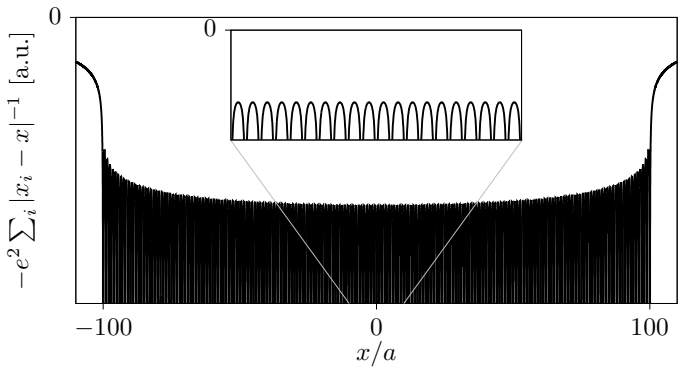

Figure 2.3.:
Coulomb interaction between an electron and a one dimensional array of positive charges at positions $x_i = ia$, with $-100 \leq i \leq 100$.

where the potential can in principle affect both the electron momentum and spin, and the Coulomb interaction renders (left as an exercise):

$$V_{\mathbf{q}} = \frac{4\pi e^2}{|\mathbf{q}|^2}. \tag{2.32}$$

2.3. The *jellium* model

The Sommerfeld model called the attention on the relevance of quantum many-body physics and the need of a quantum mechanical description for understanding some properties of macroscopic objects. Despite its remarkable success, a curious mind cannot be satisfied with simply assuming that electrons in metals as a gas of non-interacting particles obeying Fermi-Dirac statistics.

The *jellium* model provides a justification of at least some aspects of the Sommerfeld model. One gets a more physical picture of the problem, but in essence, it reaches the same conclusions that were described in the previous section.[4] It is built on two main assumptions: (i) the ions of the lattice form a homogeneous positively-charged background, and (ii) the interaction with the rest of free electrons is also homogeneous. The first one is easy to justify if one wants to concentrate on the description of the conduction electrons (one can also become convinced by looking at Fig. 2.3). The second one, let us just assume it for the moment.

The hamiltonian of the system, written in the form of Eq. (2.25) contains the terms:

$$\hat{H}_{\text{ion,jel}} = \frac{e^2}{2}\int d^3\mathbf{r}' d^3\mathbf{r}\; \mathfrak{n}(\mathbf{r})\mathfrak{n}(\mathbf{r}')\frac{\mathrm{e}^{-a|\mathbf{r}-\mathbf{r}'|}}{|\mathbf{r}-\mathbf{r}'|} = \frac{e^2}{2}\frac{N^2}{\mathcal{V}^2}\int d^3\mathbf{r}' d^3\mathbf{r}\frac{\mathrm{e}^{-a|\mathbf{r}-\mathbf{r}'|}}{|\mathbf{r}-\mathbf{r}'|} \tag{2.33}$$

$$\hat{H}_{\text{ion-el,jel}} = -e^2\sum_i \int d^3\mathbf{r}\; \mathfrak{n}(\mathbf{r})\frac{\mathrm{e}^{-a|\mathbf{r}-\mathbf{r}_i|}}{|\mathbf{r}-\mathbf{r}_i|} = -e^2\frac{N}{\mathcal{V}}\sum_i \int d^3\mathbf{r}\frac{\mathrm{e}^{-a|\mathbf{r}-\mathbf{r}_i|}}{|\mathbf{r}-\mathbf{r}_i|}, \tag{2.34}$$

where we have introduced the Yukawa potential for the screened Coulomb interaction (including the screening length, a) to avoid divergences. These integrals can be done exactly, so we do not need to *second-quantize* them. The electronic term, for $\mathbf{q} = 0$ reads:

$$\hat{H}_{\text{el,jel}} = \hat{T}_{\text{el}} + \frac{2\pi e^2}{\mathcal{V}a^2}\sum_{\sigma_1\sigma_2}\sum_{\mathbf{k}_1\mathbf{k}_2}\hat{c}^\dagger_{\mathbf{k}_1,\sigma_1}\hat{c}^\dagger_{\mathbf{k}_2,\sigma_2}\hat{c}_{\mathbf{k}_2,\sigma_2}\hat{c}_{\mathbf{k}_1,\sigma_1}. \tag{2.35}$$

One can easily than verify that the contribution of Eqs. (2.33) and (2.34) cancel the one of Eq. (2.35), up to a thermodynamically negligible value (left as an exercise)[5]. The only remaining terms are therefore,

[4] In this section, we will follow the discussion in Ref. [2.3], and sometimes also Ref. [2.4]
[5] For this, it is useful to compute their contribution to the energy per particle.

the kinetic term and the potential generated by the ions (look again to Fig. 2.3):

$$\hat{H}_{\text{jel}} = \hat{T} + \hat{V}_{\text{jel}}, \tag{2.36}$$

where $\hat{V}_{\text{jel}}$ is constant in a region of volume $\mathcal{V} = L_x L_y L_z$ where the electrons move. Therefore, the ions simply introduce boundary conditions to the free electron problem (see below).

2.3.1. Constructing the many-body state

The many-body state can then be written in terms of the single-particle wavefunction. From the kinetic term of the hamiltonian, see Eq. (2.29), we get the energies $\varepsilon_{\mathbf{k}\sigma} = \hbar^2|\mathbf{k}|^2/2m$ [6] and the wavefunctions

$$\psi_{\mathbf{k}\sigma}(\mathbf{r}) = \frac{1}{\sqrt{\mathcal{V}}} e^{i\mathbf{k}\mathbf{r}} \chi_\sigma, \tag{2.37}$$

for electrons of wavenumber $\mathbf{k}$ and spin σ. The periodic boundary conditions established by the ionic potential can be written as:

$$\psi(0,y,z) = \psi(L_x,y,z), \qquad \psi(x,0,z) = \psi(x,L_y,z) \qquad \text{and} \qquad \psi(x,y,0) = \psi(x,y,L_z),$$

and analogously for the derivatives:

$$\psi'(0,y,z) = \psi'(L_x,y,z), \qquad \psi'(x,0,z) = \psi'(x,L_y,z) \qquad \text{and} \qquad \psi'(x,y,0) = \psi'(x,y,L_z),$$

which impose that the wavenumber is quantized:

$$k_\alpha = \pm\frac{2\pi}{L_\alpha} j_\alpha, \quad \text{with} \quad j_\alpha \in \mathbb{N}. \tag{2.38}$$

Once that we have a complete description of the single-particle states, we write the many-body state by filling the vacuum with N electrons, each of them with a wavenumber $\mathbf{k}_i$ and a spin $\sigma = \uparrow, \downarrow$. For this, we need to take into account their fermionic statistics. If we order them from smaller to higher energy, so $\varepsilon_i \leq \varepsilon_j$, if $i < j$,[7] they will occupy all available states bellow $\varepsilon_{N/2}$,[8] resulting in the ground state[9]:

$$|\Psi_0\rangle = \hat{c}^\dagger_{\mathbf{k}_1\downarrow}\hat{c}^\dagger_{\mathbf{k}_1\uparrow}\hat{c}^\dagger_{\mathbf{k}_2\downarrow}\hat{c}^\dagger_{\mathbf{k}_2\uparrow}\ldots|0\rangle. \tag{2.39}$$

It is commonly known as the *Fermi sphere*. With these, we will compute the expectation values

$$\left\langle \hat{O} \right\rangle = \langle\Psi_0|\hat{O}|\Psi_0\rangle \tag{2.40}$$

of a general operator $\hat{O}$.

The energy of the last electron sets the Fermi energy, $E_{\text{F}}(T{=}0) = \varepsilon_{N/2}$ (the radius of the Fermi sphere), which will dominate the macroscopic properties of the system. Depending on the problem at hands, this definition can be rewritten in more useful ways by expressing it as a wavenumber, as a wavelength or as a velocity:

$$k_{\text{F}} = |\mathbf{k}_{N/2}| = \frac{1}{\hbar}\sqrt{2mE_{\text{F}}}, \qquad \lambda_{\text{F}} = \frac{2\pi}{k_{\text{F}}} \qquad \text{and} \qquad v_{\text{F}} = \frac{\hbar k_{\text{F}}}{m}, \tag{2.41}$$

[6] We assume there is no magnetic field, for simplicity.
[7] Remember from the rules of second quantization that the order is important for fermions.
[8] Is this always true?
[9] If this is the ground state, what are the excited states?

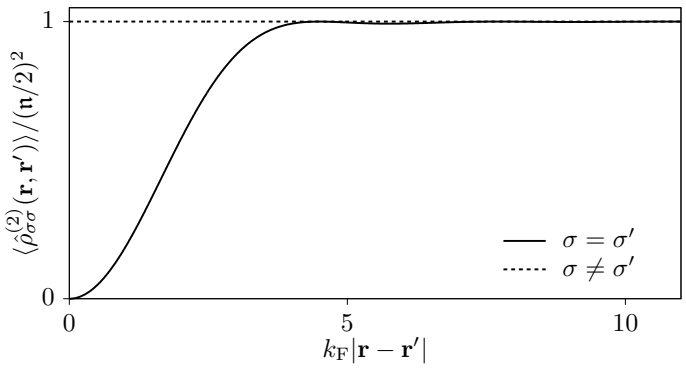

Figure 2.4.:
Spatial dependence of the spin components of the two-particle density. Exchange correlations between electrons with the same spin reduce it for short distances.

respectively. In particular, by calculating the number of particles, the Fermi wavelength can be related in a simple way to the electronic density, $\mathfrak{n}$, which is something one can estimate easily[10]:

$$\mathfrak{n} = \frac{1}{\mathcal{V}}\langle\hat{n}_{\mathbf{k}\sigma}\rangle = \frac{1}{\mathcal{V}}\sum_{|\mathbf{k}|<k_\mathrm{F},\sigma} n_{\mathbf{k}\sigma} = \frac{2}{\mathcal{V}}\int d^3\mathbf{r}\int_{|\mathbf{k}|<k_\mathrm{F}}\frac{d^3\mathbf{k}}{(2\pi)^3} = \frac{k_\mathrm{F}^3}{3\pi^2}, \tag{2.42}$$

so we get:

$$k_\mathrm{F} = \left(3\pi^2\mathfrak{n}\right)^{1/3} \quad \text{and} \quad E_\mathrm{F} = \frac{(3\pi^2\mathfrak{n})^{2/3}}{2m}\hbar^2. \tag{2.43}$$

We can now calculate the total energy of the ground state:

$$E_0 = \left\langle\hat{H}_\mathrm{jel}\right\rangle = \sum_{\mathbf{k}\sigma}\frac{\hbar^2|\mathbf{k}|^2}{2m} = 2\mathcal{V}\int_{|\mathbf{k}|\leq k_\mathrm{F}}\frac{d^3\mathbf{k}}{(2\pi)^3}\frac{\hbar^2|\mathbf{k}|^2}{2m} = \frac{3}{5}NE_\mathrm{F}(T{=}0), \tag{2.44}$$

where we have used Eqs. (2.41) and (2.42).

Recovering thermodynamics

Note that at zero temperature, the integral in the number of particles can be rewritten as:

$$N = 2\mathcal{V}\int_{|\mathbf{k}|\leq k_\mathrm{F}}\frac{d^3\mathbf{k}}{(2\pi)^3} = 8\pi\mathcal{V}\int_0^\infty\frac{k^2dk}{(2\pi)^3}\Theta(k_\mathrm{F}-k), \tag{2.45}$$

and equally for the energy E_0. Note that the Heaviside function plays the role of the occupation of the electronic states. It is then clear that at finite temperatures, this needs to be replaced by the Fermi distribution:

$$N = 8\pi\mathcal{V}\int_0^\infty\frac{k^2dk}{(2\pi)^3}f(\varepsilon_k). \tag{2.46}$$

Changing from wavenumber to energy variables, we then obtain the integrals of Eqs. (2.7), from which we recover all the results in Sec. 2.1.

2.3.2. The exchange hole

The many-body properties manifest clearly in the particle-particle correlations, even in the non-interacting state. A remarkable example is the spin resolved two-particle density[11]:

$$\hat{\rho}^{(2)}_{\sigma\sigma'}(\mathbf{r},\mathbf{r}') = \frac{1}{\mathcal{V}^2}\sum_{\mathbf{k},\mathbf{k}'}\sum_{\mathbf{q},\mathbf{q}'}\mathrm{e}^{i\mathbf{q}\mathbf{r}}\mathrm{e}^{i\mathbf{q}'\mathbf{r}'}\hat{c}^\dagger_{\mathbf{k}\sigma}\hat{c}^\dagger_{\mathbf{k}'\sigma'}\hat{c}_{\mathbf{k}'+\mathbf{q}',\sigma'}\hat{c}_{\mathbf{k}+\mathbf{q},\sigma}. \tag{2.47}$$

[10] ... and control it experimentally.
[11] One obtains it by second-quantizing the product $\hat{\rho}(\mathbf{r})\hat{\rho}(\mathbf{r}')$.

Its expectation value can be factorized in two terms using Eq. (1.53). The first term is finite only for $\mathbf{q} = \mathbf{q}' = 0$, the second one for $\sigma = \sigma'$. Transforming the sums in $\mathbf{k}$ and $\mathbf{k}'$ into integrals, we arrive at[12]

$$\left\langle \hat{\rho}^{(2)}_{\sigma\sigma'}(\mathbf{r}, \mathbf{r}') \right\rangle = \left(\frac{\mathfrak{n}}{2}\right)^2 \left[1 - G(k_\mathrm{F}|\mathbf{r} - \mathbf{r}'|)^2 \delta_{\sigma\sigma'}\right], \tag{2.48}$$

as shown in Fig. 2.4, where we have defined

$$G(x) = 3\frac{\sin x - x\cos x}{x^3}. \tag{2.49}$$

It is constant (and proportional to square of the spin density $\langle \hat{\rho}_\sigma \rangle = \mathfrak{n}/2$) for electrons with opposite spin: they are uncorrelated. However, the Pauli exclusion principle avoids two electrons with the same spin to be close to each other, resulting in a reduced density. This effect is known as the exchange hole.

2.3.3. Orders of magnitude

For every physical problem, it is important to know what are the orders of magnitude of the relevant quantities. We have seen above that most of them can be related to the electronic density. If we then consider a metal with one conduction electron per ion (such as Na), and assume that the ions are separated by 2 Å, we get a density $\mathfrak{n} \sim 10^{29}\,\mathrm{m}^{-3}$, giving:

$k_\mathrm{F} \sim 10\,\mathrm{nm}^{-1}$	$v_\mathrm{F} \sim 4 \times 10^{-3} c$	$\lambda_\mathrm{F} \sim 1\,\mathrm{nm}$	$E_\mathrm{F} \sim 1$–$10\,\mathrm{eV}$

We can readily interpret this:

- ☞ as $v_\mathrm{F} \ll c$, we can safely neglect relativistic effects in most cases (no surprise);
- ☞ room temperature ($k_\mathrm{B} T_r \sim 0.03\,\mathrm{eV}$) is low temperature for a metal: since $E_\mathrm{F} \gg k_\mathrm{B} T_r$, only a small part of the electrons will be affected by thermal fluctuations.

Also, one needs to go to the nanoscale to observe effects of the single-particle interference.

Relevance of the electron-electron interaction

A rough estimation of the Coulomb interaction requires knowing the average distance between electrons. We get this from the density: Assuming that each electron occupies a sphere of radius r_0:

$$r_0 = \left(\frac{3}{4\pi\mathfrak{n}}\right)^{1/3} = \left(\frac{9\pi}{4}\right)^{1/3} k_\mathrm{F}^{-1}, \tag{2.50}$$

we obtain the interaction between two electrons as:

$$E_\mathrm{e-e} = \frac{e^2}{2r_0} = \frac{e^2}{2}\left(\frac{4\pi}{3}\right)^{1/3} \mathfrak{n}^{1/3}. \tag{2.51}$$

We need to compare this with the kinetic energy, that we calculated in Eq. (2.44), in particular, with the kinetic energy per electron,

$$E_\mathrm{kin} = \frac{3}{5} E_\mathrm{F}(0) = \frac{3}{5}\frac{(3\pi^2\mathfrak{n})^{2/3}}{2m}\hbar^2. \tag{2.52}$$

Note that, apart from several constants, both Eqs. (2.51) and (2.52) only depend on density, giving:

$$\frac{E_\mathrm{e-e}}{E_\mathrm{kin}} \propto \mathfrak{n}^{-1/3}. \tag{2.53}$$

This implies a quite counterintuitive result:

[12] Left as an exercise.

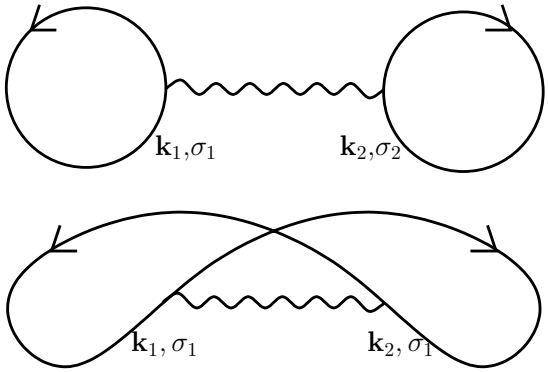

Figure 2.5.:
Feynman diagrams of the direct and exchange contributions to the first order expansion of the Coulomb interaction of two electrons with initial states $|\mathbf{k}_1,\sigma_1\rangle$ and $|\mathbf{k}_2,\sigma_2\rangle$. Note that the exchange term imposes that the two electrons have the same spin.

☞ the effect of Coulomb interaction decreases with increasing density!

Sometimes, the relative contribution of the Coulomb interaction is associated to the dimensionless distance:

$$r_s = \frac{r_0}{a_0} \propto \mathfrak{n}^{-1/3}, \tag{2.54}$$

written in terms of the Bohr radius, $a_0 = \hbar^2/e^2m \approx 0.5292\,\text{Å}$. The weak interaction regime is then defined by small r_s. For the opposite regime, $r_s \gg 1$, the interactions are so strong that electrons are expected to crystalize[13], what is known as a Wigner crystal [2.6]. Note that most metals are in the intermediate regime, $2 < r_s < 6$, cf. Ref. [2.7]. A phenomenological description of this regime is given by Landau's Fermi liquid theory [2.8] which introduces the fundamental notion of quasiparticles[14].

2.4. Perturbation theory

In the high density limit, the effect of interactions is hence expected to be small. It is natural then to perform a perturbative expansion in terms of n^{-1}. We parametrize it with the dimensionless distance r_s. We will also restrict to the $T = 0$ situation. The 0-th order will of course be given by the non-interacting description given in the previous section:

$$E^{(0)} = \langle\Psi_0|\hat{H}_{\text{jel}}|\Psi_0\rangle = \frac{3}{5}NE_{\text{F}}, \tag{2.55}$$

as we did in Eq. (2.44). We are ultimately interested in the energy per particle, which can be written as:

$$\frac{E^{(0)}}{N} = \frac{3}{5}\left(\frac{9\pi}{4}\right)^{2/3}\frac{e^2}{2a_0}r_s^{-2} \approx (2.2\,\text{Ry})r_s^{-2}, \tag{2.56}$$

where we have used Eq. (2.50) and the definition of the Bohr radius. The energy is expressed in Rybergs (remember, the ionization energy of the Hidrogen atom, $1\,\text{Ry} = e^2/2a_0 \approx 13.6\,\text{eV}$).

2.4.1. First order

We apply the standard perturbation theory (see your favourite book on quantum mechanics):

$$E^{(1)} = \left\langle\hat{H}_{\text{e-e}}\right\rangle = \frac{1}{2\mathcal{V}}\sum_{\sigma_1\sigma_2}\sum_{\mathbf{k}_1\mathbf{k}_2}\sum_{\mathbf{q}\neq 0}\frac{4\pi e^2}{q^2}\left\langle\hat{c}^\dagger_{\mathbf{k}_1+\mathbf{q},\sigma_1}\hat{c}^\dagger_{\mathbf{k}_2-\mathbf{q},\sigma_2}\hat{c}_{\mathbf{k}_2,\sigma_2}\hat{c}_{\mathbf{k}_1,\sigma_1}\right\rangle, \tag{2.57}$$

[13] Only very recently this has been measured in one-dimensional systems [2.5]. Why in 1-D and not (yet) in 2-D or 3-D?
[14] Quasi-electrons, in this case.

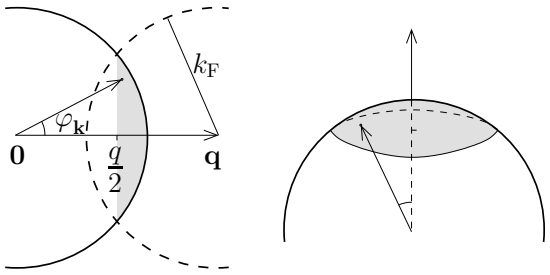

Figure 2.6.:
Interpretation of the integral over $d^3\mathbf{k}$ in Eq. (2.62) as the overlap of two spheres of radium k_F separated by $\mathbf{q}$. The total overlap is twice the shaded region.

where we have used Eq. (2.31)[15]. Not all terms of the sums in the previous expression contribute: The Fermi sphere imposes important restrictions. We know that at zero temperature, all states $|\mathbf{k}_1| < k_F$ are occupied, and empty otherwise. This means, in particular:

$$\hat{c}_{\mathbf{k}_1,\sigma_1}|\Psi_0\rangle = 0, \quad \text{if } |\mathbf{k}_1| > k_F \tag{2.58}$$

$$\langle\Psi_0|\hat{c}^\dagger_{\mathbf{k}_1+\mathbf{q},\sigma_1} = 0, \quad \text{if } |\mathbf{k}_1 + \mathbf{q}| > k_F. \tag{2.59}$$

Following this argumentation, it is easy to find that there are only two possibilities giving a finite contribution to the sums in Eq. (2.57):

i) $\mathbf{k}_1 + \mathbf{q} = \mathbf{k}_1$ and $\mathbf{k}_2 - \mathbf{q} = \mathbf{k}_2$ (direct interaction)

ii) $\mathbf{k}_1 + \mathbf{q} = \mathbf{k}_2$, with $\sigma_1 = \sigma_2$ (exchange interaction),

which are represented pictorially in Fig. 2.5. Note that the direct interaction implies $\mathbf{q} = 0$, so we do not need to consider it[16]. From the remaining term:

$$E^{(1)} = \frac{1}{2\mathcal{V}}\sum_{\mathbf{k},\sigma}\sum_{\mathbf{q}\neq 0}\frac{4\pi e^2}{q^2}\left\langle\hat{c}^\dagger_{\mathbf{k}+\mathbf{q},\sigma}\hat{c}^\dagger_{\mathbf{k},\sigma}\hat{c}_{\mathbf{k}+\mathbf{q},\sigma}\hat{c}_{\mathbf{k},\sigma}\right\rangle = -\frac{1}{2\mathcal{V}}\sum_{\mathbf{k},\sigma}\sum_{\mathbf{q}\neq 0}\frac{4\pi e^2}{q^2}\left\langle\hat{n}_{\mathbf{k},\sigma}\hat{n}_{\mathbf{k}+\mathbf{q},\sigma}\right\rangle. \tag{2.60}$$

Note the minus sign[17]. Here we used the number operator $\hat{n}_{\mathbf{k},\sigma} = \hat{c}^\dagger_{\mathbf{k},\sigma}\hat{c}_{\mathbf{k},\sigma}$, cf. Eq. (1.19). In this case, we can replace them by Heaviside step functions: $\langle\Psi_0|\hat{n}_{\mathbf{k},\sigma}|\Psi_0\rangle = \Theta(k_F - |\mathbf{k}|)$, with the spin degree of freedom being summed up to two:

$$E^{(1)} = -\frac{4\pi e^2}{\mathcal{V}}\sum_{\mathbf{k}}\sum_{\mathbf{q}\neq 0}\frac{1}{q^2}\Theta(k_F - |\mathbf{k}|)\Theta(k_F - |\mathbf{k}+\mathbf{q}|) = -\frac{4\pi e^2}{\mathcal{V}}\left(\frac{\mathcal{V}}{8\pi^3}\right)^2\mathcal{I}. \tag{2.61}$$

In the last step, we have replaced the remaining sums by integrals, giving:

$$\mathcal{I} = \int d^3\mathbf{q}\frac{1}{q^2}\int d^3\mathbf{k}\Theta(k_F - |\mathbf{k}|)\Theta(k_F - |\mathbf{k}+\mathbf{q}|). \tag{2.62}$$

To calculate it, it is useful to make a geometrical interpretation, realizing that the Fermi spheres are actually spheres, and that for a given $\mathbf{q}$, the integral in $\mathbf{k}$ is nothing but the volume of their overlap. Furthermore, we notice that this overlap is twice the volume of the section of the sphere over a horizontal plane at $(k_x, k_y, q/2)$, as indicated by a shaded region in Fig. 2.6. We can write them in

[15] Why is the sum restricted to $\mathbf{q} \neq 0$?
[16] This will not the case in general, if the periodicity of the lattice is taken into account.
[17] We could have arrived to this result by using Eq. (1.53). Indeed, a similar calculation was done this way in Sec. 2.3.2.

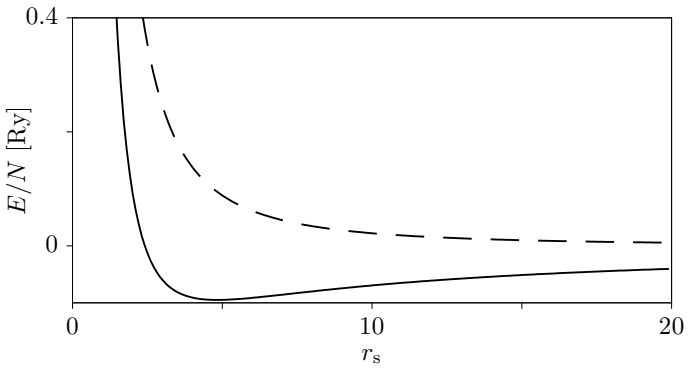

Figure 2.7.:
Perturbative correction of the energy per particle of a degenerate electron gas, $E=\left(E^{(0)}+E^{(1)}\right)/N$, according to Eq. (2.65), as a function of the dimensionless electron distance, r_s. The noninteracting case is shown with a dashed line, for comparison.

spherical[18] coordinates $(q, \theta_{\mathbf{q}}, \varphi_{\mathbf{q}})$ and $(k, \theta_{\mathbf{k}}, \varphi_{\mathbf{k}})$. Let us then fix $\mathbf{q}$, which is restricted by its modulus to $0 \leq q \leq 2k_{\mathrm{F}}$, and chose the zenith direction of the k-coordinates to be parallel to $\mathbf{q}$. Looking at Fig. 2.6, it is easy to fix the ranges of integration for the shaded region: $q/2 \leq k_{\mathrm{F}} \cos\varphi_{\mathbf{k}} \leq k_{\mathrm{F}}$, $q/2 \leq k\cos\varphi_{\mathbf{k}}$ and $0 \leq \theta_{\mathbf{k}} \leq 2\pi$. Integrating over all possible $\mathbf{q}$, we then have:

$$\mathcal{I} = 2\int_0^{2\pi} d\theta_{\mathbf{q}} \int_{-1}^{1} d\cos\varphi_{\mathbf{q}} \int_0^{2k_{\mathrm{F}}} dq q^2 \frac{1}{q^2} \int_0^{2\pi} d\theta_{\mathbf{k}} \int_{q/2k_{\mathrm{F}}}^{1} d\cos\varphi_{\mathbf{k}} \int_{q/2\cos\theta_{\mathbf{k}}}^{k_{\mathrm{F}}} dk k^2, \tag{2.63}$$

with the factor 2 accounting for the non-shaded region of the overlap. This integral can be easily performed, leading to the final result:

$$E^{(1)} = -\frac{e^2}{4\pi^3}\mathcal{V}k_{\mathrm{F}}^4. \tag{2.64}$$

Replacing $\mathcal{V} = N/\mathfrak{n}$, we get to:

$$\frac{E^{(0)} + E^{(0)}}{N} \approx \left(2.2r_s^{-2} - 0.9r_s^{-1}\right)\mathrm{Ry}. \tag{2.65}$$

This result is plotted in Fig. 2.7. Remarkably, it shows a minimum in the energy per particle at $r_s^*\approx 4.89$:

☞ the electron gas becomes stable thanks to the repulsive Coulomb interaction!

We can argue that the distance r_s^* is associated to the exchange interaction, i.e. it is a spin effect[19]. Note that, contrary to the direct term, the exchange interaction has no classical analogue.

2.4.2. Second order

We can open again our favourite book and find that the second order correction to the energy is given by:

$$E^{(2)} = \sum_{|\nu\rangle\neq|\Psi_0\rangle} \frac{\langle\Psi_0|\hat{H}_{\mathrm{e-e}}|\nu\rangle\langle\nu|\hat{H}_{\mathrm{e-e}}|\Psi_0\rangle}{E^{(0)} - E_\nu}, \tag{2.66}$$

where $|\nu\rangle$ are the possible excited states[20]. Using the same arguments as in the first order, we find that the term $\langle\nu|\hat{H}_{e-e}|\Psi_0\rangle$ makes two electrons with states $|\mathbf{k}_1,\sigma_1\rangle$ and $|\mathbf{k}_2,\sigma_2\rangle$ in the Fermi sphere (so $|\mathbf{k}_1|, |\mathbf{k}_2| < k_{\mathrm{F}}$) exchange a momentum $\hbar\mathbf{q}$, promoting them over the Fermi level, so $|\mathbf{k}_1+\mathbf{q}|, |\mathbf{k}_2-\mathbf{q}| > k_{\mathrm{F}}$. The other term, $\langle\Psi_0|\hat{H}_{\mathrm{e-e}}|\nu\rangle$, makes them interact again and recover the initial ground state.

[18] of course
[19] Another manifestation of the exchange hole discussed in Sec. 2.3.2.
[20] How is the ground state excited?

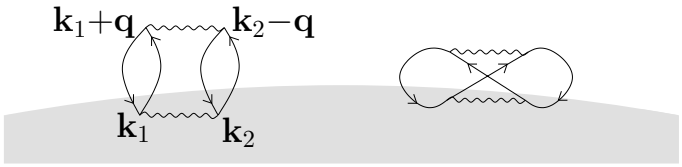

Figure 2.8.:
Diagrams contributing to the second order of the perturbative expansion.

This process can again occur in two different ways, a direct and a exchange interaction, which are represented in Fig. 2.8. As for the first order case, the exchange term imposes $\sigma_1 = \sigma_2$.

For our purposes here, we do not need to calculate the corresponding integrals. Even more, we will consider only the direct term, with the intermediate state[21]:

$$|\nu\rangle_{\rm dir} = \Theta(|\mathbf{k}_1+\mathbf{q}| - k_{\rm F})\Theta(|\mathbf{k}_2-\mathbf{q}| - k_{\rm F})\Theta(k_{\rm F} - |\mathbf{k}_1|)\Theta(k_{\rm F} - |\mathbf{k}_2|)\hat{c}^\dagger_{\mathbf{k}_1+\mathbf{q},\sigma_1}\hat{c}^\dagger_{\mathbf{k}_2-\mathbf{q},\sigma_2}\hat{c}_{\mathbf{k}_2,\sigma_2}\hat{c}_{\mathbf{k}_1,\sigma_1}|\Psi_0\rangle. \quad (2.67)$$

It gives the energy:

$$E^{(2)}_{\rm dir} = \frac{1}{\mathcal{V}^2}\sum_{\mathbf{q}}\sum_{\mathbf{k}_1,\mathbf{k}_2}\sum_{\sigma_1,\sigma_2}\frac{(V_{\mathbf{q}}/2)^2}{E^{(0)} - E_\nu}\Theta(|\mathbf{k}_1+\mathbf{q}| - k_{\rm F})\Theta(|\mathbf{k}_2-\mathbf{q}| - k_{\rm F})\Theta(k_{\rm F} - |\mathbf{k}_1|)\Theta(k_{\rm F} - |\mathbf{k}_2|). \quad (2.68)$$

Let us now consider the limit $\mathbf{q} \to 0$ and estimate the leading order contributions. Then,

$$(V_{\mathbf{q}})^2 \sim q^{-4} \quad (2.69)$$

$$E^{(0)} - E_\nu \sim \mathbf{k}_1^2 + \mathbf{k}_2^2 - (\mathbf{k}_1 + \mathbf{q})^2 - (\mathbf{k}_2 - \mathbf{q})^2 \sim \mathbf{q} + O(\mathbf{q}^2) \quad (2.70)$$

$$\sum_{\mathbf{k}_1}\Theta(|\mathbf{k}_1+\mathbf{q}| - k_{\rm F})\Theta(k_{\rm F} - |\mathbf{k}_1|) \sim q. \quad (2.71)$$

Then, when doing the necessary integral in $\mathbf{q}$:

$$E^{(2)}_{\rm dir} \sim \int dq q^2 \frac{1}{q^4}\frac{1}{q}qq = \int dq\frac{1}{q} = \ln \mathbf{q}, \quad (2.72)$$

i.e., it diverges! Not everything is lost, though. The divergence is *only* logarithmic. In order to cure it, one can regularize it by including contributions of higher order terms[22].

We get a more physical picture if we notice that using the Yukawa interaction (rather than the bare Coulomb one), the divergence disappears[23]. This emphasizes the important role of the long-range nature of the Coulomb interactions, and suggests that screening will be crucial. This issue will be discussed in the next chapter.

Bibliography

[2.1] A. Sommerfeld. Zur Elektronentheorie der Metalle auf Grund der Fermischen Statistik. *Z. Phys.*, 47(1):43–60, Jan 1928.

[2.2] W. Greiner, L. Neise, and H. Stöcker. *Thermodynamics and Statistical Mechanics*. Springer-Verlag, New York, NY, USA, 1995.

[21] How does the exchanged excitation look like?
[22] Far from the scope of this course!
[23] How?

[2.3] H. Bruus and K. Flensberg. *Many-Body Quantum Theory in Condensed Matter Physics*. Oxford University Press, Sep 2004.

[2.4] A. Altland and B. Simons. *Condensed Matter Field Theory*. Cambridge University Press, Cambridge, England, UK, Jun 2006.

[2.5] I. Shapir, A. Hamo, S. Pecker, C. P. Moca, Ö. Legeza, G. Zarand, and S. Ilani. Imaging the electronic Wigner crystal in one dimension. *Science*, 364(6443):870–875, May 2019.

[2.6] E. Wigner. On the Interaction of Electrons in Metals. *Phys. Rev.*, 46(11):1002–1011, Dec 1934.

[2.7] N. W. Ashcroft and N. D. Mermin. *Solid State Physics*. Brooks Cole, Jan 1976.

[2.8] L. D. Landau. The Theory of a Fermi Liquid. *Sov. Phys. JETP*, 3(6):920–925, Jan 1957.

Further reading

- ☞ H. Bruus and K. Flensberg, *Many-Body Quantum Theory in Condensed Matter Physics* (Oxford Univ. Press, Oxford, 2004)
- ☞ A. Altland and B. Simmons, *Condensed Matter Field Theory* (Cambridge Univ. Press, Cambridge, 2006)
- ☞ P. Phillips, *Advanced solid state physics* (Cambridge Univ. Press, 2012)
- ☞ G. D. Mahan, *Condensed matter in a nutshell* (Princeton Univ. Press, Princeton, 2010)

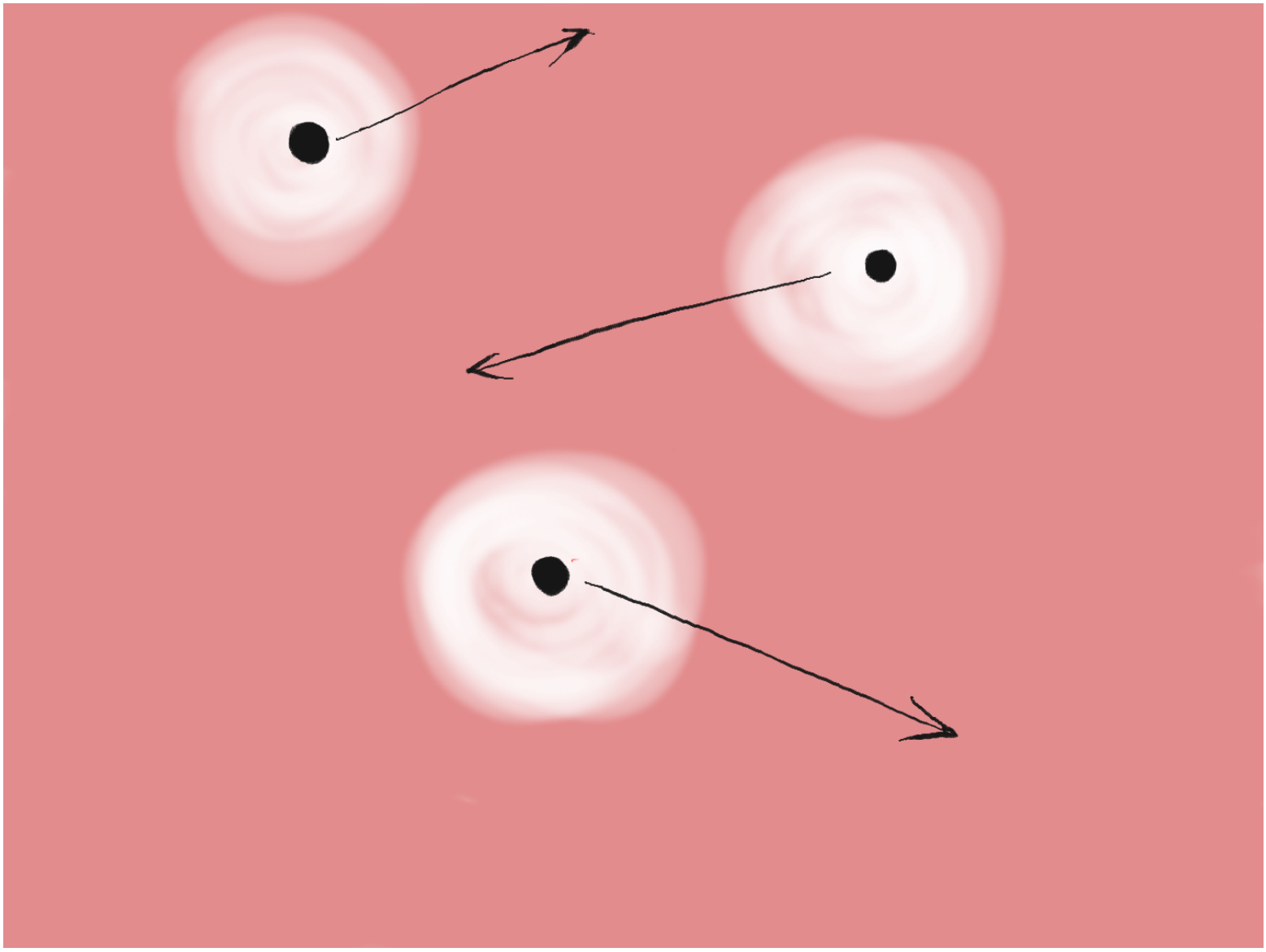

3. Mean field approaches. Hartree-Fock approximation

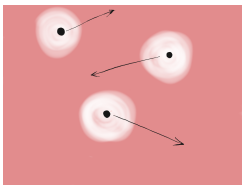

In the previous chapter, the perturbative treatment of the Coulomb interaction was introduced. We will now delve into this problem by connecting it to mean field approaches (very common in condensed matter theory), what is called as the Hartree-Fock approximation (also useful in atomic and molecular physics). We will particularize it to the jellium model. Again, issues related to the long-range character of the Coulomb interaction will show up. These are solved by taking screening effects into account properly.

3.1. Mean field approximations

Condensed matter systems are complicated for containing many degrees of freedom. Interactions between the many particles introduce correlations that make the problem difficult to solve but makes its physics very rich: Very similar systems (or even the same system in different configurations, e.g., at different temperatures) can show very different behaviours, However, not all of these correlations are always relevant for all observables. The interest is then to identify what particles and what interactions play a role in the physical phenomena of interest and be able to obtain a sufficiently general model that provides a good understanding of the underlying physics and a description of the important effects. Quite often, this leads to new concepts that would be hidden in a (if possible) exact description of the whole system.

A way to do this is to consider that the correlations between particles (of the same or of different types) generated by their interaction can be neglected[1]. The interaction then occurs between each particle and an average (a mean field) of all the others.

Following Ref. [3.1], we show this with a simple example consisting on a system with two ensembles of particles (described by creation operators $\hat{a}^\dagger_\alpha$ and $\hat{b}^\dagger_\beta$) that interact[2]. The microscopic hamiltonian is $\hat{H} = \hat{H}_\mathrm{A} + \hat{H}_\mathrm{B} + \hat{H}_\mathrm{AB}$, where

$$\hat{H}_\mathrm{A} = \sum_\alpha \varepsilon^A_\alpha \hat{a}^\dagger_\alpha \hat{a}_{\alpha'} \quad \text{and} \quad \hat{H}_\mathrm{B} = \sum_\beta \varepsilon^B_\beta \hat{b}^\dagger_\beta \hat{b}_{\beta'} \tag{3.1}$$

describe the non-interacting free particles, with their interaction being

$$\hat{H}_\mathrm{AB} = \sum_{\alpha\alpha',\beta\beta'} V_{\alpha\beta\alpha'\beta'} \hat{a}^\dagger_\alpha \hat{b}^\dagger_\beta \hat{b}_{\beta'} \hat{a}_{\alpha'}. \tag{3.2}$$

The mean field approximation assumes that each particle interacts with an average of the others. This can be justified by the deviation operators:

$$\hat{d}^A_{\alpha\alpha'} = \hat{a}^\dagger_\alpha \hat{a}_{\alpha'} - \left\langle \hat{a}^\dagger_\alpha \hat{a}_{\alpha'} \right\rangle \quad \text{and} \quad \hat{d}^B_{\beta\beta'} = \hat{b}^\dagger_\beta \hat{b}_{\beta'} - \left\langle \hat{b}^\dagger_\beta \hat{b}_{\beta'} \right\rangle \tag{3.3}$$

[1] Two observables, $\mathcal{A}$ and $\mathcal{B}$, are correlated if $\langle \mathcal{A}\mathcal{B} \rangle \neq \langle \mathcal{A} \rangle \langle \mathcal{B} \rangle$.

[2] Can you think of an example where both types of particles are electrons?

giving small expected values. Then, one approximates $\hat{d}^A_{\alpha\alpha'}\hat{d}^B_{\beta\beta'} \approx 0$, such that the interaction term becomes:

$$\hat{H}_{\mathrm{AB}} \approx \sum_{\alpha\alpha',\beta\beta'} V_{\alpha\beta\alpha'\beta'} \left(\hat{a}^\dagger_\alpha \hat{a}_{\alpha'} \left\langle \hat{b}^\dagger_\beta \hat{b}_{\beta'} \right\rangle + \hat{b}^\dagger_\beta \hat{b}_{\beta'} \left\langle \hat{a}^\dagger_\alpha \hat{a}_{\alpha'} \right\rangle - \left\langle \hat{a}^\dagger_\alpha \hat{a}_{\alpha'} \right\rangle \left\langle \hat{b}^\dagger_\beta \hat{b}_{\beta'} \right\rangle \right), \tag{3.4}$$

in the form of two single-particle hamiltonians. We can then write $\hat{H} \approx \hat{H}_{\mathrm{MF}}$, with

$$\hat{H}_{\mathrm{MF}} = \sum_{\alpha\alpha'} \tilde{\varepsilon}^A_{\alpha\alpha'} \hat{a}^\dagger_\alpha \hat{a}_{\alpha'} + \sum_{\beta\beta'} \tilde{\varepsilon}^B_{\beta\beta'} \hat{b}^\dagger_\beta \hat{b}_{\beta'} + E_0, \tag{3.5}$$

where E_0 only contains products of averages. $\hat{H}_{\mathrm{MF}}$ could be easily solved, were not the coefficients $\tilde{\epsilon}^A_{\alpha\alpha'}$ and $\tilde{\epsilon}^B_{\beta\beta'}$ depend on the other particle averages:

$$\tilde{\epsilon}^A_{\alpha\alpha'} = \varepsilon^A_\alpha \delta_{\alpha\alpha'} + \sum_{\beta\beta'} V_{\alpha\beta\alpha'\beta'} \langle \hat{b}^\dagger_\beta \hat{b}_{\beta'} \rangle \tag{3.6}$$

$$\tilde{\epsilon}^B_{\beta\beta'} = \varepsilon^B_\beta \delta_{\beta\beta'} + \sum_{\alpha\alpha'} V_{\alpha\beta\alpha'\beta'} \langle \hat{a}^\dagger_\alpha \hat{a}_{\alpha'} \rangle, \tag{3.7}$$

so they cannot be solved separately[3]. The problem is then reduced to calculating the averages $\langle \hat{a}^\dagger_\alpha \hat{a}_{\alpha'} \rangle$ and $\langle \hat{b}^\dagger_\beta \hat{b}_{\beta'} \rangle$, which is usually done in a *self-consistent* manner: one solves the system iteratively by using the result of the previous step, starting by solving the uncoupled systems. This is then repeated until the solution converges appropriately.

3.2. Hartree-Fock approximation

Let us apply these ideas to the system of interacting electrons described by the hamiltonian

$$\hat{H} = \hat{H}_0 + \hat{H}_{\mathrm{e-e}} = \sum_{mn} h^{(0)}_{mn} \hat{c}^\dagger_m \hat{c}_n + \frac{1}{2} \sum_{mnlp} h^{\mathrm{e-e}}_{mn,pl} \hat{c}^\dagger_m \hat{c}^\dagger_n \hat{c}_l \hat{c}_p, \tag{3.8}$$

with the coefficients $h^{(0)}_{mn}$ and $h^{\mathrm{e-e}}_{mn,pl}$ obtained from the elements of the single and two-particle operators

$$\hat{h}^{(0)} = -\frac{\hbar^2}{2m} \nabla^2_{\mathbf{r}} + V_{\mathrm{el-ion}}(\mathbf{r}) \qquad \text{and} \qquad \hat{h}^{\mathrm{e-e}} = \frac{e^2}{|\mathbf{r} - \mathbf{r}'|}. \tag{3.9}$$

according to Eqs. (1.5) and (1.49), respectively. For simplicity, we use a compressed notation where the indices m, n, l and p include orbital and spin degrees of freedom[4]. The spin will be made explicit only when it plays a role. Note however, that $\sigma_m = \sigma_p$ and $\sigma_n = \sigma_l$.

The main approximation consists on assuming that the ground state is not affected by electron-electron interactions:

$$|\Psi_0\rangle = \prod_n \hat{c}^\dagger_n |0\rangle. \tag{3.10}$$

With this, we evaluate the energy:

$$\left\langle \hat{H} \right\rangle = \left\langle \Psi_0 \left| \hat{H} \right| \Psi_0 \right\rangle. \tag{3.11}$$

[3] Note that $\tilde{\varepsilon}^A_{\alpha\alpha'}$ and $\tilde{\varepsilon}^B_{\beta\beta'}$ are not diagonal.

[4] Please, do not confuse the index m with the mass of the electron!

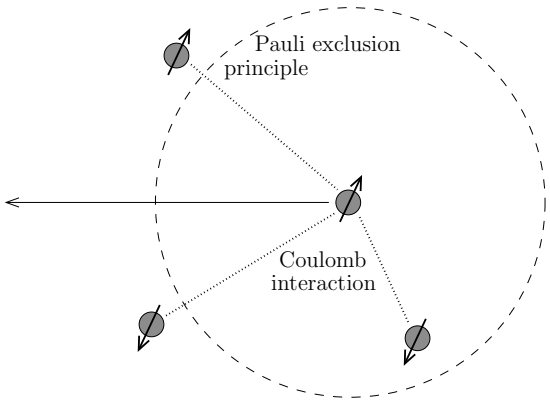

Figure 3.1.:
Exchange hole: correlations originated from the Pauli exclusion principle keep electrons with parallel spins separated (represented by the dashed circle). Hence, their Coulomb interaction will on average be smaller than that between electrons with antiparallel spins.

We need to evaluate two types of expectation values (see Sec. 1.3.1):

$$\left\langle \hat{c}_m^\dagger \hat{c}_p \right\rangle = \langle \hat{n}_m \rangle \, \delta_{mp} \tag{3.12}$$

$$\left\langle \hat{c}_m^\dagger \hat{c}_n^\dagger \hat{c}_l \hat{c}_p \right\rangle = \left\langle \hat{c}_m^\dagger \hat{c}_p \right\rangle \left\langle \hat{c}_n^\dagger \hat{c}_l \right\rangle - \left\langle \hat{c}_m^\dagger \hat{c}_l \right\rangle \left\langle \hat{c}_n^\dagger \hat{c}_p \right\rangle = \langle \hat{n}_m \rangle \langle \hat{n}_n \rangle \, (\delta_{mp}\delta_{nl} - \delta_{np}\delta_{ml}), \tag{3.13}$$

where $\hat{n}_m = \hat{c}_m^\dagger \hat{c}_m$ is the number operator. The result in Eq. (3.13) can be obtained by a direct application of Wick's theorem or from simple commutation relations (left as an exercise, it should take two lines). The first term in the right hand side corresponds to the direct interaction of two electrons sitting in states $|m\rangle$ and $|m\rangle$. The second term, describes the exchange interaction and will be finite provided the two electrons have the same spin. We then arrive at:

$$\langle \hat{H}_0 \rangle = \sum_m h^{(0)}_{mm} \langle \hat{n}_m \rangle, \qquad \text{and} \qquad \langle \hat{H}_{\text{e-e}} \rangle = \frac{1}{2} \sum_{mn} (U_{mn} - J_{mn}\delta_{\sigma_m \sigma_n}) \, (1 - \delta_{mn}) \langle \hat{n}_m \rangle \langle \hat{n}_n \rangle, \tag{3.14}$$

with the direct (Hartree) and exchange (Fock) contributions given by $U_{mn} = h^{\text{e-e}}_{mn,mn}$ and $J_{mn} = h^{\text{e-e}}_{mn,nm}$, respectively. From the definition of J_{mn} it should become clear where it is actually called exchange. From Eq. (3.14) we learn that contribution to the Coulomb interaction is smaller between electrons with the same spin (a ferromagnetic contribution). This is due to the Pauli exclusion principle which avoids electrons with the same spin to be nearby, what is known as the *exchange hole*[5], as represented in Fig. 3.1.[6] The total Hartree-Fock energy is hence:

$$E_{\text{HF}} = \left\langle \hat{H}_0 \right\rangle + \frac{1}{2} \sum_{mn} (U_{mn} - J_{mn}\delta_{\sigma_m \sigma_n}) \, (1 - \delta_{mn}) \langle \hat{n}_m \rangle \langle \hat{n}_n \rangle. \tag{3.15}$$

We still need to obtain the wavefunctions $\psi_\nu(\mathbf{r})$. For this, we take a variational approach by minimizing E_{HF} under the condition that the wave function is normalized, i.e., $\int d^3\mathbf{r} |\psi_\nu(\mathbf{r})|^2 = 1$. This is done by introducing Lagrange multipliers (see e.g., Ref. [3.3]):

$$\tilde{E}_{\text{HF}} = E_{\text{HF}} - \sum_\nu \varepsilon_\nu \left(\int d^3\mathbf{r} \, |\psi_\nu(\mathbf{r})|^2 - 1 \right). \tag{3.16}$$

We now minimize the functional $\tilde{E}_{\text{HF}}(\psi_\nu)$ by taking the functional derivative and solving:

$$\frac{\delta \tilde{E}_{\text{HF}}}{\delta \psi^*_\nu(\mathbf{r})} = 0. \tag{3.17}$$

[5] Sounds familiar?
[6] A detailed discussion of this point is given in Ref. [3.2].

It takes a few lines, but there is nothing really complicated in getting to the self-consistent Hartree-Fock equations (by using the integral definitions of U_{mn} and J_{mn} given by Eq. (1.49)):

$$\varepsilon_m \psi_m(\mathbf{r}) = \hat{h}^{(0)}(\mathbf{r})\psi_m(\mathbf{r}) + \sum_{n\neq m} \int d^3\mathbf{r}' \frac{e^2}{|\mathbf{r}-\mathbf{r}'|} \left(\left|\psi_n(\mathbf{r}')\right|^2 \psi_m(\mathbf{r}) - \delta_{\sigma_m\sigma_n} \psi_n^*(\mathbf{r}')\psi_m(\mathbf{r}')\psi_n(\mathbf{r}) \right). \tag{3.18}$$

Each equation includes the wavefunctions corresponding to all the (many) *occupied* states, so a complete solution becomes intractable. However, they can be solved iteratively (self-consistently) as described at the end of Sec. 3.1.

☞ The dependence of the wavefunction $\psi_m(\mathbf{r})$ on all other occupied states introduces the notion of *quasiparticles*.

3.2.1. Interpretation

We do not want to solve Eqs. (3.18) here. However, they are not useless. If we multiply it by $\psi_m^*(\mathbf{r})$ and integrate, we get to the expression for the energies:

$$\varepsilon_m = h_{mm}^{(0)} \psi_m(\mathbf{r}) + \sum_n \left(U_{mn} - J_{mn}\delta_{\sigma_m\sigma_n}\right) \langle \hat{n}_n \rangle, \tag{3.19}$$

which relate to the total energy as:

$$E_{\mathrm{HF}} = \sum_m \varepsilon_m \langle \hat{n}_m \rangle - \frac{1}{2} \sum_{m,n} \left(U_{mn} - J_{mn}\delta_{\sigma_m\sigma_n}\right)(1-\delta_{mn}) \langle \hat{n}_m \rangle \langle \hat{n}_n \rangle. \tag{3.20}$$

Hence, we can argue that the energy ε_m does not correspond to the energy of a single particle in state $|m\rangle$ but rather includes the interaction with all other particles. In the same way, E_{HF} is not the sum of the single-particle energies. However, by inspecting Eq. (3.15) we notice that the energy of the highest occupied orbital, ε_{m_N}, is:

$$\varepsilon_{m_N} \approx E_{\mathrm{HF}}^N - E_{\mathrm{HF}}^{N-1}, \tag{3.21}$$

i.e., it corresponds to the minimal energy needed to add a quasiparticle to the system[7,8]. This is known as Koopmans' theorem [3.4].

3.3. Hartree-Fock for the jellium model

We apply now this approximation to the jellium model introduced in Sec. 2.3. In this case, we use

$$\hat{H}_{\mathrm{e-e}} = \frac{1}{2\mathcal{V}} \sum_{\mathbf{k}_1\mathbf{k}_2} \sum_{\sigma_1\sigma_2} \sum_{\mathbf{q}\neq 0} V_{\mathbf{q}} \hat{c}^\dagger_{\mathbf{k}_1+\mathbf{q},\sigma_1} \hat{c}^\dagger_{\mathbf{k}_2-\mathbf{q},\sigma_2} \hat{c}_{\mathbf{k}_2,\sigma_2} \hat{c}_{\mathbf{k}_1,\sigma_1}. \tag{3.22}$$

The first step is to take its expectation value with the noninteracting Fermi sphere using Eq. (3.13):

$$\left\langle \hat{c}^\dagger_{\mathbf{k}_1+\mathbf{q},\sigma_1} \hat{c}^\dagger_{\mathbf{k}_2-\mathbf{q},\sigma_2} \hat{c}_{\mathbf{k}_2,\sigma_2} \hat{c}_{\mathbf{k}_1,\sigma_1} \right\rangle = \left\langle \hat{n}_{\mathbf{k}_1,\sigma_1} \right\rangle \left\langle \hat{n}_{\mathbf{k}_2,\sigma_2} \right\rangle \left(\delta_{\mathbf{q},\mathbf{0}} - \delta_{\mathbf{k}_1+\mathbf{q},\mathbf{k}_2} \delta_{\sigma_1,\sigma_2} \right). \tag{3.23}$$

Once more, these two terms correspond to the direct and exchange contributions. Again, the direct term, proportional to $\delta_{\mathbf{q},0}$, is excluded from the sum in Eq. (3.22), so we get:

$$\left\langle \hat{H}_{\mathrm{e-e}} \right\rangle = -\frac{1}{2\mathcal{V}} \sum_{\mathbf{k},\sigma} \sum_{\mathbf{q}\neq 0} V_{\mathbf{q}} \left\langle \hat{n}_{\mathbf{k},\sigma} \right\rangle \left\langle \hat{n}_{\mathbf{k}+\mathbf{q},\sigma} \right\rangle. \tag{3.24}$$

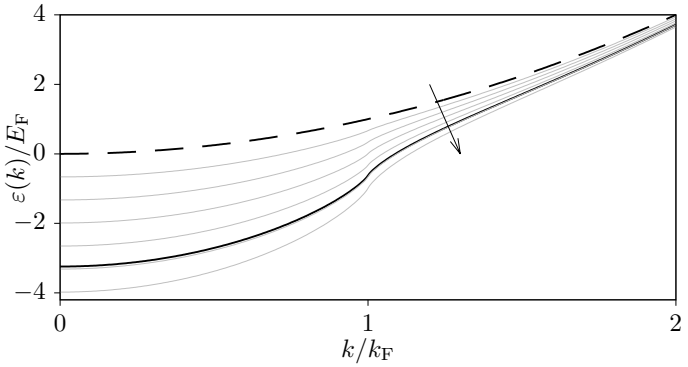

Figure 3.2.:
Hartree-Fock dispersion relation for the jellium model. The arrow points the increase of the dimensionless electron distance from $r_s = 1$ to $r_s = 6$, plotted with gray lines. In black are the free-electron (dashed) and $r_s^* = 4.89$ (solid line) cases.

The Hartree-Fock equations have the form[9]:

$$-\frac{\hbar^2}{2m}\nabla^2_{\mathbf{r}}\psi_{\mathbf{k},\sigma}(\mathbf{r}) - \sum_{\mathbf{k}'\neq\mathbf{k}}\int d^3\mathbf{r}'\psi^*_{\mathbf{k}',\sigma}(\mathbf{r}')\psi_{\mathbf{k},\sigma}(\mathbf{r}')\frac{e^2}{|\mathbf{r}-\mathbf{r}'|}\psi_{\mathbf{k}',\sigma}(\mathbf{r}) = \varepsilon_{\mathbf{k},\sigma}\psi_{\mathbf{k},\sigma}(\mathbf{r}). \tag{3.25}$$

Solving them is easier than expected: It turns out that the plane waves are eigenstates of the previous equation (you can just check it), with the eigenenergies:

$$\varepsilon_{\mathbf{k},\sigma} = \frac{\hbar^2|\mathbf{k}|^2}{2m} - \frac{e^2}{\mathcal{V}}\sum_{\mathbf{k}'\neq\mathbf{k}}\int d^3\mathbf{r}'\frac{e^{i\mathbf{k}(\mathbf{r}-\mathbf{r}')}e^{i\mathbf{k}'(\mathbf{r}'-\mathbf{r})}}{|\mathbf{r}-\mathbf{r}'|}. \tag{3.26}$$

Transforming the sum into an integral and using the Fourier transform of the Coulomb interaction, cf. Eq. (1.65), we get:

$$\varepsilon(\mathbf{k},\sigma) = \frac{\hbar^2|\mathbf{k}|^2}{2m} - e^2\int_0^{k_F}\frac{d^3\mathbf{k}}{(2\pi)^3}\frac{4\pi}{(\mathbf{k}-\mathbf{k}')^2}. \tag{3.27}$$

The remaining integral can be performed invoking a book of tables[10]. In a few lines, we arrive to the dispersion relation:

$$\varepsilon(\mathbf{k},\sigma) = \frac{\hbar^2|\mathbf{k}|^2}{2m} - \frac{e^2k_F}{\pi}\left(1 + \frac{k_F^2-|\mathbf{k}|^2}{2|\mathbf{k}|k_F}\ln\left|\frac{k_F+|\mathbf{k}|}{k_F-|\mathbf{k}|}\right|\right), \tag{3.28}$$

which is plotted in Fig. 3.2 for different distances r_s.

We gain more insight by rewriting the exchange term as

$$\varepsilon_x(k) = -\frac{2e^2k_F}{\pi}F\left(\frac{k}{k_F}\right), \quad \text{with} \quad F(y) = \frac{1}{2} + \frac{1-y^2}{4y}\ln\left|\frac{1+y}{1-y}\right|. \tag{3.29}$$

Note that $\varepsilon_x(k) < 0$, if $k < k_F$. In particular, $F(y) \to 1/2$, when $y \to 0$ gives $\varepsilon_x(0) = -e^2k_F/\pi$. As $k_F \propto 1/r_s$, the exchange hole will be *deeper* when the electron density increases. At the Fermi level,

[7] Why is Eq. (3.21) approximate and not an identity?

[8] Can a similar expression obtained for the energy required to remove one particle? Does the initial state of that particle play any role?

[9] Compare them with Eq. (3.18)

[10]
$$\int dx\frac{1}{1-ax} = -\frac{1}{a}\ln|1-ax| \qquad \text{and} \qquad \int dx\, x\ln|x+a| = \frac{x^2-a^2}{2}\ln|x+a| - \frac{1}{4}(x-a)^2$$

$y = 1$, we have $F(1) = 1/2$, giving $\varepsilon_x(k_F) = -e^2 k_F/\pi$.[11] However by inspecting the derivative:

$$\left.\frac{dF(y)}{dy}\right|_{y=1} \approx \frac{1}{2}\ln\left|\frac{1-y}{2}\right|, \tag{3.30}$$

we find that it diverges! We understand the consequences of this divergence by noticing that it gives a vanishing density of states[12] at the Fermi energy, which is unphysical[13]:

$$\upsilon(\varepsilon_F) \to 0. \tag{3.31}$$

This would imply for instance that transport coefficients (which depend on the density of states at the Fermi energy) vanish[14].

This pathological behaviour is related to the one in the perturbative expansion in chapter 2, due to the long-ranged electron-electron interaction. As in that case, it is simple to show that a screened Coulomb interaction (Yukawa) circumvents this problem. How to treat screening properly is the subject of the following section.

3.4. Screening

3.4.1. Brief reminder

A charge in a polarizable media attracts opposite charges, inducing a charge distribution around it that *screens* it. Classically, the potential generated by an external charge distribution, ϱ_{ext}, and the induced charge, ϱ_{ind} is given by the (Fourier transformed) Poisson equation[15]:

$$q^2\phi(\mathbf{q}) = 4\pi[\varrho_{ext}(\mathbf{q}) + \varrho_{ind}(\mathbf{q})]. \tag{3.32}$$

Writing $q^2\phi_{ext}(\mathbf{q}) = 4\pi\varrho_{ext}(\mathbf{q})$, and introducing the susceptibility $\chi(\mathbf{q})$ that relates $\varrho_{ind} = \chi(\mathbf{q})\phi(\mathbf{q})$, we arrive at:

$$\phi(\mathbf{q}) = \left[1 - \frac{4\pi}{q^2}\chi(\mathbf{q})\right]^{-1}\phi_{ext}(\mathbf{q}). \tag{3.33}$$

From this equation, we relate the susceptibility and the dielectric constant:

$$\epsilon(\mathbf{q}) = 1 - \frac{4\pi}{q^2}\chi(\mathbf{q}). \tag{3.34}$$

[11] Rewriting it as $\varepsilon_x(k_F) = -2e^2/\lambda_F$ suggests that the diameter of the exchange hole is the Fermi wavelength.

[12] Recovering the expression for the number of states, Eq. (2.5), we get for the density of states:

$$\upsilon(\varepsilon_k) = \frac{k^2}{\pi^2}\left(\frac{d\varepsilon_k}{dk}\right)^{-1}.$$

The same result is obtained by defining $\upsilon(E) = \sum_{\mathbf{k},\sigma}\delta(E - \varepsilon_{\mathbf{k}})$.

[13] Another version of the same problem is that the effective mass of electrons at the Fermi energy, defined from

$$\frac{1}{m^*} = \frac{1}{\hbar^2 k_F}\left.\frac{\partial\varepsilon(k)}{\partial k}\right|_{k=k_F},$$

gives $m^* = 0$.

[14] J. Bardeen [*Electron exchange in the theory of metals*, Phys. Rev. **50**, 1098 (1936)] showed that this result leads to a specific heat proportional to $c_V \sim -T/\ln T$ when $T \to 0$, which deviates from the experimental observations. Is this result consistent at finite temperature?

[15] Notation: the density ϱ has units of charge per volume; not to confuse with the density operator $\hat{\rho}$. For the same reason, we will below use $\mathfrak{n}$ for the electron density (per unit volume).

The question is now how to calculate $\chi(\mathbf{q})$, for which one usually needs to invoke the appropriate approximations. The most typical are: (i) Thomas-Fermi approximation (semiclassical limit of the Hartree interaction), and (ii) Lindhard or random-phase approximation (which we will treat below).

Thomas-Fermi semiclassical approximation

This approximation assumes that the electrons move freely in a potential that varies smoothly along distances much larger than the electron wavelength: $\Delta r \sim \hbar/\Delta k \gg \lambda$. The electron energy is then

$$\varepsilon(\mathbf{k}) = \frac{\hbar^2 k^2}{2m} - e\phi(\mathbf{r}). \tag{3.35}$$

The electron density can be approximated by:

$$\mathfrak{n}(\mathbf{r}) = \frac{1}{4\pi^3}\int d^3\mathbf{k} f(\varepsilon(\mathbf{k}) - \mu), \tag{3.36}$$

in terms of the Fermi distribution. The induced charge density is then:

$$\varrho_{\text{ind}}(\mathbf{r}) = -e[\mathfrak{n}(\mathbf{r}) - \mathfrak{n}_0(\mu)], \tag{3.37}$$

where $\mathfrak{n}_0$ is the density without the external charge (obtained by making $\phi = 0$ in Eq. (3.36)). We can linearize it $\mathfrak{n}(\mathbf{r}) \approx \mathfrak{n}_0(\mu) + e\phi(\mathbf{r})\partial\mathfrak{n}_0/\partial\mu$, so after simplifying and Fourier-transforming, we obtain the susceptibility

$$\chi(\mathbf{q}) = -e^2\frac{\partial\mathfrak{n}_0}{\partial\mu}. \tag{3.38}$$

Defining the Thomas-Fermi wavenumber from $k_{\text{TF}}^2 = 4\pi e^2\partial\mathfrak{n}_0/\partial\mu$, the dielectric constant reads[16]:

$$\epsilon_{\text{TF}} = 1 + \frac{k_{\text{TF}}^2}{q^2}, \tag{3.39}$$

which gives the screened potential[17]

$$\phi(\mathbf{q}) = \phi_{\text{ext}}(\mathbf{q})\frac{q^2}{q^2 + k_{\text{TF}}^2}. \tag{3.40}$$

3.4.2. Quantum treatment: linear response to a potential

We want to see how the charge distribution of a gas of (free) electrons changes when it is in the presence of an external potential, $U_{\text{ext}}(\mathbf{r}, t)$. In general, the potential can be time dependent, giving a hamiltonian:

$$\hat{H}(t) = \hat{H}_0 + \hat{H}_U(t) = \sum_{\mathbf{k},\sigma}\varepsilon_{\mathbf{k}\sigma}\hat{c}^\dagger_{\mathbf{k}\sigma}\hat{c}_{\mathbf{k}\sigma} + \sum_{\mathbf{k},\mathbf{k}'}\sum_{\sigma}\left(\frac{1}{\mathcal{V}}\int d^3\mathbf{r}\mathrm{e}^{-i\mathbf{k}'\mathbf{r}}U_{\text{ext}}(\mathbf{r}, t)\mathrm{e}^{i\mathbf{k}\mathbf{r}}\right)\hat{c}^\dagger_{\mathbf{k}'\sigma}\hat{c}_{\mathbf{k}\sigma}, \tag{3.41}$$

where we have considered the planewave basis, and $\varepsilon_{\mathbf{k}\sigma}$ are the free-electron energies. We assume that the external potential is periodic in space and time, allowing for a Fourier decomposition, of which we

[16] We can estimate k_{TF} by approximating $\partial\mathfrak{n}_0/\partial\mu$ by the density of states at the Fermi energy (exercise).
[17] In the case that the potential is caused by a charge e, $\phi_{\text{ext}}(\mathbf{q}) = e/q^2$, we get the Yukawa potential $\phi(\mathbf{q}) = e(q^2 + k_{\text{TF}}^2)^{-1}$.

are interested only in the component corresponding to the potential characteristic vector $\mathbf{q}'$ and a single oscillatory frequency ω (for simplicity). Hence:

$$U_{\text{ext}}(\mathbf{r},t) = U_{\text{ext}}(\mathbf{q}',\omega)\mathrm{e}^{i(\mathbf{q}'\mathbf{r}-\omega t)}\mathrm{e}^{\eta t} + \text{h.c.}, \tag{3.42}$$

The small parameter $\eta \to 0^+$ warranties the adiabatic switching of the potential at $t = 0$. Therefore:

$$\hat{H}_U(t) = \sum_{\mathbf{k},\sigma}\left(U_{\text{ext}}(\mathbf{q}',\omega)\mathrm{e}^{-i\omega t}\mathrm{e}^{\eta t}\hat{c}^\dagger_{\mathbf{k}\sigma}\hat{c}_{\mathbf{k}+\mathbf{q},\sigma} + U^*_{\text{ext}}(\mathbf{q}',\omega)\mathrm{e}^{i\omega t}\mathrm{e}^{\eta t}\hat{c}^\dagger_{\mathbf{k}\sigma}\hat{c}_{\mathbf{k}-\mathbf{q},\sigma}\right). \tag{3.43}$$

The charge distribution is given by the density operator[18], which in reciprocal space reads:

$$\hat{\rho}_{\mathbf{q}} = \sum_{\mathbf{k},\sigma}\hat{c}^\dagger_{\mathbf{k}\sigma}\hat{c}_{\mathbf{k}+\mathbf{q},\sigma} = \sum_{\mathbf{k},\sigma}\hat{n}_{\mathbf{k}\mathbf{q}\sigma}, \tag{3.44}$$

where the operator $\hat{n}_{\mathbf{k}\mathbf{q}\sigma}$ generalizes the number operator, cf. Eq. (1.19) (recovering it for $\mathbf{q} = 0$).

The dynamic response is given by the Heisenberg equation of motion applied to the density operator:

$$i\hbar\frac{d}{dt}\hat{n}_{\mathbf{k}\mathbf{q}\sigma} = [\hat{n}_{\mathbf{k}\mathbf{q}\sigma},\hat{H}(t)] = [\hat{n}_{\mathbf{k}\mathbf{q}\sigma},\hat{H}_0] + [\hat{n}_{\mathbf{k}\mathbf{q}\sigma},\hat{H}_U(t)]. \tag{3.45}$$

We will need to compute the averages:

$$\left\langle i\hbar\frac{d}{dt}\hat{n}_{\mathbf{k}\mathbf{q}\sigma}\right\rangle = \underbrace{\left\langle[\hat{n}_{\mathbf{k}\mathbf{q}\sigma},\hat{H}_0]\right\rangle}_{(r1)} + \underbrace{\left\langle[\hat{n}_{\mathbf{k}\mathbf{q}\sigma},\hat{H}_U(t)]\right\rangle}_{(r2)}. \tag{3.46}$$

Let us go step by step and calculate the different terms separately. The algebra simplifies considerably knowing that

$$[\hat{c}^\dagger_\mu\hat{c}_{\mu'},\hat{c}^\dagger_\nu\hat{c}_{\nu'}] = \hat{c}^\dagger_\mu\hat{c}_{\nu'}\delta_{\mu'\nu} - \hat{c}^\dagger_\nu\hat{c}_{\mu'}\delta_{\mu\nu'}. \tag{3.47}$$

$(r1)$ This term is easy to calculate using Eq. (3.47), yielding:

$$\left\langle[\hat{n}_{\mathbf{k}\mathbf{q}\sigma},\hat{H}_0]\right\rangle = (\varepsilon_{\mathbf{k}+\mathbf{q},\sigma} - \varepsilon_{\mathbf{k}\sigma})\left\langle\hat{n}_{\mathbf{k}\mathbf{q}\sigma}\right\rangle. \tag{3.48}$$

$(r2)$ Again using Eq. (3.47), the second term results in:

$$\begin{aligned}\left\langle[\hat{n}_{\mathbf{k}\mathbf{q}\sigma},\hat{H}_U(t)]\right\rangle =& U_{\text{ext}}(\mathbf{q}',\omega)\mathrm{e}^{-i\omega t}\mathrm{e}^{\eta t}\left(\left\langle\hat{c}^\dagger_{\mathbf{k}\sigma}\hat{c}_{\mathbf{k}+\mathbf{q}-\mathbf{q}',\sigma}\right\rangle - \left\langle\hat{c}^\dagger_{\mathbf{k}+\mathbf{q}',\sigma}\hat{c}_{\mathbf{k}+\mathbf{q},\sigma}\right\rangle\right)\\ &+ U^*_{\text{ext}}(\mathbf{q}',\omega)\mathrm{e}^{i\omega t}\mathrm{e}^{\eta t}\left(\left\langle\hat{c}^\dagger_{\mathbf{k}\sigma}\hat{c}_{\mathbf{k}+\mathbf{q}+\mathbf{q}',\sigma}\right\rangle - \left\langle\hat{c}^\dagger_{\mathbf{k}-\mathbf{q}',\sigma}\hat{c}_{\mathbf{k}+\mathbf{q},\sigma}\right\rangle\right).\end{aligned} \tag{3.49}$$

Note that the terms within brackets in the right-hand side couple the time evolution of $\left\langle\hat{n}_{\mathbf{k}\mathbf{q}\sigma}\right\rangle$ with other contributions[19] which may in principle also depend on time. Therefore, our problem results in a system of coupled differential equations. We are interested in the linear response, for which it is sufficient to assume that the only time dependence in Eq. (3.49) is the one explicitly introduced by the potential. Henceforth, the other contributions are considered as stationary coefficients, which we can evaluate using Eq. (3.12). Out of these terms, we will in the end keep only those with $\mathbf{q} = \mathbf{q}'$ when taking the expectation values: e.g., $\left\langle\hat{c}^\dagger_{\mathbf{k}\sigma}\hat{c}_{\mathbf{k}+\mathbf{q}-\mathbf{q}',\sigma}\right\rangle = f(\varepsilon_{\mathbf{k}\sigma})\delta_{\mathbf{q}\mathbf{q}'}$. We end with[20]:

$$\left\langle[\hat{n}_{\mathbf{k}\mathbf{q}\sigma},\hat{H}_U(t)]\right\rangle = U_{\text{ext}}(\mathbf{q},\omega)\mathrm{e}^{-i\omega t}\mathrm{e}^{\eta t}\left[f(\varepsilon_{\mathbf{k}\sigma}) - f(\varepsilon_{\mathbf{k}+\mathbf{q},\sigma})\right]. \tag{3.50}$$

[18] We second-quantized it in Sec. 1.3.2.

[19] For example, $\left\langle\hat{n}_{\mathbf{k},\mathbf{q}+\mathbf{q}',\sigma}\right\rangle$.

[20] What happens with the terms proportional to $U^*_{\text{ext}}(\mathbf{q}',\omega)$?

Gathering all the terms in Eq. (3.46), we get the differential equation:

$$i\hbar\frac{d}{dt}\left\langle\hat{n}_{\mathbf{kq}\sigma}\right\rangle = (\varepsilon_{\mathbf{k}+\mathbf{q},\sigma} - \varepsilon_{\mathbf{k}\sigma})\left\langle\hat{n}_{\mathbf{kq}\sigma}\right\rangle + U_{\text{ext}}(\mathbf{q},\omega)[f(\varepsilon_{\mathbf{k}\sigma}) - f(\varepsilon_{\mathbf{k}+\mathbf{q},\sigma})]. \tag{3.51}$$

As there is only one remaining time dependence, we can use the ansatz:

$$\left\langle\hat{n}_{\mathbf{kq}\sigma}(t)\right\rangle = \left\langle\hat{n}_{\mathbf{kq}\sigma}\right\rangle \mathrm{e}^{-i\omega t}\mathrm{e}^{\eta t}, \tag{3.52}$$

which involves that the the electronic density follows the potential U_{ext}[21]. Replacing Eq. (3.52) in Eq. (3.51), we finally obtain the expression for the stationary density:

$$\left\langle\hat{\rho}_{\mathbf{q}}\right\rangle = \sum_{\mathbf{k}\sigma}\left\langle\hat{n}_{\mathbf{kq}\sigma}\right\rangle = \sum_{\mathbf{k}\sigma}\frac{f(\varepsilon_{\mathbf{k}\sigma}) - f(\varepsilon_{\mathbf{k}+\mathbf{q},\sigma})}{\hbar\omega + \varepsilon_{\mathbf{k}\sigma} - \varepsilon_{\mathbf{k}+\mathbf{q},\sigma} + i\hbar\eta}U_{\text{ext}}(\mathbf{q},\omega). \tag{3.53}$$

This finally gives the susceptibility:

$$\chi_0(\mathbf{q},\omega) = \frac{1}{\mathcal{V}}\sum_{\mathbf{k}\sigma}\frac{f(\varepsilon_{\mathbf{k}\sigma}) - f(\varepsilon_{\mathbf{k}+\mathbf{q},\sigma})}{\hbar\omega + \varepsilon_{\mathbf{k}\sigma} - \varepsilon_{\mathbf{k}+\mathbf{q},\sigma} + i\hbar\eta}, \tag{3.54}$$

which is known as the Lindhard function [3.5]. It is useful to split it into real and imaginary parts, $\chi_0(\mathbf{q},\omega) = \chi_0^R(\mathbf{q},\omega) + i\chi_0^I(\mathbf{q},\omega)$, which we can write as[22]:

$$\chi_0^R(\mathbf{q},\omega) = \frac{1}{\mathcal{V}}\sum_{\mathbf{k}\sigma}P\left[\frac{f(\varepsilon_{\mathbf{k}\sigma}) - f(\varepsilon_{\mathbf{k}+\mathbf{q},\sigma})}{\hbar\omega + \varepsilon_{\mathbf{k}\sigma} - \varepsilon_{\mathbf{k}+\mathbf{q},\sigma}}\right] \tag{3.55}$$

$$\chi_0^I(\mathbf{q},\omega) = \frac{\pi}{\mathcal{V}}\sum_{\mathbf{k}\sigma}\Big[f(\varepsilon_{\mathbf{k}\sigma}) - f(\varepsilon_{\mathbf{k}+\mathbf{q},\sigma})\Big]\delta(\hbar\omega + \varepsilon_{\mathbf{k}\sigma} - \varepsilon_{\mathbf{k}+\mathbf{q},\sigma}), \tag{3.56}$$

using the Cauchy principal value. They contain different information: while $\chi_0^R(\mathbf{q},\omega)$ describes the instabilities of the electron gas, the spectral function $\chi_0^I(\mathbf{q},\omega)$ has the form of the Fermi golden rule describing the rate of transitions in response to a time-dependent perturbation. In this case, these are the electron-hole excitations of the Fermi sea. In this sense, the Dirac-delta in $\chi_0^I(\mathbf{q},\omega)$ introduces the conditions for the elementary electron-hole excitations to be possible (via the conservation of energy)[23]:

$$\hbar\omega = \frac{\hbar^2}{2m}\left(q^2 + 2\mathbf{kq}\right). \tag{3.57}$$

For the undriven case, $\omega = 0$, excitations are restricted to $q \leq 2k_{\text{F}}$. This bound can be broken for $\omega \neq 0$: A time dependent potential modulates this condition as long as the frequency lays between $|\omega_-| \leq \omega \leq \omega_+$, with

$$\omega_\pm = \frac{\hbar}{2m}(q^2 \pm 2k_{\text{F}}q). \tag{3.58}$$

The corresponding region, where $\chi_0^I(q) \neq 0$, is shaded in grey in Fig. 3.3.

- ☞ The static response $\chi_0(\mathbf{q},0)$ contains (as the linear term in a $\mathbf{q}$ expansion) the Thomas-Fermi screening.
- ☞ Still non-interacting!

[21] Like a cork in a pond.

[22] Remember:

$$\lim_{\eta\to 0^+}\frac{1}{\omega + i\eta} = P\left(\frac{1}{\omega}\right) - i\pi\delta(\omega).$$

[23] Are they possible in 2-D? And in 1-D?

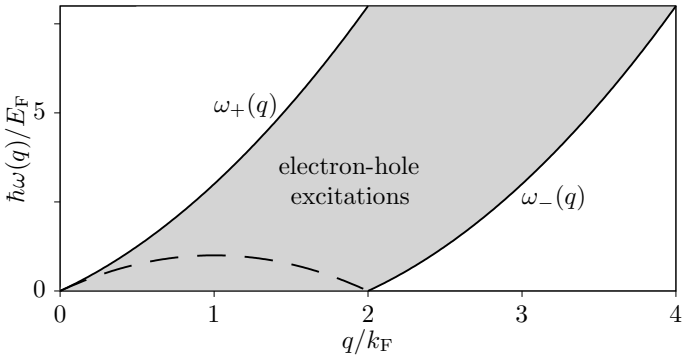

Figure 3.3.:
Regime of electron-hole excitations according to the Lindhard spectral function $\chi_0^I(q)$.

3.4.3. Including the Coulomb interaction. Random-phase approximation

Let us now consider the electron-electron interaction:

$$\hat{H}_{e-e} = \frac{1}{2\mathcal{V}} \sum_{\sigma'\sigma''} \sum_{\mathbf{k}'\mathbf{k}''} \sum_{\mathbf{q}'\neq 0} V_{\mathbf{q}} \hat{c}^\dagger_{\mathbf{k}'+\mathbf{q}',\sigma'} \hat{c}^\dagger_{\mathbf{k}''-\mathbf{q}',\sigma''} \hat{c}_{\mathbf{k}''\sigma''} \hat{c}_{\mathbf{k}'\sigma'}. \tag{3.59}$$

In this case, the commutator $[\hat{n}_{\mathbf{kq}\sigma}, \hat{H}_{e-e}]$ requires a bit more algebra, as it includes terms of the form $[\hat{c}^\dagger_{\mathbf{k}\sigma}\hat{c}_{\mathbf{k}+\mathbf{q},\sigma}, \hat{c}^\dagger_{\mathbf{k}'+\mathbf{q}',\sigma'}\hat{c}^\dagger_{\mathbf{k}''-\mathbf{q}',\sigma''}\hat{c}_{\mathbf{k}''\sigma''}\hat{c}_{\mathbf{k}'\sigma'}]$, but nothing we cannot do with patience in a couple of paper sides[24]. The result is:

$$[\hat{n}_{\mathbf{kq}\sigma}, \hat{H}_{e-e}] = \frac{1}{\mathcal{V}} \sum_{\mathbf{q}'\neq 0} V_{\mathbf{q}'} \hat{\rho}_{\mathbf{q}'} \left(\hat{c}^\dagger_{\mathbf{k}\sigma} \hat{c}_{\mathbf{k}+\mathbf{q}-\mathbf{q}',\sigma} - \hat{c}^\dagger_{\mathbf{k}+\mathbf{q}',\sigma} \hat{c}_{\mathbf{k}+\mathbf{q},\sigma} \right). \tag{3.60}$$

It is now convenient to keep only the terms with $\mathbf{q}' = \mathbf{q}$. This rather drastic but remarkably successful approximation is known as the *random-phase approximation* (RPA). It leads to:

$$\left\langle [\hat{n}_{\mathbf{kq}\sigma}, \hat{H}_{e-e}] \right\rangle_{RPA} = \frac{1}{\mathcal{V}} V_{\mathbf{q}} \left\langle \hat{\rho}_{\mathbf{q}} \right\rangle \left[f(\varepsilon_{\mathbf{k}\sigma}) - f(\varepsilon_{\mathbf{k}+\mathbf{q},\sigma}) \right], \tag{3.61}$$

where the time dependence is implicit in $\left\langle \hat{\rho}_{\mathbf{q}} \right\rangle$. Adding this term to the non-interacting contributions in Eq. (3.51) gives:

$$\left\langle \hat{\rho}_{\mathbf{q}} \right\rangle = \sum_{\mathbf{k}\sigma} \frac{f(\varepsilon_{\mathbf{k}\sigma}) - f(\varepsilon_{\mathbf{k}+\mathbf{q},\sigma})}{\hbar\omega + \varepsilon_{\mathbf{k}\sigma} - \varepsilon_{\mathbf{k}+\mathbf{q},\sigma} + i\hbar\eta} \left[U_{ext}(\mathbf{q},\omega) + \frac{4\pi e^2}{q^2} \frac{1}{\mathcal{V}} \left\langle \hat{\rho}_{\mathbf{q}} \right\rangle \right]. \tag{3.62}$$

The term into brackets is the effective potential, $V(\mathbf{q},\omega) = U_{ext}(\mathbf{q},\omega) + V_{pol}(\mathbf{q},\omega)$, which includes the polarization potential $V_{pol}(\mathbf{q},\omega) = 4\pi e^2 \left\langle \hat{\rho}_{\mathbf{q}} \right\rangle / q^2 \mathcal{V}$ induced by the external charge distribution. Hence, in the RPA, the screened susceptibility coincides with that of the non-interacting electrons, $\chi_{RPA} = \chi_0$, with the effective potential playing the role of the external potential, and the dielectric constant is:

$$\epsilon_{RPA} = 1 - \frac{4\pi e^2}{q^2} \chi_0(\mathbf{q},\omega). \tag{3.63}$$

[24] The most complicated operations are renaming variables in the $\mathbf{k}'$ summation, sometimes.

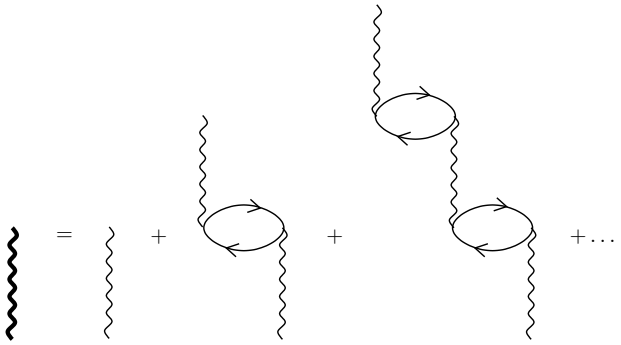

Figure 3.4.:
RPA diagrammatic expansion of the interaction.

3.4.4. Interpretation of the RPA

Introducing the screening susceptibility[25], we write the induced charge density (per unit volume) as $\mathfrak{n}(\mathbf{q},\omega) = \chi_{\rm sc} V(\mathbf{q},\omega)$. Hence, the potential is:

$$V(\mathbf{q},\omega) = U_{\rm ext}(\mathbf{q}) + \frac{4\pi e^2}{q^2}\chi_{\rm sc} V(\mathbf{q},\omega), \tag{3.64}$$

which can be rewritten as

$$V(\mathbf{q},\omega) = \left[1 - \frac{4\pi e^2}{q^2}\chi_{\rm sc}\right]^{-1} U_{\rm ext}(\mathbf{q}). \tag{3.65}$$

Let us now compare this with what we obtain from the RPA i.e., $\chi_{\rm sc} = \chi_0$, and from considering that the Coulomb interaction as the external potential, $U_{\rm ext}(\mathbf{q}) = 4\pi e^2/q^2$. Then, Eq. (3.64) reads:

$$V(\mathbf{q},\omega) = U_{\rm ext}(\mathbf{q})\left[1 + \chi_0 V(\mathbf{q},\omega)\right]. \tag{3.66}$$

This expression allows for an iterative expansion:

$$\begin{aligned} V(\mathbf{q},\omega) &= U_{\rm ext}(\mathbf{q})\left\{1 + \chi_0 U_{\rm ext}(\mathbf{q})\left[1 + \chi_0 V(\mathbf{q},\omega)\right]\right\} \\ &= U_{\rm ext}(\mathbf{q})\left\{1 + \chi_0 U_{\rm ext}(\mathbf{q}) + \left[\chi_0 U_{\rm ext}(\mathbf{q})\right]^2 + \ldots\right\} = \frac{U_{\rm ext}(\mathbf{q})}{1 - \chi_0 U_{\rm ext}(\mathbf{q})}, \end{aligned} \tag{3.67}$$

where in the last step we have made the geometric sum. It recovers the result $\epsilon_{\rm RPA} = 1 - \chi_0 U_{\rm ext}(\mathbf{q})$. Most interestingly, the series in Eq. (3.67) can be interpreted as a perturbative expansion of the interaction to all orders, including only the density-density (Hartree) interactions (see Fig. 3.4 for a diagrammatic representation). It can be argued that these dominate over the (Fock) exchange terms [3.7]. Therefore, the RPA approximation coincides with the dominant contribution of the perturbative expansion to all orders in the Coulomb interaction[26].

3.4.5. Collective excitations

We have seen how the Lindhard function describes the (electron-hole) excitations of the system. A different type of excitation emerges around the zeroes of the dielectric function. There, small perturbations give rise to large system responses, since $V(\mathbf{q},\omega) = U(\mathbf{q},\omega)/\epsilon_{\rm RPA}(\mathbf{q},\omega)$. Let us concentrate on the low $\mathbf{q}$ regime. We can show (another excercise):

$$\lim_{\mathbf{q}\to 0} \chi_0(\mathbf{q},\omega) = \frac{nq^2}{m\omega^2}, \tag{3.68}$$

[25] We follow Ref. [3.6] here.
[26] Remember the discussion at the end of Sec. 2.4.

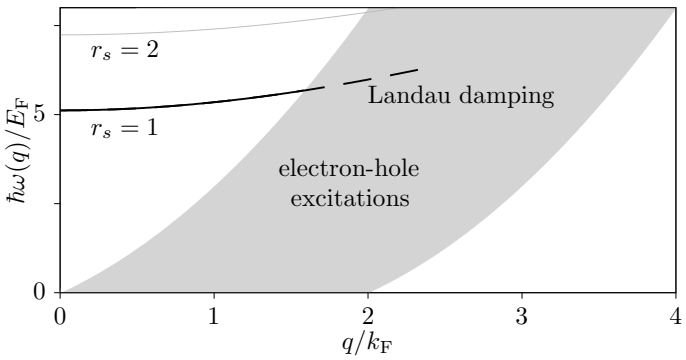

Figure 3.5.:
Electron plasma excitations. Two cases for different inverse densities (parametrized by the dimensionless distance r_s) are plotted.

resulting in a dielectric function:

$$\epsilon_{\text{RPA}}(0,\omega) = 1 - \frac{\omega_p^2}{\omega^2}, \tag{3.69}$$

where we have defined the electron plasma frequency:

$$\omega_p = \sqrt{\frac{n4\pi e^2}{m}} \tag{3.70}$$

which describes the collective oscillations of the electron gas.

We can extend the expansion to the leading order in q, getting:

$$\epsilon_{\text{RPA}}(\mathbf{q},\omega) = 1 - \frac{\omega_p^2}{\omega^2}\left[1 + \frac{3}{5}\left(\frac{qv_{\text{F}}}{\omega}\right)^2\right]. \tag{3.71}$$

The frequency ω that makes $\epsilon_{\text{RPA}}(\mathbf{q},\omega) = 0$ is plotted in Fig. 3.5. The plasmon mode is damped in the electron-hole continuum.

3.4.6. Friedel oscillations

In the opposite case of static excitations (for $\omega = 0$), we have [27]:

$$\epsilon_{\text{RPA}} = 1 + \frac{k_{\text{TF}}^2}{q^2} F\left(\frac{q}{2k_{\text{F}}}\right), \tag{3.72}$$

with $F(y)$ defined in Eq. (3.29). As we did for the Thomas-Fermi potential, we get:

$$V(\mathbf{q},0) = \frac{q^2}{q^2 + k_{\text{TF}}^2 F\left(\frac{q}{2k_{\text{F}}}\right)} U_{\text{ext}}(\mathbf{q},0). \tag{3.73}$$

The real space interaction is given by the inverse Fourier transform. Using the bare Coulomb interaction as the external potential:

$$V(\mathbf{r}) = \frac{e^2}{2\pi^2 r}\int dq \frac{q\sin(qr)}{q^2 + k_{\text{TF}}^2 F\left(\frac{q}{2k_{\text{F}}}\right)}. \tag{3.74}$$

[27] It is not complicated to get it from Eq. (3.54) at $T = 0$ (we did this integral before). The general case for finite temperatures is derived in Ref. [3.8].

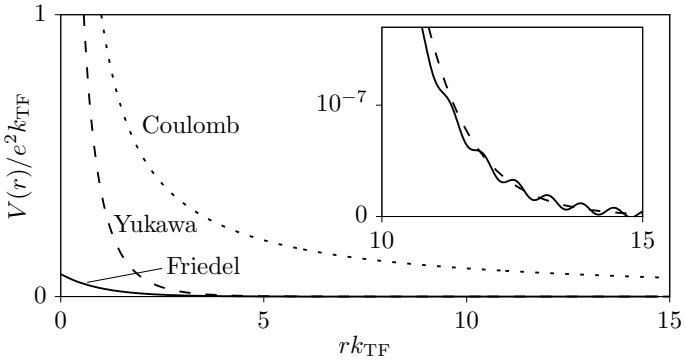

Figure 3.6.:
Comparison of the screened Yukawa and Friedel (for $k_{\mathrm{F}} = 5k_{\mathrm{TF}}$) interactions with the (unscreened) Coulomb interaction. The inset shows a detail of the Friedel oscillations.

The integral is not simple to do, so we will be happy to show the numerical solution in Fig. 3.6. However, it can be shown (see e.g., Ref. [3.8]) that the resulting potential oscillates at long distances around the Yukawa solution of the (semiclassical) Thomas-Fermi screening [3.9]:

$$V(\mathbf{r}) \propto \frac{\cos(2k_{\mathrm{F}}r)}{r^3}, \tag{3.75}$$

see the inset in Fig. 3.6. The oscillations can be understood from the phase shift suffered by an electron at the Fermi energy when being scattered by the external potential.

Bibliography

[3.1] H. Bruus and K. Flensberg. *Many-Body Quantum Theory in Condensed Matter Physics*. Oxford University Press, Sep 2004.

[3.2] D. Pines. *Elementary Excitations in Solids Lectures on Protons, Electrons, and Plasmons*. Taylor & Francis, Andover, England, UK, May 2019.

[3.3] G. B. Arfken and H. J. Weber. *Mathematical Methods for Physicists*. Academic Press Inc, Sep 1995.

[3.4] T. Koopmans. Über die Zuordnung von Wellenfunktionen und Eigenwerten zu den Einzelnen Elektronen Eines Atoms. *Physica*, 1(1):104–113, Jan 1934.

[3.5] J. Lindhard. On the properties of a gas of charged particles. *Det Kgl. Danske Vid. Selskab, Matematisk-Fysiske Meddelelser*, 28(8):1–57, 1954.

[3.6] P. Phillips. *Advanced Solid State Physics*. Cambridge University Press, Cambridge, England, UK, Mar 2012.

[3.7] A. Altland and B. Simons. *Condensed Matter Field Theory*. Cambridge University Press, Cambridge, England, UK, Jun 2006.

[3.8] A. L. Fetter and J. D. Walecka. *Quantum Theory of Many-particle Systems*. Dover Publications, Mineola, NY, USA, 2003.

[3.9] J. Friedel. XIV. The distribution of electrons round impurities in monovalent metals. *London, Edinburgh, and Dublin Philosophical Magazine and Journal of Science*, 43(337):153–189, Feb 1952.

Further reading

- ☞ H. Bruus and K. Flensberg, *Many-Body Quantum Theory in Condensed Matter Physics* (Oxford Univ. Press, Oxford, 2004)
- ☞ D. Pines, *Elementary excitations in solids* (Taylor & Francis, Boca Raton, 1999)
- ☞ A. L. Fetter and J. D. Walecka, *Quantum Theory of Many-Particle Systems* (McGraw-Hill, New York, 1971)
- ☞ A. Altland and B. Simmons, *Condensed Matter Field Theory* (Cambridge Univ. Press, Cambridge, 2006)
- ☞ P. Phillips, *Advanced solid state physics* (Cambridge Univ. Press, 2012)
- ☞ N. W. Ashcroft and N. D. Mermin, *Solid State Physics* (Saunders College Publ., New York, 1976)
- ☞ S. M. Girvin and K. Yang, *Modern Condensed Matter Physics* (Cambridge Univ. Press, Cambridge, 2019)
- ☞ G. D. Mahan, *Condensed matter in a nutshell* (Princeton Univ. Press, Princeton, 2010)

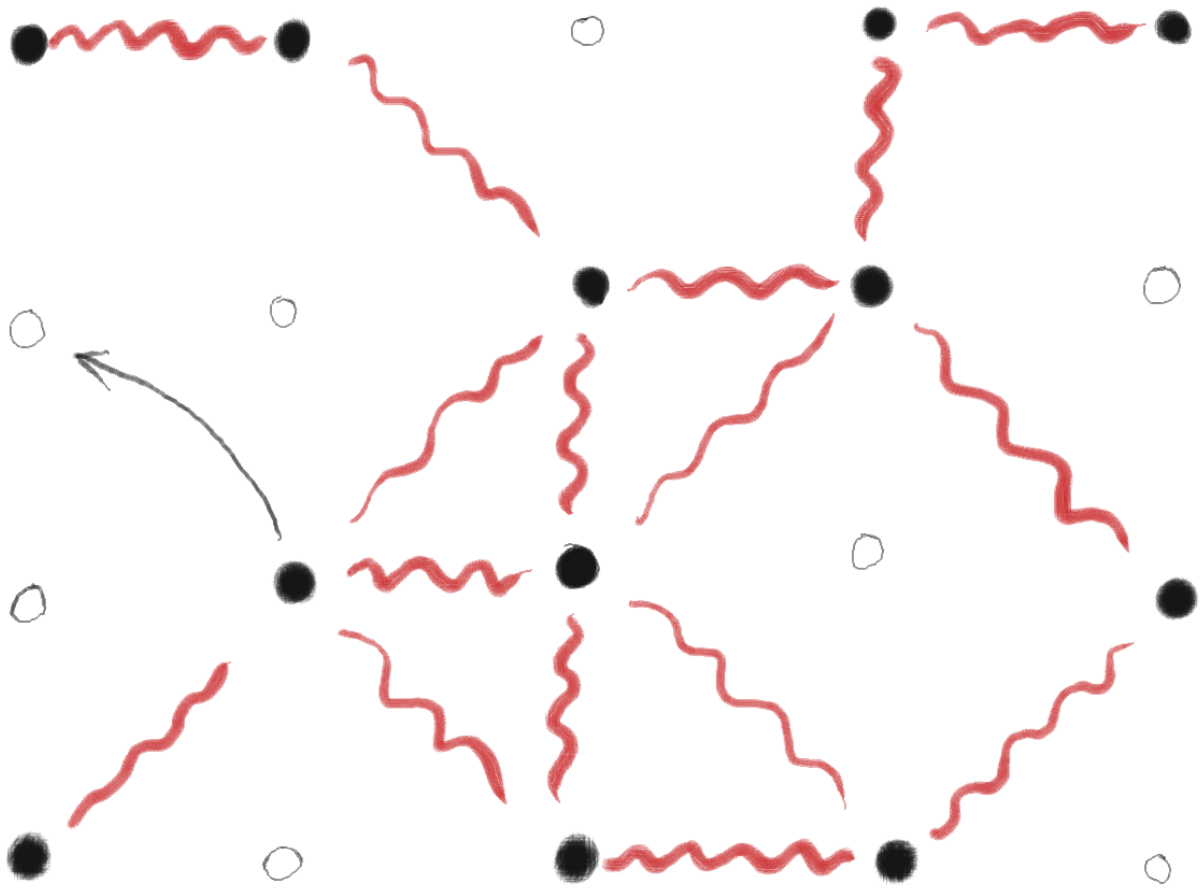

4. Lattice based descriptions

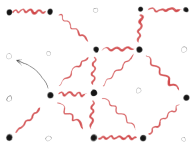

So far we discussed how the electron-electron interactions are treated in systems that allow for a description based on delocalized (either plane waves or Bloch) wave functions. This applies to metals where the conduction electrons come from extended orbitals. This is of course not always the case. In this chapter, we will show how the properties of the lattice influence the electronic properties when orbitals are localized. A prominent example of this is graphene. The Coulomb interactions are not so easily screened and give rise to the rich physics of strongly correlated electrons. A glance of the appearance of quantum phase transitions will be given using the Hubbard model as an illustration.

4.1. Tight binding approach

The description made in the previous chapters, is mostly based on treating electrons a free particles moving freely (except for the interactions) or in a band that extends over the while system. The structure of the lattice was either just a modulation (entering in the wave function as Bloch waves) or was directly neglected (the jellium model, in which case plane waves was an appropriate basis). This is a good approximation when the valence electrons of the atoms in the lattice correspond to orbitals that extend over several atom-atom distances. It also helps if they are isotropic, as for s orbitals. This is why it works particularly well for alkali metals.

However, this is obviously not always the case. In many situations (e.g., transition metals), conduction electrons occupy d or f orbitals which are strongly localized around the nuclei or oriented along well defined directions. Then, translational invariance is broken and, rather than plane waves or Bloch vectors, a description in terms of localized states is useful. This is done by writing the Bloch states as:

$$\psi_n(\mathbf{k},\mathbf{r}) = \frac{1}{\sqrt{\mathcal{V}_0}} \sum_j \mathrm{e}^{i\mathbf{k}\mathbf{R}_j} \mathcal{W}_n(\mathbf{r}-\mathbf{R}_j), \tag{4.1}$$

where $\mathcal{V}_0$ is the volume of the unit cell, and the Wannier functions [4.1]

$$\mathcal{W}_n(\mathbf{r}-\mathbf{R}_j) = \langle \mathbf{r}\,|nj\rangle = \sqrt{\mathcal{V}_0} \int_{\mathrm{BZ}} \frac{d^3\mathbf{k}}{(2\pi)^3} \mathrm{e}^{-i\mathbf{k}\mathbf{R}_j} \psi_n(\mathbf{k},\mathbf{r}-\mathbf{R}_j) \tag{4.2}$$

are centered at the positions of the atoms, and $\mathbf{R}_j$ are the vectors of the unit cell. It can be useful to discretize the reciprocal space in which case we have:

$$\mathcal{W}_n(\mathbf{r}-\mathbf{R}_j) = \frac{1}{\sqrt{\mathcal{N}}} \sum_{\mathbf{k}} \mathrm{e}^{-i\mathbf{k}\mathbf{R}_j} \psi_n(\mathbf{k},\mathbf{r}), \tag{4.3}$$

where $\mathcal{N}$ is the number of unit cells. In this case, it is convenient to use the definition

$$\psi_n(\mathbf{k},\mathbf{r}) = \frac{1}{\sqrt{\mathcal{N}}} \sum_j \mathrm{e}^{i\mathbf{k}\mathbf{R}_j} \mathcal{W}_n(\mathbf{r}-\mathbf{R}_j) \tag{4.4}$$

that normalizes the Wannier functions[1]:

$$\langle ni|mj\rangle = \int d^3\mathbf{r}\mathcal{W}_n^*(\mathbf{r}-\mathbf{R}_i)\mathcal{W}_m(\mathbf{r}-\mathbf{R}_j) = \delta_{ij}\delta_{nm}. \tag{4.5}$$

In this basis, we second-quantize the kinetic term of the Hamiltonian as:

$$\hat{H}_0 = \sum_{ij}\sum_{nm} T_{ij}^{nm}\hat{c}_{ni}^\dagger\hat{c}_{mj}, \tag{4.6}$$

with the operators $\hat{c}_{mi}$ annihilating an electron of band m in the site i, and where[2]

$$T_{ij}^{nm} = \left\langle ni\left|\hat{H}_0\right|mj\right\rangle = T_{ij}^n\delta_{n,m}. \tag{4.7}$$

Using this last equality[3], we get:

$$\hat{H}_0 = \sum_{ij}\sum_{n} T_{ij}^n\hat{c}_{ni}^\dagger\hat{c}_{nj}. \tag{4.8}$$

From this, we readily see that the Wannier functions are not eigenstates of the hamiltonian. The nondiagonal elements in Eq. (4.8) describe the system dynamics as a series of transitions where the electrons tunnel between two sites (or atoms) of the lattice. For this reason it is typically referred to as the *hopping hamiltonian*. It is the base for tight-binding models which (based on the knowledge of the chemical bounds in the lattice) make assumptions on the different contributions of the terms T_{ij}^n to extract the electronic properties.

4.2. Electrons in graphene

We will illustrate the use of tight-binding models using graphene as an example [4.3]. Thought for decades to be just a nice theoretical problem impossible to realize experimentally[4], the discovery of graphene [4.4] revealed a huge amount of phenomena which have transcended the field of fundamental physics to find industrial applications.

Graphene is formed by a monolayer[5] two-dimensional honeycomb lattice of carbon atoms, see Fig. 4.1. The two unit cell atoms, denoted by A and B, form two Bravais sublattices. The atomic bonds, of the type sp^2, are very strong[6]. Hence, the contribution of all other orbitals can be neglected. The B atoms are connected to their nearest neighbours by the vectors

$$\boldsymbol{\delta}_1 = \frac{a}{2}\left(1,\sqrt{3}\right), \qquad \boldsymbol{\delta}_2 = \frac{a}{2}\left(1,-\sqrt{3}\right) \qquad \text{and} \qquad \boldsymbol{\delta}_3 = -a\,(1,0)\,, \tag{4.9}$$

with the interatomic distance $a \approx 1.42$ Å.

With these, we write the tight binding hamiltonian, where we distinguish the diagonal and the off-diagonal terms:

$$\hat{H} = E_0\sum_{j\sigma}\left(\hat{a}_{j\sigma}^\dagger\hat{a}_{j\sigma} + \hat{b}_{j\sigma}^\dagger\hat{b}_{j\sigma}\right) + \tau\sum_{j\sigma}\sum_{\delta_l}\left(\hat{a}_{j+\delta_l,\sigma}^\dagger\hat{b}_{j\sigma} + \hat{b}_{j\sigma}^\dagger\hat{a}_{j+\delta,\sigma}\right), \tag{4.10}$$

[1] In most cases in condensed matter, the actual form of the Wannier functions is now completely determined, so there is some freedom in chosing the conventions, see e.g., Ref. [4.2].
[2] This is left as an exercise.
[3] What do the off-diagonal elements mean?
[4] It was believed that isolated two dimensional crystals could simply not exist because they could not sustain fluctuations.
[5] The properties change quite dramatically in bilayer graphene.
[6] Not surprising if you think of the same bonds in diamond.

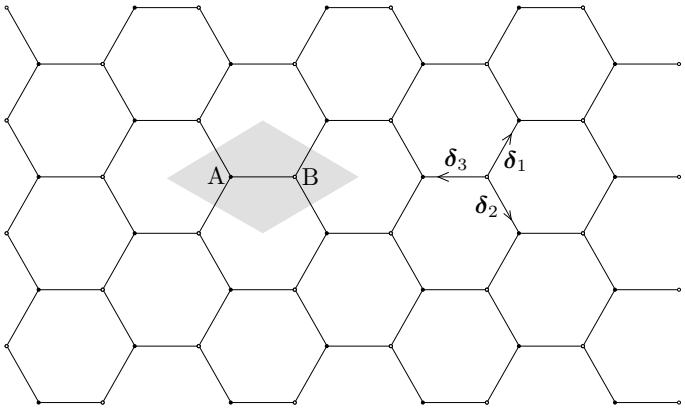

Figure 4.1.:
Graphene honeycomb lattice. The unit cell is formed by two inequivalent atoms (A and B, marked by black and white circles, respectively). Vectors $\boldsymbol{\delta}_i$ point to the nearest neightbours of B atoms.

where the operators $\hat{a}_{j\sigma}$ and $\hat{b}_{j\sigma}$ annihilate electrons in site $\mathbf{R}_j$ of sublattices A and B, respectively. Indices $j + \delta_l$ indicate the neightbouring sites $\mathbf{R}_j + \boldsymbol{\delta}_l$. In the Bloch state basis:

$$\hat{a}_{j\sigma} = \frac{1}{\sqrt{\mathcal{N}}} \sum_{\mathbf{k}} e^{i\mathbf{k}\mathbf{R}_j} \hat{a}_{\mathbf{k}\sigma} \qquad \text{and} \qquad \hat{b}_{j\sigma} = \frac{1}{\sqrt{\mathcal{N}}} \sum_{\mathbf{k}} e^{i\mathbf{k}\mathbf{R}_j} \hat{b}_{\mathbf{k}\sigma}. \tag{4.11}$$

Let us show explicitly one of the hopping terms in Eq. (4.10). On one hand:

$$\sum_j \hat{a}^\dagger_{j+\delta_l,\sigma} \hat{b}_{j\sigma} = \frac{1}{\mathcal{N}} \sum_{\mathbf{k}\mathbf{k}'} \sum_j e^{-i\mathbf{k}(\mathbf{R}_j+\delta_l)} \hat{a}^\dagger_{\mathbf{k}\sigma} \hat{b}_{\mathbf{k}'\sigma} e^{i\mathbf{k}'\mathbf{R}_j} = \sum_{\mathbf{k}} e^{-i\mathbf{k}\vec{\delta}_l} \hat{a}^\dagger_{\mathbf{k}\sigma} \hat{b}_{\mathbf{k}\sigma}. \tag{4.12}$$

On the other hand,

$$\sum_{\delta_l} e^{-i\mathbf{k}\vec{\delta}_l} = e^{ik_x a} + e^{-i(k_x+\sqrt{3})a/2} + e^{-i(k_x-\sqrt{3})a/2} = e^{i\theta_x} + 2e^{-i\theta_x} \cos\left(\frac{\sqrt{3}}{2}\theta_y\right) \equiv \gamma(\mathbf{k}), \tag{4.13}$$

where we have defined $\theta_i = k_i a$. This leaves the hamiltonian as:

$$\hat{H} = E_0 \sum_{\mathbf{k}\sigma} \left(\hat{a}^\dagger_{\mathbf{k}\sigma}\hat{a}_{\mathbf{k}\sigma} + \hat{b}^\dagger_{\mathbf{k}\sigma}\hat{b}_{\mathbf{k}\sigma}\right) + \tau \sum_{\mathbf{k}\sigma} \left[\gamma(\mathbf{k})\hat{a}^\dagger_{\mathbf{k}\sigma}\hat{b}_{\mathbf{k}\sigma} + h.c.\right], \tag{4.14}$$

which is easily diagonalizable[7], giving the eigenvalues (spin degenerate):

$$E_\pm(\mathbf{k}) = E_0 \pm \tau|\gamma(\mathbf{k})|. \tag{4.15}$$

The second term introduces a gap between the two bands, as shown in Fig. 4.2.

We can identify several special points in the Brilloin zone, which are denoted as Γ, M, K and K′ in Fig. 4.2. At $\mathbf{k}_\Gamma = 0$, we find the maximum and minimum of the conduction and valence bands, given by $E_\pm(\mathbf{k}_\Gamma) = E_0 \pm 3\tau$. At $\mathbf{k}_\mathrm{M} = (2\pi/3, 0)$, there is a saddle point which results in van Hove singularities of the density of states.

Special attention needs to be paid to the K and K′ points, where $|\gamma(\mathbf{k}_\mathrm{K})| = |\gamma(\mathbf{k}_{\mathrm{K}'})| = 0$. There, the conduction and valence bands touch each other: $E_\pm(\mathbf{k}_\mathrm{K}) = E_\pm(\mathbf{k}_{\mathrm{K}'}) = E_0$. The gap closes, which allows (in principle) electron-hole excitations to occur at these points.

[7] Write it as a 2×2 matrix for each $\mathbf{k}$ and each σ.

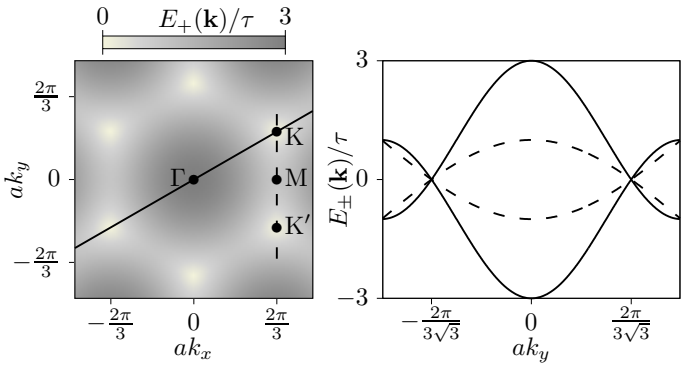

Figure 4.2.:
Dispersion relation of monolayer graphene, for $E_0 = 0$. The special points of the reciprocal lattice are highlighted. The right panel shows cuts along the solid and dashed lines traced in the left one.

4.2.1. Low energy dispersion

Let us focus on the K and K′ points, located at $\mathbf{k}_{n\pm} = \frac{4\pi}{3a}\left(n, \pm 1/\sqrt{3}\right)$. In the following, for concreteness, we will focus on the case $\mathbf{k}_{0\pm}$ (+ gives a K′, and − a K point). We are interested on the behaviour around E_0, for which we consider small deviations $\mathbf{k} = \mathbf{k}_{0\pm} + \delta\mathbf{k}$ and we perform an expansion of the dispersion relation. In a few lines we arrive at:

$$\gamma(\mathbf{k}_{0\pm}+\delta\mathbf{k}) \approx \frac{3ia}{2}(\delta k_x \mp i\delta k_y). \tag{4.16}$$

Defining the Fermi velocity $v_\mathrm{F} = 3\tau a/2\hbar$, we get two different terms:

$$H_\mathrm{K} = \begin{pmatrix} E_0 & i\hbar v_\mathrm{F}(\delta k_x - i\delta k_y) \\ -i\hbar v_\mathrm{F}(\delta k_x - i\delta k_y) & E_0 \end{pmatrix}, \tag{4.17}$$

and $H_{\mathrm{K}'}(\delta k_x, \delta k_y) = H_\mathrm{K}(\delta k_x, -\delta k_y)$. With them, we write the effective hamiltonian:

$$H_\mathrm{K} = \begin{pmatrix} H_\mathrm{K} & 0 \\ 0 & H_{\mathrm{K}'} \end{pmatrix}, \tag{4.18}$$

The K and K′ terms give rise to the valley degree of freedom (often also called isospin). Diagonalizing the different blocks, we get that the dispersion relation

$$E_\pm(\mathrm{K}) = E_\pm(\mathrm{K}') = E_0 \pm \frac{3}{2}a\tau\left|\delta k_x + i\delta k_y\right| \tag{4.19}$$

turns out to be linear[8]. Note this also means that the density of states at these points vanishes:

$$\upsilon(E_0+\delta E) \approx \frac{1}{2\pi\hbar^2 v_\mathrm{F}^2}|\delta E|. \tag{4.20}$$

Therefore, differently from what we saw in the previous chapter, electron-hole excitations are not possible at arbitrarily low energies around the Fermi energy[9].

The eigenstates read:

$$\psi^\pm_\mathrm{K}(\mathbf{k}) = \frac{1}{\sqrt{2}}\begin{pmatrix} \mathrm{e}^{-i\phi_\mathbf{k}/2} \\ \pm\mathrm{e}^{i\phi_\mathbf{k}/2} \end{pmatrix}, \qquad \text{with} \qquad \phi_\mathbf{k} = \arctan\left(\frac{k_x}{k_y}\right). \tag{4.21}$$

[8] For this reason and one that will become clear soon, the dispersion in the K and K' is said to form *Dirac cones*, and the K and K' are the *Dirac points*. Two sections of the Dirac cones can indeed be appreciated in the right panel of Fig. 4.2.

[9] But... what is the Fermi energy in (undoped) graphene?

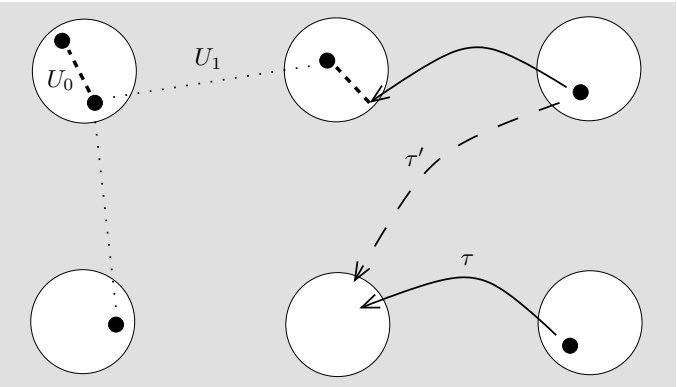

Figure 4.3.:
Hubbard model in a square lattice. Dashed and dotted lines represent the Coulomb interaction between electrons in the same or in different atomic sites. Hoppings to neighbouring available sites are represented by arrows.

Note that the wave function gains a minus sign upon a 2π-rotation (a geometrical Berry phase [4.5] originating from the lattice duplicity[10]). As the spin, it has a 4π-periodicity, for which reason this degree of freedom is called pseudospin.

This is not *totally* surprising because the valley matrices H_{K} and $H_{\mathrm{K}'}$ have the form of a Dirac hamiltonian for massless fermions[11]:

$$\hat{H}_{\mathrm{Dirac}} = v\hat{\boldsymbol{\sigma}}\hat{\mathbf{p}}, \tag{4.22}$$

where $\hat{\boldsymbol{\sigma}}$ are the Pauli matrices and $\hat{\mathbf{p}}$ is the momentum. The Dirac equation is a relativistic analogue of the Schrödinger equation which introduces naturally the notion of the electron spin. Remarkably, relativistic dynamics emerge in graphene for $v_{\mathrm{F}} \approx 8.4 \times 10^5\,\mathrm{ms}^{-1} \ll c$, and are experimentally relevant [4.7]. It has furthermore allowed for the demonstration of the Klein paradox for the perfect tunneling of helical particles [4.8], predicted so long ago that it was done in German [4.9] in the context of relativistic quantum mechanics[12]. In graphene, holes below the Fermi level play the role of positrons in quantum electrodynamics.

4.3. Strong correlations. The Hubbard model

Interactions in narrow band conductors (due to transitions between localized states, e.g., d orbitals in transition metals) have several contributions. On one hand, the interaction between electrons in different sites, i.e., well separated spatially, will likely be screened by electrons in broad bands (delocalized over the system). On the other hand, electrons in the same site will interact strongly and cannot be disregarded.

Following this kind of ideas, J. Hubbard proposed an effective model based on mean field approaches using a Wannier function description [4.11] (see also Refs. [4.12] and [4.13] for similar arguments applied to magnetic materials). All the electrons in narrow band states are treated with a Hartree-Fock approximation (pretty much like how it was done in chapter 3). The remaining electrons are assumed to hop between the narrow band orbitals following the kinetic description of the hamiltonian in Eq. (4.8).

[10] Remember sites A and B?

[11] Not so long ago there were no evidence of the existence of any massless Dirac fermion, see e.g., Ref. [4.6]. This is another manifestation of the fundamental interest of quasiparticles. This agrees with the semiclassical expression for the effective mass

$$m^* = \hbar^2 k \left(\frac{dE}{dk}\right)^{-1}.$$

Note that the usual definition in terms of the second derivative d^2E/dk^2 gives a diverging effective mass.

[12] See Ref. [4.10] for more modern discussions.

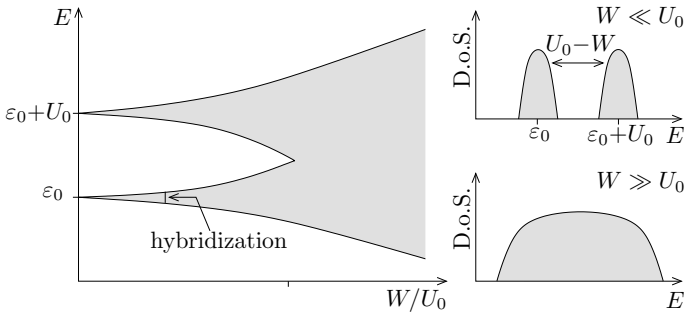

Figure 4.4.:
Illustration of the metal to Mott insulator transition as the electron-electron-correlations, U_0, overcome the (kinetic) bandwidth, W.

The fact that electrons are sitting in localized sites introduces the separation between atoms, d_{ij}, as the relevant distance for the electron-electron interactions. This way, assuming that they are screened over distances $d_{\text{scr}} \ll d_{ij}$, one can neglect the contribution of the terms $\left\langle ij\left|\hat{H}_{\text{e-e}}\right|ij\right\rangle$ when $i \neq j$. In particular:

$$\left\langle ij\left|\hat{H}_{\text{e-e}}\right|ij\right\rangle \ll \left\langle ii\left|\hat{H}_{\text{e-e}}\right|ii\right\rangle \equiv U_0, \tag{4.23}$$

where U_0 is the mean-field interaction between electrons in the same site, i. For the simple case where each site is has all orbitals full except for one level (admitting up to two electrons), the hamiltonian reads:

$$\hat{H}_{\text{Hubbard}} = \sum_{ij}\sum_{\sigma} T_{ij}\hat{c}^{\dagger}_{i\sigma}\hat{c}_{j\sigma} + U_0\sum_{i}\hat{n}_{i\sigma}\hat{n}_{i,-\sigma}, \tag{4.24}$$

where $\hat{n}_{i\sigma} = \hat{c}^{\dagger}_{i\sigma}\hat{c}_{i\sigma}$ counts the number of electrons in site i with spin σ. Despite its apparent simplicity, this model includes a high complexity not only in the number of physical phenomena it describes[13], but also in the difficulties in finding proper solutions.

The model hence introduces the dynamical suppression of events that involve the tunneling of an electron into an occupied site: it requires an additional energy U_0.[14]

Single-site Hubbard model:
For a single (spin degenerate) atomic site, with state $|1\sigma\rangle$:

$$\hat{H}_1 = \sum_{\sigma}\varepsilon_0\hat{n}_{\sigma} + U_0\sum_{\sigma}\hat{n}_{\sigma}\hat{n}_{-\sigma}.$$

The matrix elements are $\left\langle 1\sigma\left|\hat{H}_1\right|1\sigma\right\rangle = \varepsilon_0$, for singly-occupied, and $\left\langle 1\uparrow,1\downarrow\left|\hat{H}_1\right|1\uparrow,1\downarrow\right\rangle = 2\varepsilon_0 + U_0$, for doubly-occupied states. This way, we interpret ε_0 as the energy required to add an electron to an empty site, and $\varepsilon_0 + U_0$ as the energy required to add it when the site already contains one electron.

4.3.1. Metal to insulator transition

Let us consider the simplest case with hopping to nearest-neightbours given by:

$$T^{\text{near}}_{ij} = \frac{W}{2}, \tag{4.25}$$

[13] As we will see, metal-insulating transitions, but also models of high-T_c superconductors (cuprates), ultra-cold atomic systems. It is furthermore used as a benchmark of quantum simulators in different platforms: atomic lattices [4.14], artificial lattices [4.15], nitrogen vacancies [4.16], or quantum dots [4.17].

[14] Also known as *charging energy*.

and the all other contributions $T_{ij}^{\text{non-near}} = 0$. Then, the constant W corresponds to the band width. In this case, we can distinguish two limiting regimes, depending on the relative contribution of kinetic and correlation terms (see Fig. 4.4):

(i) $U \ll W$: electrons are free;

(ii) $U \gg W$: electrons are localized.

In the first case, the system tends to behave as a metal[15]. The second one is more involved. Consider the particular half-filled case (with one electron per site). Then, the ground state is clearly given by the system with one electron in each site. Charge fluctuations are strongly suppressed by U,[16] and the system behaves as an insulator. This is a *Mott insulator* [4.18]. Note this is very different to band insulators which rely on having completely full bands[17], but rather on electron-electron correlations.

4.3.2. Related hamiltonians: Anderson impurity model

Tunneling to a localized orbital was proposed by P. W. Anderson as a model for magnetic impurities in metals [4.19]: a single site occupied by an electron with spin σ is tunnel-coupled to *itinerant* electron in metallic widebands:

$$\hat{H}_{\text{Anderson}} = \sum_{\sigma} \left(\varepsilon_{\sigma} \hat{n}_{0\sigma} + U \hat{n}_{0\sigma} \hat{n}_{0,-\sigma} \right) + \sum_{k\sigma} \varepsilon_{k\sigma} \hat{c}^{\dagger}_{k\sigma} \hat{c}_{k\sigma} + \sum_{k\sigma} \left(V_{k\sigma} \hat{d}^{\dagger}_{0\sigma} \hat{c}_{k\sigma} + \text{h.c.} \right). \tag{4.26}$$

The first term describes the impurity (similarly to the single-site Hubbard model in the previous section), where $\hat{n}_{0\sigma} = \hat{d}^{\dagger}_{0\sigma} \hat{d}_{0\sigma}$[18] is the number operator of electrons with spin σ in the impurity, ε_{σ} is the energy of the electron, and U the charging energy. The second term describes the free electrons in the metal, and the last one in brackets, the tunneling of an electron between the local site and the free-electron bands.

The impurity is then described by four states, depending on its occupation: $|0\rangle$, $|\sigma\rangle$ (with spin $\sigma = \uparrow, \downarrow$), and $|\uparrow,\downarrow\rangle$. Transitions between them are induced by tunneling and will depend on the occupation of the impurity: electrons will need an additional energy U to tunnel into an impurity containing an electron than it would if the impurity was empty.

Consider for example the case where U is large enough such that $\varepsilon_{\sigma} + U > \mu > \varepsilon_{\sigma}$ (with μ being the Fermi energy of the metal). Then, the doubly occupation is not energetically available, so the impurity will be occupied by one electron with spin σ. Single-electron tunneling events will be hence suppressed by the Coulomb interaction[19]. However, if the coupling $V_{k\sigma}$ is sufficiently strong, higher order tunneling transitions are possible where the occupation of the impurity changes by *virtually* occupying either $|0\rangle$ or $|\uparrow,\downarrow\rangle$. In that case, the spin of the impurity is allowed to fluctuate, e.g. via transitions $|\uparrow\rangle \rightarrow (|0\rangle) \rightarrow |\downarrow\rangle$.[20] These transitions correlate the spin of the impurity with the cloud of surrounding spins, forming a singlet[21], an effect known as spin screening. This spin-mediated increase of the scattering leads to an increase of resistance at low temperatures (known as the Kondo effect [4.20]).

The Anderson hamiltonian is also widely used to describe transport in quantum dot systems: the impurity role is played by a quantum dot exchanging electrons with one or more electronic reservoirs across tunnel barriers [4.21][22]. Currents are therefore strongly affected by charge and spin correlations,

[15] Can you think on an exception?

[16] (at sufficiently low temperatures)

[17] See your favourite solid state book.

[18] For clarity, the creation operators in the impurity are denoted differently than those in the wideband: $\hat{d}^{\dagger}_{\sigma}$ (originally for being intended to describe d orbitals) vs. $\hat{c}^{\dagger}_{k\sigma}$.

[19] Another way of saying that energy is not conserved in the process.

[20] The brackets are to emphasize that the state is only viartually occupied.

[21] Why a singlet?

[22] Indeed, they serve as model systems to investigate the Kondo effect [4.22, 4.23].

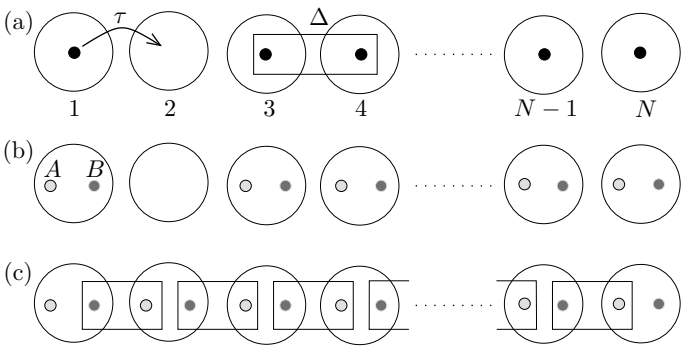

Figure 4.5.:
(a) N-site wire coupled by a hopping τ and pairing Δ. (b) Electrons (black circles) can be decomposed as pairs of Majorana fermions A and B (grey circles). The configuration in (b) corresponds to (a) for $\tau = \Delta = 0$. (c) Majorana wire with $\mu = 0$ and $\tau = \Delta$: A and B recombine non-locally.

allowing to measure them down to the single-electron level. We will discuss this problem in chapter **??**.

4.4. Majorana fermions in nanowires

A particularly interesting case is a one dimensional (but finite) array of sites with p-wave superconducting correlations[23]. This model is known as the Kitaev chain [4.24], depicted in Fig. 4.5(a). Assuming non-interacting electrons and that each site can host up to one electron, the hamiltonian for an N-site chain reads:

$$\hat{H} = -\mu \sum_{i=1}^{N} \left(\hat{c}_i^\dagger \hat{c}_i - \frac{1}{2} \right) + \sum_{i=1}^{N-1} \left[-\tau \left(\hat{c}_i^\dagger \hat{c}_{i+1} + \hat{c}_{i+1}^\dagger \hat{c}_i \right) + \Delta \left(\hat{c}_i \hat{c}_{i+1} + \hat{c}_{i+1}^\dagger \hat{c}_i^\dagger \right) \right], \tag{4.27}$$

where μ is the on-site energy, τ is the hopping, and Δ is the superconducting gap. Note that spin plays no role. It is convenient to introduce the Majorana operators that separate the real and imaginary parts of the electron operators:

$$\hat{c}_i = \frac{1}{2} \left(\hat{\gamma}_{iA} + i \hat{\gamma}_{iB} \right). \tag{4.28}$$

> Majorana fermions are real solutions of the Dirac equation [4.25], which involves that they are their own antiparticles, see e.g., Ref. [4.26]. Necessarily, this also implies that they have no charge nor mass. Furthermore, stationary solutions are possible only at zero energy. This involves the algebra:
>
> $$\{\hat{\gamma}_i, \hat{\gamma}_j\} = 2\delta_{ij}, \quad \hat{\gamma}_i = \hat{\gamma}_i^\dagger \quad \text{and} \quad \hat{\gamma}_i^2 = (\hat{\gamma}_i^\dagger)^2 = 1.$$

We can check that the operators $\hat{\gamma}_{i\alpha}$ verify:

$$\{\hat{\gamma}_{i\alpha}\hat{\gamma}_i, \hat{\gamma}_{j\beta}\hat{\gamma}_i\} = 2\delta_{ij}\delta_{\alpha\beta}, \quad \hat{\gamma}_{i\alpha} = (\hat{\gamma}_{i\alpha})^\dagger, \quad \text{and} \quad \hat{\gamma}_{i\alpha}^2 = (\hat{\gamma}_{i\alpha}^\dagger)^2 = 1. \tag{4.29}$$

We can then say that an electron is composed of two Majorana fermions. Note also that one cannot write a number operator for Majorana fermions: $\hat{\gamma}_{i\alpha}\hat{\gamma}_{i\alpha}^\dagger = \hat{\gamma}_{i\alpha}^\dagger \hat{\gamma}_{i\alpha} = 1$.

The system hamiltonian is then transformed into:

$$\hat{H} = -\frac{i\mu}{2} \sum_{i=1}^{N} \hat{\gamma}_{iA}\hat{\gamma}_{iB} + \frac{i}{2} \sum_{i=1}^{N-1} \left[(\Delta + \tau)\hat{\gamma}_{iB}\hat{\gamma}_{i+1,A} + (\Delta - \tau)\hat{\gamma}_{iA}\hat{\gamma}_{i+1,B} \right]. \tag{4.30}$$

[23] Differently from the usual s-wave superconductors, p-wave Cooper pairs are spin triplets.

In this form, the hamiltonian couples different Majorana modes in the same site (first term, proportional to μ) or in different sites (second term). The case $\Delta = \tau = 0$ recovers the *trivial* hamiltonian of a system of uncoupled electrons, each in its own site, as shown in Fig. 4.5(b).

In the case $\Delta = \tau$ and $\mu = 0$, the hamiltonian reduces to

$$\hat{H} = i\tau \sum_{i=1}^{N-1} \hat{\gamma}_{iB}\hat{\gamma}_{i+1,A}, \tag{4.31}$$

i.e., only the terms with coupling between first neightbouring sites survive. The fact that there is no coupling between Majorana operators in the same site is highly remarkable, because they describe the same electron!

Looking carefully into Eq. (4.31), you may miss two operators: $\hat{\gamma}_{1A}$ and $\hat{\gamma}_{NB}$, i.e., two Majorana operators at the two ends of the chain, remain uncoupled, see Fig. 4.5(c). If we recombine the Majorana operators into non-local fermions:

$$\hat{d}_i = \frac{1}{2}\left(\hat{\gamma}_{iB} + i\hat{\gamma}_{i+1,A}\right), \tag{4.32}$$

we get a non-interacting (diagonal) hamiltonian:

$$\hat{H} = 2\tau \sum_{i=1}^{N-1} \left(\hat{d}_i^\dagger \hat{d}_i - \frac{1}{2}\right), \tag{4.33}$$

which describes the superconducting bulk of the wire, with a non-local fermion

$$\hat{f} = \frac{1}{2}\left(\hat{\gamma}_{1A} + i\hat{\gamma}_{NB}\right) \tag{4.34}$$

delocalized at its two ends.

Bibliography

[4.1] G. H. Wannier. The Structure of Electronic Excitation Levels in Insulating Crystals. *Phys. Rev.*, 52(3):191–197, Aug 1937.

[4.2] N. Marzari, A. A. Mostofi, J. R. Yates, I. Souza, and D. Vanderbilt. Maximally localized Wannier functions: Theory and applications. *Rev. Mod. Phys.*, 84(4):1419–1475, Oct 2012.

[4.3] A. H. Castro Neto, F. Guinea, N. M. R. Peres, K. S. Novoselov, and A. K. Geim. The electronic properties of graphene. *Rev. Mod. Phys.*, 81(1):109–162, Jan 2009.

[4.4] K. S. Novoselov, D. Jiang, F. Schedin, T. J. Booth, V. V. Khotkevich, S. V. Morozov, and A. K. Geim. Two-dimensional atomic crystals. *Proc. Natl. Acad. Sci. U.S.A.*, 102(30):10451–10453, Jul 2005.

[4.5] M. V. Berry. Quantal Phase Factors Accompanying Adiabatic Changes. *Proc. R. Soc. London A - Math. Phys. Sci.*, 392(1802):45–57, Mar 1984.

[4.6] W. Greiner, L. Neise, and H. Stöcker. *Thermodynamics and Statistical Mechanics*. Springer-Verlag, New York, NY, USA, 1995.

[4.7] K. S. Novoselov, A. K. Geim, S. V. Morozov, D. Jiang, M. I. Katsnelson, I. V. Grigorieva, S. V. Dubonos, and A. A. Firsov. Two-dimensional gas of massless Dirac fermions in graphene. *Nature*, 438:197–200, Nov 2005.

[4.8] A. F. Young and P. Kim. Quantum interference and Klein tunnelling in graphene heterojunctions. *Nat. Phys.*, 5:222–226, Mar 2009.

[4.9] O. Klein. Die Reflexion von Elektronen an einem Potentialsprung nach der relativistischen Dynamik von Dirac. *Z. Phys.*, 53(3):157–165, Mar 1929.

[4.10] C. W. J. Beenakker. Colloquium: Andreev reflection and Klein tunneling in graphene. *Rev. Mod. Phys.*, 80(4):1337–1354, Oct 2008.

[4.11] J. Hubbard. Electron Correlations in Narrow Energy Bands. *Proc. R. Soc. London A - Math. Phys. Sci.*, 276(1365):238–257, Nov 1963.

[4.12] M. C. Gutzwiller. Effect of Correlation on the Ferromagnetism of Transition Metals. *Phys. Rev. Lett.*, 10(5):159–162, Mar 1963.

[4.13] J. Kanamori. Electron Correlation and Ferromagnetism of Transition Metals. *Prog. Theor. Phys.*, 30(3):275–289, Sep 1963.

[4.14] L. Tarruell and L. Sanchez-Palencia. Quantum simulation of the Hubbard model with ultracold fermions in optical lattices. *C. R. Phys.*, 19(6):365–393, Sep 2018.

[4.15] A. Singha, M. Gibertini, B. Karmakar, S. Yuan, M. Polini, G. Vignale, M. I. Katsnelson, A. Pinczuk, L. N. Pfeiffer, K. W. West, and V. Pellegrini. Two-Dimensional Mott-Hubbard Electrons in an Artificial Honeycomb Lattice. *Science*, 332(6034):1176–1179, Jun 2011.

[4.16] J. Salfi, J. A. Mol, R. Rahman, G. Klimeck, M. Y. Simmons, L. C. L. Hollenberg, and S. Rogge. Quantum simulation of the Hubbard model with dopant atoms in silicon. *Nat. Commun.*, 7(11342):1–6, Apr 2016.

[4.17] T. Hensgens, T. Fujita, L. Janssen, Xiao Li, C. J. Van Diepen, C. Reichl, W. Wegscheider, S. Das Sarma, and L. M. K. Vandersypen. Quantum simulation of a Fermi–Hubbard model using a semiconductor quantum dot array. *Nature*, 548:70–73, Aug 2017.

[4.18] N. F. Mott. The Basis of the Electron Theory of Metals, with Special Reference to the Transition Metals. *Proc. Phys. Soc. A*, 62(7):416–422, Jul 1949.

[4.19] P. W. Anderson. Localized Magnetic States in Metals. *Phys. Rev.*, 124(1):41–53, Oct 1961.

[4.20] J. Kondo. Resistance Minimum in Dilute Magnetic Alloys. *Prog. Theor. Phys.*, 32(1):37–49, Jul 1964.

[4.21] R. Hanson, L. P. Kouwenhoven, J. R. Petta, S. Tarucha, and L. M. K. Vandersypen. Spins in few-electron quantum dots. *Rev. Mod. Phys.*, 79(4):1217–1265, Oct 2007.

[4.22] D. Goldhaber-Gordon, Hadas Shtrikman, D. Mahalu, David Abusch-Magder, U. Meirav, and M. A. Kastner. Kondo effect in a single-electron transistor. *Nature*, 391:156–159, Jan 1998.

[4.23] W. G. van der Wiel, S. De Franceschi, T. Fujisawa, J. M. Elzerman, S. Tarucha, and L. P. Kouwenhoven. The Kondo Effect in the Unitary Limit. *Science*, 289(5487):2105–2108, Sep 2000.

[4.24] A. Yu Kitaev. Unpaired Majorana fermions in quantum. *Phys.-Usp.*, 44(10S):131–136, Oct 2001.

[4.25] E. Majorana. Teoria simmetrica dell'elettrone e del positrone. *Nuovo Cim.*, 14(4):171–184, Apr 1937.

[4.26] R. Aguado. Majorana quasiparticles in condensed matter. *La Rivista del Nuovo Cimento 40, 523 (2017)*, 40:523–593, Oct 2017.

Further reading

☞ G. D. Mahan, *Condensed matter in a nutshell* (Princeton Univ. Press, Princeton, 2010)
☞ H. Bruus and K. Flensberg, *Many-Body Quantum Theory in Condensed Matter Physics* (Oxford Univ. Press, Oxford, 2004)
☞ T. Ihn, *Semiconductor Nanostructures: Quantum states and electronic transport* (Oxford Univ. Press, Oxford, 2009)
☞ A. H. Castro Neto, F. Guinea, N. M. R. Peres, K. S. Novoselov and A. K. Geim, *The electronic properties of graphene*, Rev. Mod. Phys **81**, 109 (2009).
☞ M. Imada, A. Fujimori, and Y. Tokura, *Metal-insulator transitions*, Rev. Mod. Phys **70**, 1039 (1998).
☞ P. Barthelemy and L. M. K. Vandersypen, *Quantum dot systems: a versatile platform for quantum simulations*, Ann. Phys. **525**, 808 (2013).

Part II.

Artificial quantum systems

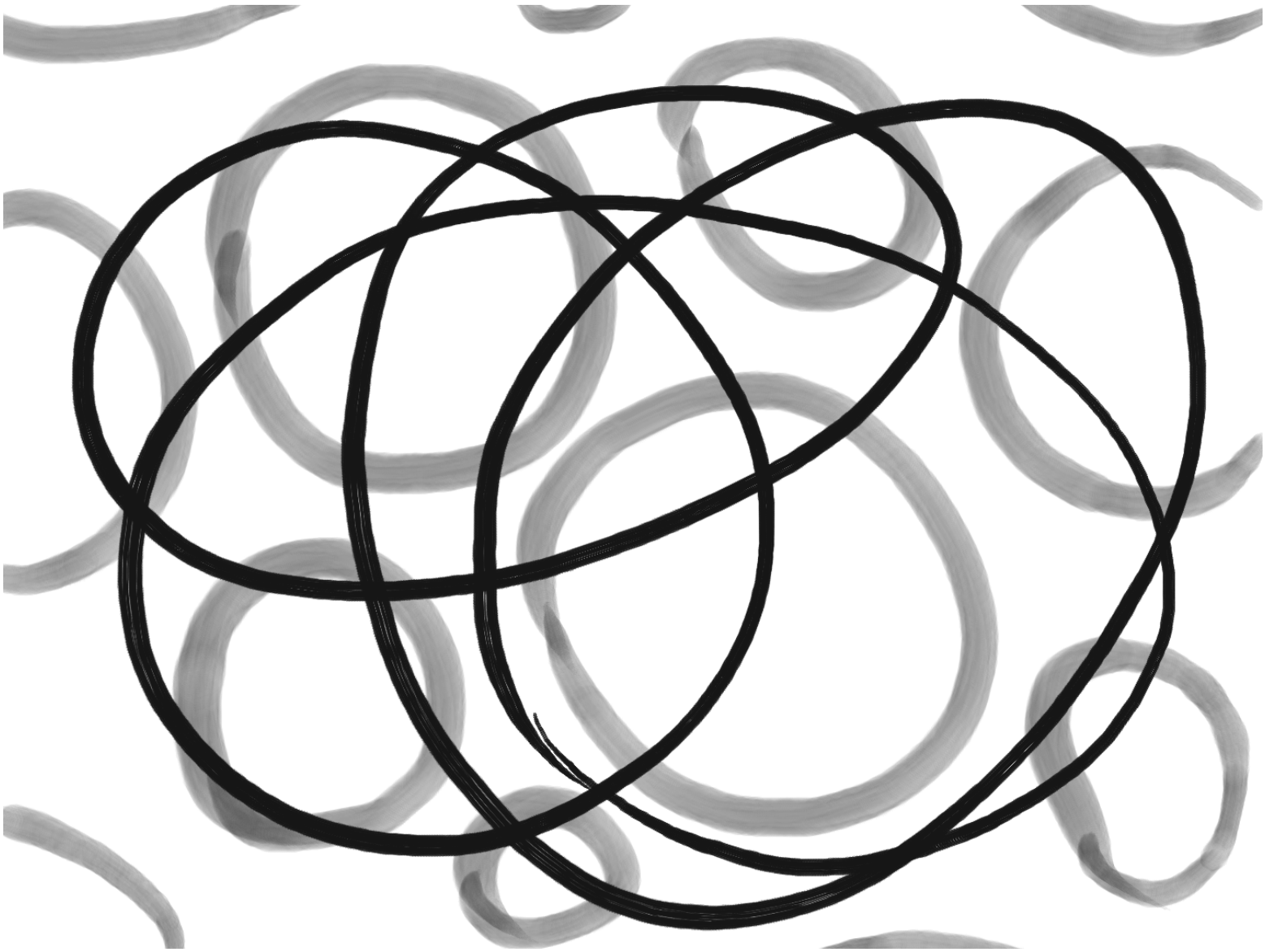

In the previous chapters, we have discussed how quantum many body effects appear in condensed matter systems existing in nature (with more or less help from humans with scotch tapes, in some cases). However, we are not restricted to that: experimental advances allow to construct and manipulate systems where the quantum nature of electrons manifest in all its glory (artificial atoms, interferometers, qubits...), and where new effects and quasiparticles emerge (conductance quantization, resonant tunneling, Majorana fermions...). These are prominent as the system dimensionality (not necessarily its dimensions) is reduced. The best example of this was the discovery of the quantum Hall effect in two dimensional electron gases[24], which we will see below.

[24] K. von Klitzing, G. Dorda, M. Pepper, New method for high-accuracy determination of the fine-structure constant based on quantized Hall resistance, Phys. Rev. Lett. **45**, 494 (1980).

5. Low dimensional systems: From the real to the Hilbert space

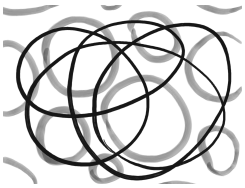

In the last decades –mainly since the ability to isolate high quality two dimensional electron gases (2DEG) in the 80's– there has been huge advances in the design and control of systems where quantum effects can be measured and manipulated, opening new platforms for the investigation of some of the underlying mechanisms in condensed matter (e.g., Coulomb correlations, spin interactions...) and some prominent quantum mechanical effects (manifestations of the Pauli exclusion principle, quantum superpositions, electronic interferences...). Most remarkably, new effects have been discovered in systems with electrons confined in one or more spatial dimensions (such as the mentioned 2DEGS, quantum wires, quantum dots, atomic junctions, qubits of different types...), with unexpected quasiparticles showing up: chiral electrons in edge states, anyons (not fermions nor bosons)... We will see how this has opened new fields of research (quantum and topological transport, quantum open systems, quantum information...). There are many dots (. . .) in this paragraph because the list of new phenomena is endless... and open!

This chapter is organized in three main parts, one for each reduced dimensionality from 2-D to 0-D configurations. Each of them is formed by two sections: the first one discusses general properties and experimental implementations (for which we mainly follow Refs. [5.1] and [5.2]), followed by another section describing some examples of prominent physical phenomena (the quantum Hall effect in 2DEGs, conductance quantization in quantum point contacts, single-electron transport and qubits in quantum dots) related to them.

5.1. Two dimensional electron gas

In Sec. 4.2 we already saw a purely two-dimensional system (graphene), where electrons are restricted to move over a single-atom thick layer. We discuss now how to obtain a 2DEG from thicker pieces of material. We know from quantum mechanics that energy is quantized when motion along one direction is confined (remember the particle in a box problem). If we consider a system in which electrons can move freely along two dimensions (say x and y) but is confined in the third one (due to e.g., a hard wall potential), the wave function is of the form:

$$\psi_{n\sigma}(x,y) = \frac{1}{\sqrt{\mathcal{A}}} e^{ik_x x} e^{ik_y y} \phi_n(z) \chi_\sigma, \tag{5.1}$$

where $\mathcal{A}$ is the area, χ_σ is the spinor, and the transverse modes $\phi_n(z)$ depend on the confinement potential. Denoting the energy of these modes as ε_n, electrons have a total energy:

$$\varepsilon_{k_x k_y n} = \frac{\hbar^2}{2m}(k_x^2 + k_y^2) + \varepsilon_n, \tag{5.2}$$

where we have neglected spin effects.

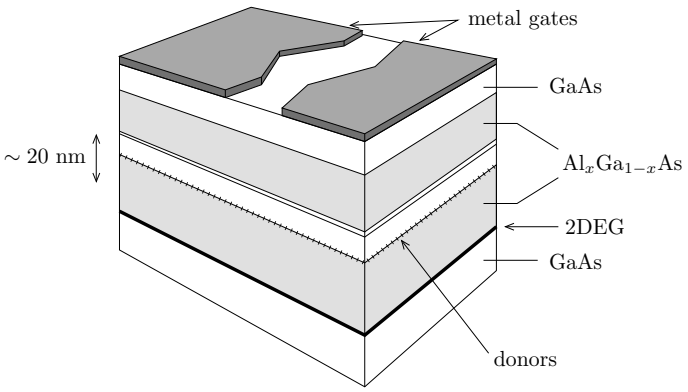

Figure 5.1.:
Semiconductor heterostructure with a 2DEG formed in the interface of GaAS and AlGaAs layers. On top of it, metal gates are deposited that deplete the electronic gas below, forming a nanostructure.

The above wavefunction is still three-dimensional, no matter how narrow the z-confinement is, as soon as electrons can distribute over the different modes $\phi_n(z)$. In order to effectively have a two-dimensional electron gas, where the n degree of freedom plays no role, electrons must stay in the ground state n=1. This will be the case if thermal fluctuations are suppressed, that is, when

$$\varepsilon_2 - (\varepsilon_1 + E_F) \gg k_B T. \tag{5.3}$$

Considering a square well potential of width a,[1] with energies $\varepsilon_n = (n\pi\hbar)^2/2ma^2$,[2] and for typical Fermi energies of 10 meV, this will happen even at room temperature ($k_B T_{room} \approx 0.02$ eV) provided that $a \ll 120a_0$, i.e., if the well is a few nanometer wide[3]. However, condition (5.3) is easily met at subkelvin temperatures, where most experiments are performed[4].

5.1.1. Semiconductor heterostructures

The field of mesoscopic physics developed rapidly when high mobility 2DEGs where obtained in the interface of layered semiconductors, as the one sketched in Fig. 5.1. In most of the cases, GaAS/AlGaAS interfaces are used, because they have very similar lattice constant, which helps to reduce imperfections. The key aspect is that GaAs and AlGaAs have different gaps, so the there is a mismatch of the bottom of the conduction bands at the interface. This results in charge accumulation on both sides, resulting in the band forming a narrow (of the order of 5 nm) triangular well where the 2DEG is formed, as discussed above[5].

In order to measure the properties of the sandwiched 2DEG, ohmic contacts are formed by high temperature evaporation of Ge, which diffuses across the GaAs layer. These contacts can then be wired and attached to probes that allow for transport experiments.

Furthermore, metallic gates can be deposited on top of the sample (dark regions in Fig. 5.1) which work as a capacitor with the 2DEG underneath. Upon the application of negative voltages, they reduce the charge density in the 2DEG. Then, electrons below the gates are depleted, allowing for the design of nanostructures in the gas. This way, narrow constrictions forming quantum point contacts (QPC) and tunnel barriers can be implemented and combined to form e.g., quantum dot (QD) arrays, as shown in Fig. 5.2 (we will treat these cases in the next sections).

[1] Typically, confining potentials, as those found in the configurations discussed in Sec. 5.1.1 will rather be triangular.
[2] Check your favourite book on quantum mechanics, or even a not so good one.
[3] This is a very rough estimate: typically confinement potentials are not square but triangular; also, the effective electron mass in the material is needed.
[4] For convenience, if one wants to get rid of phonon contributions.
[5] The corresponding level spacing is of the order of 20 meV.

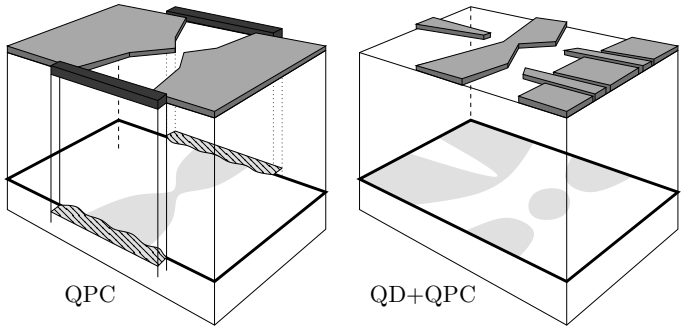

Figure 5.2.:
Formation of nanoestructures in a 2DEG by top gates. Left panel: a quantum point contact (QPC) connected to two electronic reservoirs via ohmic contacts. Right: two tunnel barriers define a quantum dot (QD). It is capacitively coupled to a QPC working as a charge detector.

5.2. The quantum Hall effect

The discovery of the integer quantum Hall effect in 2DEGs [5.3] is the starting point of the field of mesoscopic physics where quantum effects can be measured and controlled in condensed matter systems. Initially, the measurement of quantized Hall resistances $R_{\mathrm{H}} = R_K/i$, with $i \in \mathbb{N}$ and the von Klitzing resistance $R_K = h/e^2$, was proposed to serve for metrological standards[6], but it soon expanded to a plethora of phenomena, such as the fractional, the spin and the anomalous quantum Hall effects, opening the physics of topological insulators, non-abelian states, quantum optics with electrons...

The classical Hall effect:

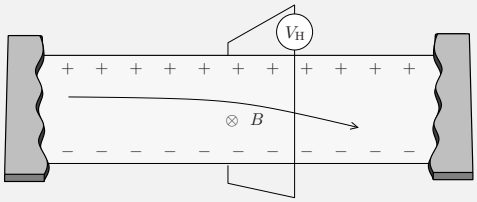

In a two dimensional metal, the Hall effect appears as a manifestation of the Lorentz force

$$\mathbf{F} = -e(\mathbf{E} + \mathbf{v} \times \mathbf{B})$$

experienced by an electron moving with a speed $\mathbf{v}$ perpendicularly to a magnetic field $\mathbf{B} = B_z\mathbf{u}_z$. The stationary solution of the equation of motion (in the Dude model for transport) relates it with the friction term

$$\mathbf{F} - \frac{1}{\tau}m\mathbf{v} = 0,$$

where τ is the time between collisions. The current density $\mathbf{J} = -en\mathbf{v}$ (with the carrier density n) can be related to the electric field in matricial form $\mathbf{J} = \sigma_D\mathbf{E}$,[a] with the conductivity

$$\sigma_D = \frac{e^2 n\tau}{m(\omega_B^2\tau^2 + 1)}\begin{pmatrix} 1 & -\omega_B\tau \\ \omega_B\tau & 1 \end{pmatrix}.$$

Here, $\omega_B = eB/m$ is the cyclotron frequency. The resistivity $\rho_D = \sigma_D^{-1}$ shows a transverse resistance $\rho_{xy} = B/en$.[b] It can be measured as a developed transverse (Hall) voltage, V_{H}, as shown in the inset figure. Remarkably different from the longitudinal resistances ρ_{xx} and ρ_{yy}, it does not depend on τ (henceforth, on the conduction properties of the metal).

[a] This is nothing but Ohm's law.
[b] Note ρ_{xy} is linear in B.

[6] Indeed, for relating two of the seven defining constants that establish the modern international system of units (redefined very recently [5.4]), it is a central measurement in metrology.

5.2.1. Landau levels

Let us start by considering the problem of an electron moving in two dimensions in the presence of a perpendicular magnetic field $\mathbf{B} = B\mathbf{u}_z$. Additionally, we assume a potential $U(y)$ which will confine the motion within the Hall bar. The hamiltonian is:

$$\hat{H} = \frac{1}{2m}\left(\hat{\mathbf{p}} + e\hat{\mathbf{A}}\right)^2 + \hat{U}(y). \tag{5.4}$$

Gauge invariance allows to chose the vector potential $\hat{\mathbf{A}}$ as long as it satisfies $\nabla \times \hat{\mathbf{A}} = \hat{\mathbf{B}}$. In particular, one chooses the Landau gauge

$$\hat{\mathbf{A}} = -\hat{y}B\mathbf{u}_x, \tag{5.5}$$

which leads to

$$\hat{H} = \frac{1}{2m}\left(\hat{p}_x - e\hat{y}B\right)^2 + \frac{\hat{p}_y^2}{2m} + \hat{U}(y). \tag{5.6}$$

It is x-translational invariant, so we can replace $\hat{p}_x = \hbar k$. Defining

$$\omega_\mathrm{B} = \frac{eB}{m} \quad \text{and} \quad l_\mathrm{B} = \sqrt{\frac{\hbar}{eB}}, \tag{5.7}$$

the cyclotron frequency and the magnetic length,[7] respectively, we arrive to the hamiltonian of a harmonic oscillator:

$$\hat{H} = \frac{\hat{p}_y^2}{2m} + \frac{1}{2}m\omega_\mathrm{B}^2\left(\hat{y} - y_k\right)^2 + \hat{U}(y), \tag{5.8}$$

displaced by $y_k = \hbar k/eB$.

The eigenenergies depend on the particular shape of the potential, which can be complicated. We can consider two limiting cases. (i) In the case $V(y) = 0$, the spectrum is quantized:

$$E_n^{(0)} = \hbar\omega_\mathrm{B}\left(n + \frac{1}{2}\right), \tag{5.9}$$

where $n = 0, 1, 2\ldots$ labels the Landau levels. They are degenerate in k, which determines the position around which each electron oscillates. (ii) If the potential is smooth, we can make a Taylor expansion

$$U(y) \approx U(y_0) + \frac{\partial U}{\partial y}(y - y_0) \tag{5.10}$$

around each position y_0. Then, ignoring the constant term, we get an effective electric field $-eE = U'$. The hamiltonian in Eq. (5.6) then becomes:

$$\hat{H} = \frac{\hat{p}_y^2}{2m} + \frac{1}{2m}\left(\hbar k - e\hat{y}B\right)^2 - eE\hat{y}. \tag{5.11}$$

Completing the square, we arrive to

$$\hat{H} = \frac{\hat{p}_y^2}{2m} + \frac{1}{2}m\omega_\mathrm{B}^2\left(\hat{y} - y_{kE}\right)^2 - eEy_{kE} + \frac{mE^2}{2B^2}, \tag{5.12}$$

[7] Orders of magnitude: $l_\mathrm{B} \approx 25$ nm for B=1 T.

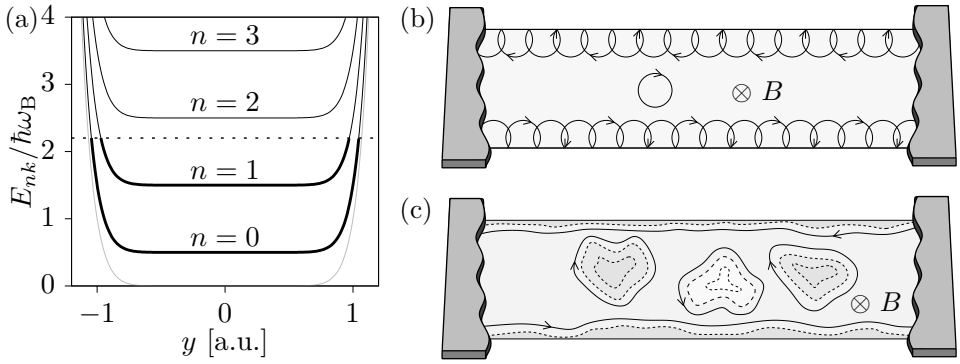

Figure 5.3.: (a) Landau level quantization in the presence of a confining potential in the y direction (grey line). The occupied states below the Fermi energy (dashed line) are highlighted. (b) Semiclassical interpretation of the edge states in terms of skipping orbits following the borders of the sample. They lead to transport between two terminals. (c) Electrons move following equipotential lines, forming closed loops due to disorder in the bulk and extended (conducting) states in the edges.

with the displacement given by $y_{kE} = y_k + mE/eB$. The eigenenergies are:

$$E_{nk} = \hbar\omega_B \left(n + \frac{1}{2}\right) - eEy_{kE} + \frac{mE^2}{2B^2}. \tag{5.13}$$

Note that k determines not only the position of the electron but also its energy. The energies follow the local electric field.

A crucial aspect of the energies in Eq. (5.13) is that the group velocity

$$v_x = \frac{1}{\hbar}\frac{\partial E_{nk}}{\partial k} = -\frac{E}{B} \tag{5.14}$$

depends on the electric field.

Going back to the smooth potential, we make two observations:

- ☞ the electron energy adapts to the local details of the potential. An example of this is plotted in Fig. 5.3(a) for $V(y) = y^{12}$ and assuming strong magnetic fields such that mE^2/B^2 is the smaller energy scale in the problem.
- ☞ the group velocity depends on the local properties of the potential:

$$v_x = \frac{1}{eB}\frac{\partial U}{\partial y}. \tag{5.15}$$

They imply that for a potential that confines electrons in one direction, as the one plotted in Fig. 5.3(a), electrons move in opposite directions on opposite edges of the potential: they are chiral! A semiclassical interpretation of this effect is sketched in Fig. 5.3(b): assuming a Hall bar with a uniform potential with hard walls, skipping orbits forms in the center of the system which give rise to propagation along the edges when interrupted by the wall[8].

In a real system, the potential is not as smooth as in Fig. 5.3(a). It will rather contain imperfections (disorder), resulting on an amount of potential hills and dips. The electron chirality will make them stick to these regions tending to form closed orbits as sketched in Fig. 5.3(c). With a reasonable

[8] Similarly to how a spinning top moves to the other side of the room when it hits the border of a carpet.

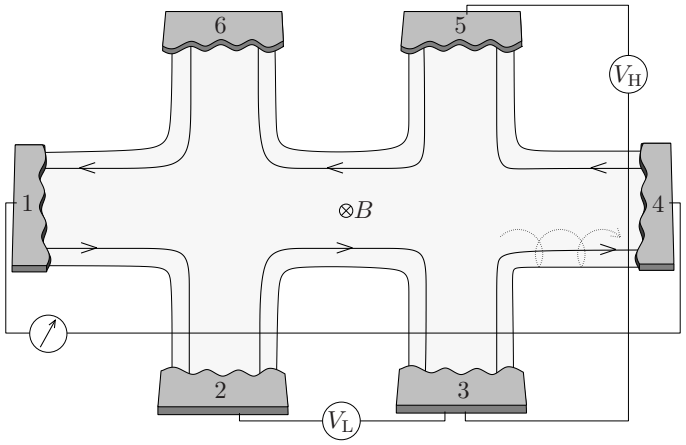

Figure 5.4.:
Quantum Hall bar coupled to six terminals. A current injected between terminals 1 and 4 generates a quantized transverse voltage difference V_H measured between terminals 3 and 5, but no longitudinal voltage between 2 and 3. This is due to electrons flowing chirally along edge states.

amount of disorder, no orbit will connect the two transverse edges of the sample. The existence of states connecting longitudinally the two ohmic contacts is enabled by topology. We will come back to the importance of disorder later.

5.2.2. Transport along edge states

Let us assume all Landau levels with $n \geq 2$ are empty i.e., only the first one is (partially) occupied. Knowing the velocity of electrons in the longitudinal direction, x, we can calculate the electric current:

$$I_x = e \int \frac{dk}{2\pi} v_x(k). \tag{5.16}$$

Using $dk = l_B^{-2} dy$ and Eq. (5.15), we arrive to

$$I_x = \frac{e}{h} \Delta U, \tag{5.17}$$

which relates the electron flow to a potential difference, ΔU. between the two edges of the system. The later can be measured by voltmeters, giving a voltage $V_H = \Delta V_y = \Delta U/e$. The result is a transverse (Hall) resistance which is quantized[9]:

$$R_K = \frac{h}{e^2} \approx 25812.8\,\Omega. \tag{5.18}$$

The measurement scheme is sketched in Fig. 5.4: a current flows between terminals 1 and 4. All other terminals represent voltage probes. Transverse voltages are measured between terminals 2 and 3 and terminals 5 and 6. Every combination will give the same result. Remarkably, the longitudinal voltage V_L (measured between terminals 2 and 3, or between 5 and 6, will be zero! This means that electrons flow without resistance along the conductor.

Note that the previous result does not imply that transport is flowing only at the edges of the sample. In principle, every state contributes. Think, for instance on a potential that is not totally flat in the center of a clean sample. If the chemical potential or the magnetic field are tuned such that the next Landau level starts to be populated. Then the resistance will continually increase between R_K and $R_K/2$, when the second level is full. This does not lead to the quantization of the resistance. In order

[9]The label K stands for von Klitzing.

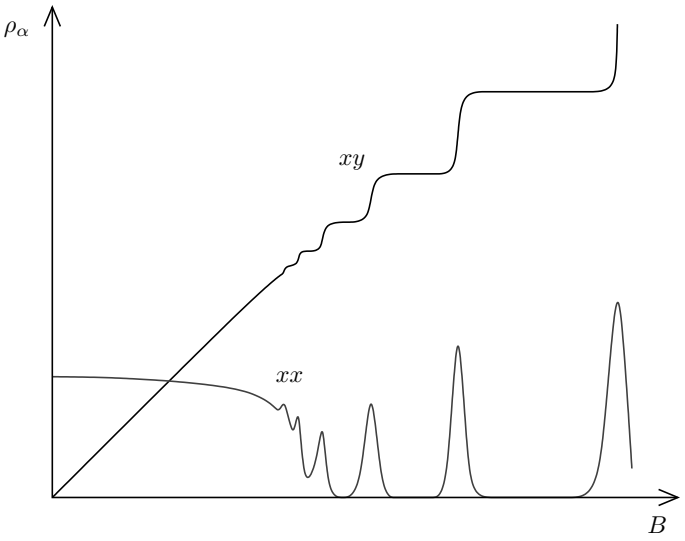

Figure 5.5.:
Experimental detection of the quantum Hall effect (sketch following Ref. [5.8]). Increasing the magnetic field, B, the transverse resistance ρ_{xy} stops being linear and shows steps at inverse multiples of h/e^2. In the plateaus, the longitudinal resistance, ρ_{xx}, vanishes.

to find it, we need to invoke again the presence of a disordered potential. As discussed above, this leads to a distribution of localized states[10] in the center of the sample and extended states close to the edges [5.6][11]. In that case, the localized states are the first to be filled, so transport reaches a *plateau*. Only when the extended states are filled the resistance jumps to the new quantized level. In the transition, the longitudinal resistance becomes finite. These are indeed the properties (sketched in Fig. 5.5) that lead to the discovery of the quantum Hall effect [5.3].

The presence of disorder is then essential for the detection of universal resistance plateaus $R_\mathrm{H} = e^2/\nu h$. The electronic chirality implies that disorder does not introduce backscattering [5.9][12]. The edge states therefore form perfect conducting channels[13]. Only when the potential is such that two (counterpropagating) edge channels are brought close to each other, transitions between them are possible. Transport then depends on the scattering properties of the constriction [5.11], which can be controlled with external voltages.

Different from the integer quantum Hall effect, the quantum anomalous [5.12] and quantum spin Hall [5.13, 5.14] effects do not need a magnetic field, but rather the presence of finite magnetization or of spin-orbit coupling, respectively. In both cases, a picture of transport based on edge-states is still commonly used[14]. However, very recent experiments seem to challenge this interpretation in the quantum anomalous Hall case [5.15, 5.16].

5.3. One dimensional conductors

If we continue to confine the electron motion along another dimension (y this time), we get:

$$\psi_{ln\sigma}(x) = \frac{1}{\sqrt{\mathcal{L}}} \mathrm{e}^{ik_x x} \zeta_l(y) \phi_n(z) \chi_\sigma, \tag{5.19}$$

[10] The occurrence of localization due to disorder was introduced by P. W. Anderson [5.5].
[11] See also Ref. [5.7] for a popular discussion of the edge state picture.
[12] Can you understand this invoking the semiclassical picture of Fig. 5.3(b)?
[13] One can then perform quantum optics experiments with electrons, using the edge states as wave guides [5.10].
[14] In the quantum spin Hall effect, electrons propagate along helical rather than chiral edge states: electrons with opposite spin move in opposite directions along the same edge.

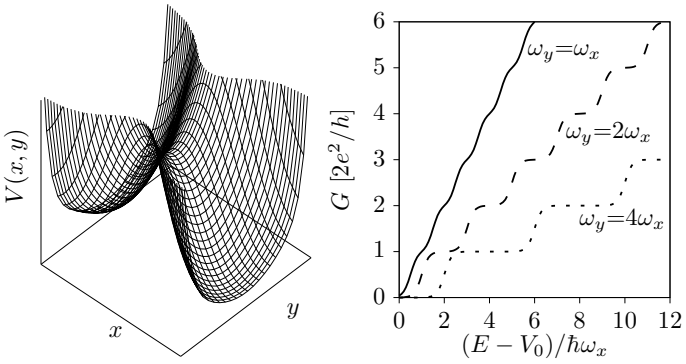

Figure 5.6.:
Conductance quantization in a quantum point contact, according to the saddle point approximation, see Eq. (5.28).

with the modes $\zeta_l(y)$ quantized. The energies now read $\varepsilon_{k_x ln} = \frac{(\hbar k_x)^2}{2m} + \varepsilon_{ln}$. Following the same arguments as in Sec. 5.1, the conditions to dynamically wash out the dimensions y and z are $\varepsilon_{10} - \varepsilon_{00} - E_F \gg k_B T$ and $\varepsilon_{01} - \varepsilon_{00} - E_F \gg k_B T$.

We can find different systems that satisfy these requirements, among them:

- ☞ Nanowires: typically grown by evaporation of the semiconductor on gold nanoparticles. Their diameter is about 20 nm, and they can be as long as several micron.
- ☞ Carbon nanotubes: take a graphene ribbon and roll it as a cigarette. Depending on the direction you roll it, it will be metallic or a semiconductor. The chirality of electrons in graphene manifests as a spin-orbit effect[15]. Level spacings are large, of the order of 1 eV, i.e., 12000 K/k_B.
- ☞ Molecular junctions: real molecules can be captured in a break-junction [5.17] or at the tip of a scanning tunneling microscope [5.18]. The electronic transport across it probes the structure of the molecular orbitals [5.19].

They can be engineered out of semiconductor 2DEGs in various ways [5.20]. For its historical and conceptual relevance, we will discuss the case of a top-gate defined quantum point contact.

5.4. Quantum point contacts

Consider a 2DEG with electrons moving along a strip along the x direction. The quantization due to the y confinement, defines the transverse modes l that can propagate along the conductor, similarly to what happens in a waveguide. Voltages applied to top gates can induce an additional potential that narrows the strip locally, as shown in Fig. 5.2. For the one-dimensional motion along x, this is as if the energy $\varepsilon_{l1}(x)$ forms a potential barrier[16].

The particular shape of the potential is in general not important. All electrons with energies well below the top of the barrier will be reflected. This is not the case close to the top of the barrier, where the potential can be approximated by a saddle point of the form [5.21]:

$$V(x,y) \approx V_0 - \frac{1}{2}m\omega_x^2 x^2 + \frac{1}{2}m\omega_y^2 y^2. \tag{5.20}$$

This is illustrated in the left panel of Fig. 5.6. The barrier can be tuned with the top gate voltages. The barrier height, V_0, controls the number of transverse modes that are allowed to propagate along the conductor. Decreasing it increases the number of modes, N, that will contribute to the current. For a single mode, this is given by [5.22]

$$I_n = v_n \Delta\rho_n, \tag{5.21}$$

[15] The orbit is defined by the (left- or right-handed) rotation of the electron around the nanotube axis.
[16] Discrete energies increase with the decreasing of the confining potential range, remember the particle in a box problem.

where v_n is the group velocity:

$$v_n = \frac{1}{\hbar} \left. \frac{\partial \varepsilon(k)}{\partial k} \right|_\mu , \tag{5.22}$$

and

$$\Delta\rho_n = e \left. \frac{\partial n}{\partial E} \right|_\mu eV = e^2 \upsilon_\mathrm{F} V \tag{5.23}$$

is the difference of charge carrier density due to a voltage difference V applied to the two sides of the barrier[17]. It depends on the density of states, which in one dimension is

$$\upsilon_\mathrm{F} = \frac{1}{\pi} \left. \frac{\partial k}{\partial \varepsilon(k)} \right|_\mu = \frac{1}{\pi\hbar v_n}. \tag{5.24}$$

The current then becomes:

$$I_n = \frac{2e^2}{h} V, \tag{5.25}$$

totally independent on the details of the material! This defines the quantum of conductance

$$G_0 = \frac{2e^2}{h}, \tag{5.26}$$

which sets the conductance $G = \partial I/\partial V$ of a fully transmitting mode. Summing to all transmitting modes, the total current is $I \approx NG_0V$.

This effect is elegantly described by the Landauer formula, which treats conduction as a scattering problem[18] and relates the conductance to the transmission probability of each mode $\mathcal{T}_n$ from one terminal to the other across the barrier:

$$G = \frac{e^2}{h} \sum_n \mathcal{T}_n. \tag{5.27}$$

The missing factor 2 is recovered by summing separately the spin degree of freedom. Note that if N modes are fully transmitting and all others are fully reflecting, the conductance reads $G = 2Ne^2/h$. Experimentally, transport quantization was observed as steps in the conductance as a function of the gate voltage applied to the constriction [5.29, 5.30].

For the potential in Eq. (5.20), the transmission probabilities can be calculated[19], giving [5.21]:

$$\mathcal{T}_n = \left(1 + \mathrm{e}^{-2\pi\alpha_n}\right)^{-1}, \quad \text{with} \quad \alpha_n = \frac{1}{\hbar\omega_x}\left[E - V_0 - \hbar\omega_y\left(n + \frac{1}{2}\right)\right]. \tag{5.28}$$

The result is plotted in Fig. 5.6, reproducing the experimental measurements. Tunneling enables a finite transmission below the steps.

Apart from confirming the scattering theory of quantum transport, the detection of conductance quantization paved the way to the field of semiconductor nanostructures. In this sense, the QPC can be seen as the minimal constituent of more complex structures: for instance, a QPC acts as the separation between two regions in the conductor. This way, a two-dimensional stripe can be divided in regions of different size (from large cavities to small small quantum dots) separated by a series of QPCs that

[17] Assuming V is small.

[18] See e.g., Refs. [5.23] and [5.11] for first hand discussions, or Ref. [5.24, 5.25] for recent reviews. Several textbooks also discuss it, see Refs. [5.1, 5.26, 5.27, 5.28].

[19] Assuming a WKB approximation.

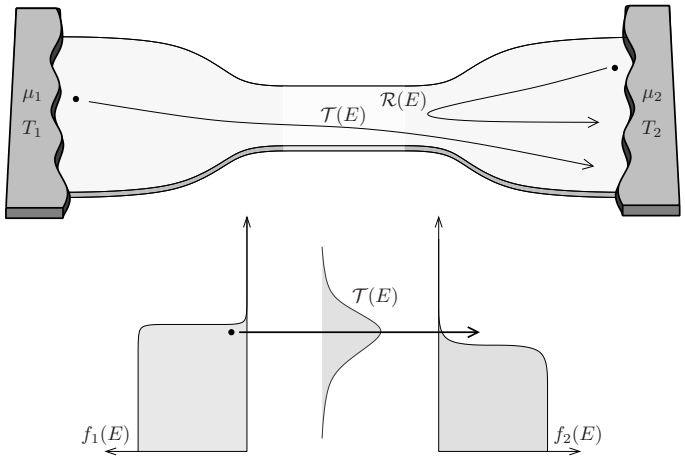

Figure 5.7.:
Two terminal quantum conductor. Electrons propagate ballistically between terminals 1 and 2 at electrochemical potential μ_i and temperature T_i. For a single mode scattering region, electrons are transmitted with probability $\mathcal{T}(E)$ and reflected with $\mathcal{R}(E) = 1 - \mathcal{T}(E)$. Transport appears in the presence of a nonequilibrium situation described by the difference of Fermi distributions $f_1(E) - f_2(E)$.

can furthermore serve to control the transfer of electrons between them (e.g., in the form of tunneling barriers). A remarkable example of this is when QPCs are defined in quantum Hall systems. Then they behave as beam splitters for electrons that propagate along the edge states: they are transmitted with probability $\mathcal{T}$ and reflected with $1 - \mathcal{T}$. This way, quantum optics experiments can be performed with electrons [5.10], including different types of interferometers[20].

5.4.1. Scattering approach to quantum transport

Equation (5.27) is strictly valid for non-interacting electrons flowing in response to a small voltage (established by a chemical potential difference between the two reservoirs) and at low temperatures. For a two terminal conductor, as the one sketched in Fig. 5.7, it can be obtained[21] from the Landauer-Büttiker expression for the charge current into terminal j:

$$I_j = -\frac{e}{h}\sum_n \int dE \mathcal{T}_n(E)[f_{j'}(E) - f_j(E)], \tag{5.29}$$

where j' denotes the other terminal and $f_i(E) = \{1 + \exp[(E - \mu_i)/k_B T_i]\}^{-1}$ introduces the occupation of the propagating mode. Obviously, charge conservation gives $I_{j'} = -I_j$. Setting a nonequilibrium situation, e.g. due to a difference of chemical potential $\Delta\mu = \mu_j - \mu_{j'}$ or of temperature $\Delta T = T_j - T_{j'}$, will result in general in a finite charge current flowing through the conductor[22].

Similarly, one can define the heat currents carried by electrons [5.31]:

$$J_j = \frac{1}{h}\sum_n \int dE(E - \mu_j)\mathcal{T}_n(E)[f_{j'}(E) - f_j(E)]. \tag{5.30}$$

The interpretation is clear: each electron with energy E dissipates an excess of energy $E - \mu_j$ when absorbed by terminal j. Note that, differently from charge currents, heat currents are not conserved:

$$J_j + J_{j'} = VI_j = -P, \tag{5.31}$$

[20] How would an electronic Fabry-Perot interferometer be built this way? Note that for the interferometer, one needs to think in terms of transmission amplitudes, rather than probabilities.

[21] Remember the Sommerfeld expansion.

[22] In the case of a temperature difference (thermoelectric effect), the transmission probability needs to depend on energy. Can you say why?

as one needs to take power dissipated by the current in the presence of a voltage difference $V = -\Delta\mu/e$ (Joule heating) into account[23]. The sign convention here means that $P < 0$ when electrons flow in favour of the electrochemical potential difference[24].

Linear regime

Note that all the effects of nonequilibrium states appear only in the distribution functions. Assuming that transport is due to small electrochemical potential ($\delta\mu_j = \mu_j - \mu \ll k_B T$) or temperature differences ($\delta T_j = T_j - T \ll T$), we can linearize

$$f_{j'}(E) - f_j(E) \approx -\partial_E f(E)\left[\delta\mu_{j'} - \delta\mu_j + \frac{E-\mu}{T}(\delta T_{j'} - \delta T_j)\right]. \tag{5.32}$$

Then, using $\delta V_{j'j} = (\delta\mu_{j'} - \delta\mu_j)/(-e)$ and $\delta T_{j'j} = \delta T_{j'} - \delta T_j$, we can write the different currents as

$$I_j = G\delta V_{j'j} + L\delta T_{j'j} \tag{5.33}$$

$$J_j = M\delta V_{j'j} + K\delta T_{j'j}, \tag{5.34}$$

where G and K are the electrical and thermal conductances, respectively, and L and M are the Seebeck and Peltier thermoelectric coefficients[25]. The electrical conductance reads:

$$G = \frac{e^2}{h}\sum_n \int dE\mathcal{T}_n(E)[-\partial_E f(E)]. \tag{5.35}$$

At low temperatures, we can make a Sommerfeld expansion and recover the Landauer expression in Eq. (5.27).

In the same way as electrical currents, heat currents are also quantized. If the linear regime, the thermal conductance $K = \partial J/\partial\delta T$ is bounded by $0 \le K \le K_0 = 2K_P$, with the quantum of thermal conductance being[26]

$$K_P = \frac{\pi^2 k_B^2 T}{3h}. \tag{5.36}$$

That the maximal heat that a single channel can support is $K_P\Delta T$ was first obtained by Pendry for photons in a waveguide [5.32]. However it turns out to be universal, irrespective of the statistics of the carriers. It was recenty measured for electrons by controlling the number of channels with QPCs [5.33] or in atomically-thin break junctions [5.34][27].

[23] To prove this is straightforward once it is clear that energy currents are conserved [5.25].

[24] In what cases can P be positive?

[25] What are their general expressions?

[26] To proof this, one can again use the Sommerfeld expansion. Note again the factor 2 coming from the spin degeneracy.

[27] Note it includes the Lorenz number

$$L_N = \frac{\pi^2 k_B^2}{3e^2} \approx 2.44 \times 10^{-8}\,\mathrm{W\Omega K^{-2}}$$

from where it is easy to relate the electrical and thermal quanta: $K_0 = L_N G_0 T$. Indeed the Sommerfeld expansion of the linear response conductances expresses the Wiedemann-Franz law: $K/G = L_N T$ for quantum conductors. It is known to be satisfied for macroscopic systems in terms of their conductivities, but nonlinearities or strong interactions challenge it in the nanoscale.

Multiterminal configurations

An extension to multiterminal configurations is possible:

$$I_j = -\frac{e}{h}\sum_{j',mn}\int dE\mathcal{T}_{jn,j'm}(E)[f_{j'}(E) - f_j(E)], \tag{5.37}$$

where $\mathcal{T}_{jn,j'm}(E)$ is the transmission probability for an electron injected from mode m connected to terminal j' to be scattered into mode n of terminal j.[28] This way for instance, four-probe measurements can be described: two terminals inject current, while another two are used to probe voltage differences along the conductor[29]. A clear example of this is the quantum Hall effect described in section 5.2: In order to obtain a simple description of the transport properties, it is sufficient to assume that electrons propagate along edge states without backscattering [5.9].

5.5. Zero dimensions

If motion in the three spatial dimensions is confined, all degrees of freedom are quantized $\psi_{lmn\sigma} = \xi_l\zeta_m\phi_n\chi_\sigma$, and result in discrete energies ε_{lmn}, analogously to what we find in atoms. For this reason, solid-state zero-dimensional systems are sometimes named as *artificial atoms*. The advantage is that they can be constructed and their properties can be manipulated externally (e.g., via electromagnetic potentials), hence controlling the energy level separation or inducing electronic transitions between some of them. One can also combine several 0-D systems in complex structures and make them interact (then, they form artificial *molecules* or lattices).

They can be constructed by spacial confinement in many different ways: by epitaxial growth of nanoparticles, by introducing inhomogeneities in the formation of nanowires, contacting C_{60} molecules (fullerene [5.35]), defining quantum corrals in metallic surface states [5.36], or by depletion of a 2DEGs with top gates, among many others. There are less obvious ways to find few level systems, for instance based on circulating currents in superconducting loops with Josephson junctions [5.37]. In each case, states will be affected by different degrees of freedom (charge, spin, valley, vibrations) and different interactions may be relevant (for instance, electron-electron or electron-phonon interactions, charge noise, spin exchange, spin-orbit coupling...).

More complex configurations can also be done where the electronic system is coupled to additional degrees of freedom, like e.g., photons in a cavity [5.38, 5.39] serving as onchip platforms for quantum electrodynamics, or coupling to mechanical oscillation modes [5.40], e.g. in a carbon nanotube [5.40], as interfaces between quantum information and mechanics[30].

These properties make them interesting for probing quantum mechanical dynamics, for quantum information processing, or quantum optics experiments. Also, they are strongly affected by fluctuations and can be easily taken far from equilibrium, hence soon giving rise to nonlinear phenomena.

5.6. Quantum dots

The most typical artificial atom is a quantum dot defined in a 2DEG, as sketched in the right panel of Fig. 5.2: by applying voltages to them, the different gates serve to define the quantum dot region and to

[28] The expressions for the heat currents are obtained by inserting $(E - \mu_j)/(-e)$ into the integral.

[29] A voltage probe is modeled by connecting the conductor to a terminal (labelled by p) with a floating chemical potential such that no current flows out of it. The measured potential is given by the solution, μ_p, of this boundary condition, $I_p = 0$.

[30] And serving for instance as detectors of minute masses.

modulate the confining potential and hence, the energy levels $\varepsilon_n(V_g)$. The level spacing is typically of the order of $10-30\,\mu$eV. How the quantum dot is coupled to the rest of the 2DEG can also be controlled by defining tunneling barriers, so its properties can be probed by transport measurements [5.41]. Series of quantum dots can also be defined forming the analogue of artificial molecules where electrons are delocalized and coherent superpositions are formed[31] [5.42].

Due to the small size of the quantum dots, Coulomb interactions are strong, so adding one electron to the system costs an energy U (charging energy, of about 1-2 meV). The charge state of the quantum dot is then quantized and can be tuned to go down to be just zero or one electron. In this case, they can be described by a single-site Hubbard hamiltonian[32]:

$$\hat{H}_{\mathrm{QD}} = \sum_{\sigma} \varepsilon_\sigma \hat{n}_\sigma + U \hat{n}_\uparrow \hat{n}_\downarrow . \tag{5.38}$$

The size of the Hubbard-like array can be increased by tunnel-coupling several quantum dots:

$$\hat{H}_{\mathrm{array}} = \sum_{i\sigma} \varepsilon_{i\sigma} \hat{n}_{i\sigma} + U \hat{n}_{i\uparrow} \hat{n}_{i\downarrow} - \sum_{i\neq j,\sigma} \left(\tau_{ij} \hat{c}^\dagger_{i\sigma} \hat{c}_{j\sigma} + \mathrm{h.c.} \right), \tag{5.39}$$

where τ_{ij} is the hopping energy between dots i and j. They can be coupled in linear, triangular or square arrangements and tuned individually, allowing for quantum simulation experiments [5.43].

With the spin of the electron, a qubit can be formed by applying a magnetic field, with the two states $|+\rangle = |\uparrow\rangle$ and $|-\rangle = |\downarrow\rangle$, and energies:

$$\varepsilon_\pm = \varepsilon \pm \frac{\hbar}{2} g \mu_{\mathrm{B}} B_z, \tag{5.40}$$

where g is the gyromagnetic factor (depending on the details of the quantum dot) and μ_{B} is the Bohr magneton. It turns out that the spin coherence is sufficiently long in GaAs quantum dots[33] to be able to perform single and double qubit operations [5.41] by using electromagnetic pulses[34]. We will discuss the former case in the next section.

5.6.1. Single-electron transport through a quantum dot

A single-level quantum dot coupled to two terminals, as the one sketched in Fig. 5.2, can be described by the single-impurity Anderson hamiltonian, see section 4.3.2:

$$\hat{H} = \sum_{\sigma} \left(\varepsilon_\sigma \hat{n}_\sigma + U \hat{n}_\sigma \hat{n}_{-\sigma} \right) + \sum_{lk\sigma} \varepsilon_{lk\sigma} \hat{c}^\dagger_{lk\sigma} \hat{c}_{lk\sigma} + \sum_{lk\sigma} \left(V_{lki\sigma} \hat{d}^\dagger_\sigma \hat{c}_{lk\sigma} + \mathrm{h.c.} \right). \tag{5.41}$$

The first term accounts for the (Hubbard-like) quantum dot with one level at the discrete energy ε_σ, the Coulomb interaction[35] given by U, and $\hat{n}_\sigma = \hat{d}^\dagger_\sigma \hat{d}_\sigma$ is the number operator of electrons in state $|\sigma\rangle$. The second one describes the electrons in terminals $l = 1, 2$. The last term describes tunneling between the quantum dot and terminal l.[36] We will assume spin degenerate states (in the absence of a magnetic field), such that $\varepsilon_\sigma = \varepsilon$, for simplicity.

In equilibrium (and at low temperatures[37]), the number of electrons in the quantum dot, N, is defined by the chemical potential of the leads: $E_N - E_{N-1} < \mu_l < E_{N+1} - E_N$. Due to their reduced size,

[31] Similar to molecular orbitals.
[32] Remember section 4.3.
[33] A few miliseconds, even longer in silicon quantum dots.
[34] This is the minimal requirement to be able to build universal quantum gate operations.
[35] a.k.a. charging energy.
[36] Note it has the same structure as the hopping terms in the tight-binding approach in section 4.1.
[37] Experiments are preformed at $T \lesssim 100$ mK.

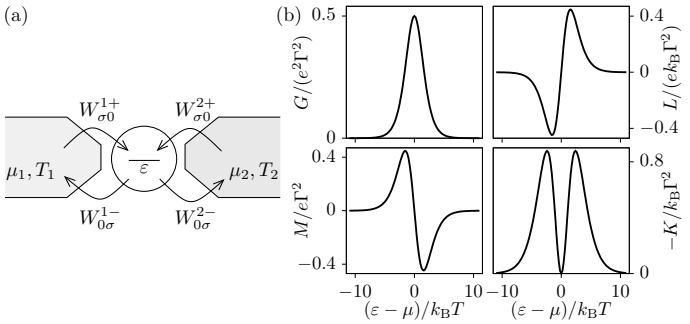

Figure 5.8.:
(b) Quantum dot tunnel-coupled to two terminals at chemical potential μ_l and temperature T_l. Electrons tunnel with rates $W^{l\pm}_{mn}$. (b) Linear response coefficients as functions of the level position, ε, for $\Gamma_1 = \Gamma_2 = \Gamma$.

the charging energy is usually large ($U \sim 1\,\text{meV}$) compared to temperature, so we can restrict the description of the system to a single level with energy ε, and consider the four states: $|0\rangle$, $|\sigma\rangle$, $|\uparrow\downarrow\rangle$. The energy costs of adding one electron are hence: $E_\sigma - E_0 = \varepsilon$, if initially the system is empty, and $E_{\uparrow\downarrow} - E_\sigma = \varepsilon + U$, if initially the system has one electron with spin σ. This means that adding a second electron to the quantum dot requires a higher energy, what defines the *Coulomb blockade* regime.

Fluctuations of the quantum dot charge will happen due to electron tunneling transitions. Assuming that the quantum dot is weakly coupled to the leads, the rate at which these transitions occur can be calculated by time-dependent perturbation theory. We consider for simplicity the case where each tunneling coupling is constant, $V_{lki\sigma} \to A_l$. At lowest order[38], these are given by the Fermi golden rule:

$$W^{l\alpha}_{m\leftarrow n} = \frac{2\pi}{\hbar}\left|A_l\langle m|\hat{D}_\alpha|n\rangle\right|^2 \upsilon_l(\alpha\Delta_{mn}) f_l(\Delta_{mn}) = \Gamma^{l\alpha}_{mn} f_l(\Delta_{mn}), \tag{5.42}$$

where $\upsilon_l(E)$ is the density of states in terminal l, and $\Delta_{mn} = E_m - E_n$. In most cases, it can be assumed to be constant in the relevant energy scales of the problem (what is known as the *wide-band limit*), so the rates $\Gamma^{l\alpha}_{mn}$ of the barriers are energy independent: $\Gamma^{l\alpha}_{mn} = \Gamma_l$. We have introduced the notation $\hat{D}_+ = \sum_\sigma \hat{d}^\dagger_\sigma$ and $\hat{D}_- = \sum_\sigma \hat{d}_\sigma$. The index α hence indicates whether the transition corresponds to an electron tunneling from terminal l into the quantum dot ($\alpha = +$), or the opposite ($\alpha = -$). The Fermi distribution function contains the thermodynamic properties of the reservoirs.

With these, we can write a set of rate equations for the occupation of each state, ρ_{ii}:[39]

$$\dot{\rho}_{mm} = \sum_{l\alpha}\sum_n \left(W^{l\alpha}_{m\leftarrow n}\rho_{nn} - W^{l\alpha}_{n\leftarrow m}\rho_{mm}\right). \tag{5.43}$$

With the occupations, we obtain the particle and heat currents flowing into each reservoir:

$$I^p_l = -\sum_{mn\alpha} \alpha W^{l\alpha}_{m\leftarrow n}\rho_{nn} \tag{5.44}$$

$$J_l = -\sum_{mn\alpha} \alpha(\alpha\Delta_{mn} - \mu_l) W^{l\alpha}_{m\leftarrow n}\rho_{nn}. \tag{5.45}$$

The electric charge current is obtained by simply multiplying the particle flow by the electric charge:

$$I_l = -eI^p_l. \tag{5.46}$$

Note that different sign conventions can be found in the literature depending on whether currents are positive when injected or absorbed by a terminal, or whether e is positive or negative. Our definition agrees with the experimental fact that negative voltages increase the electrochemical potential.

[38] ...and assuming that the electronic terminals behave as markovian reservoirs where excitations relax in times much shorter than those in which the system fluctuations occur...

[39] Technically, this is given by the diagonal elements of the reduced density matrix of the quantum dot, $\rho = \text{tr}_{\text{res}}\chi$, once all the reservoir degrees of freedom are traced out of the total (quantum dot + reservoirs) density matrix, χ.

Example: Strong Coulomb blockade regime

Let us for clarity furthermore restrict to the case $\varepsilon + U \gg \mu_l, k_B T_l$, such that we can neglect the occupation of the state $|\uparrow\downarrow\rangle$. Then, the only energy changes in the quantum dot upon a tunneling event are given by $\alpha\varepsilon$. We only need to consider the rates $W^{l+}_{\sigma 0} = \Gamma_l f_l(\varepsilon)$ and $W^{l-}_{0\sigma} = \Gamma_l[1 - f_l(\varepsilon)]$, obtained from Eq. (5.42).[40] The different transitions are sketched in Fig. 5.8(a). The stationary solution of the rate equations, $\dot{\rho} = 0$, yields

$$\rho_{00} = \gamma^{-1} \sum_l \Gamma_l[1 - f_l(\varepsilon)], \quad \text{with} \quad \gamma = \sum_l \Gamma_l \left[1 + f_l(\varepsilon)\right], \tag{5.47}$$

and $2\rho_{\sigma\sigma} = 1 - \rho_{00}$.[41] The charge current is then:

$$I_l = 2e\gamma_c \left[f_l(\varepsilon) - f_{l'}(\varepsilon)\right], \tag{5.48}$$

where $\gamma_c = \Gamma_1\Gamma_2\gamma^{-1}$ is the charge relaxation rate. Since (in this particular case) all transitions involve the same change of energy in the quantum dot (up to a sign), the heat and charge currents are proportional to each other:

$$J_l = \frac{\varepsilon - \mu_l}{-e} I_l, \tag{5.49}$$

a property known as tight energy-matter coupling[42].

In the linear regime, where electrochemical or temperature differences are small (compared to the overall temperature), $\mu_i = \mu + \delta\mu_i$ and $T_i = T + \delta T_i$, we can expand the Fermi functions as in Eq. (5.32) and write the response (Onsager) matrix (writing $-e\delta V_{ll'} = \delta\mu_l - \delta\mu_{l'}$ and $\delta T_{ll'} = \delta T_l - \delta T_{l'}$):

$$\begin{pmatrix} I_l \\ J_l \end{pmatrix} = \begin{pmatrix} G & L \\ M & K \end{pmatrix} \begin{pmatrix} \delta V_{ll'} \\ \delta T_{ll'} \end{pmatrix} = 2\partial_E f(\varepsilon)\gamma_c^{eq} \begin{pmatrix} -e^2 & -e(\varepsilon-\mu)/T \\ e(\varepsilon-\mu) & (\varepsilon-\mu)^2/T \end{pmatrix} \begin{pmatrix} \delta V_{ll'} \\ \delta T_{ll'} \end{pmatrix}, \tag{5.50}$$

where G and K are the electrical and thermal conductances[43], and L and M are the thermoelectric coefficients, related to the Seebeck effect for conversion of heat into power, and to Peltier cooling, respectively[44]. The currents strongly depend on the position of the level with respect to the chemical potential, as plotted in Fig. 5.8(b). This can be easily tuned experimentally by a lever-arm gate voltage that controls $\varepsilon = \varepsilon_0 - e\eta V_g$.[45] Here, $\gamma_c^{eq} = \Gamma_1\Gamma_2/(\Gamma_1+\Gamma_2)[1+f(\varepsilon)]$ is evaluated at equilibrium.

The conductance shows a peak whose width scales with temperature[46] when the level crosses the Fermi energy[47]. At that point, the thermal conductance, K, vanishes because electrons at the Fermi energy carry no heat. The thermoelectric coefficients change sign depending on whether transport is

[40] How are the rates for a given process (e.g., $|0\rangle \to |\sigma\rangle$) and its reversed related?

[41] Due to the trace property of the density matrix.

[42] In practice, the level broadens due to the coupling to the leads, but this is captured only by the higher order contributions to the perturbative expansion. The narrow level approximation is accurate provided $\hbar\Gamma_l \ll k_B T_l$.

[43] Sometimes the thermal conductance is defined under the condition that there is no particle flow. Proof that, in that case we get $K' = K - ML/G$.

[44] The linear thermoelectric response of a system is usually characterized by its thermopower:

$$S_{\text{th}} = -\left.\frac{\delta V}{\delta T}\right|_{I=0} = \frac{L}{G},$$

giving the voltage that develops across the system (in open circuit) due to a temperature difference. Note that, despite its name, it does not have dimensions of power.

[45] The system-dependent parameter η describes how the quantum dot potential changes with the gate voltage.

[46] Remember $k_B T \gg \hbar\Gamma$.

[47] For this property they work as single-electron transistors.

dominated by electrons (when $\varepsilon > \mu$) or by holes (when $\varepsilon < \mu$). This way, both charge and heat currents can be reversed by properly tuning the thermodynamic forces or the position of the quantum dot level. Note that the off-diagonal (thermoelectric) coefficients are proportional to each other:

$$L = -\frac{1}{T}M, \tag{5.51}$$

which expresses the Onsager reciprocity relations in this system [5.44, 5.45]. Charge currents respond to temperature differences in the same way as heat currents do to electrochemical potential differences. These relations can be extended to other fluxes and forces [5.46]. However, in general they only hold in the linear response regime.

5.7. Single qubit operations in a quantum dot

In the previous section, the role of the electron spin was almost irrelevant. This is not always the case. Indeed, electrons in quantum dots have been proposed as good candidates for spin qubits [5.47]. In order to operate the system as a useful qubit in quantum information processing, one needs to be able to controllably perform single-qubit rotations. Additionally, being able to swap two-qubit states is necessary for universal logical operations. Experimentally, the goal is to achieve these operations with high enough fidelity, see e.g. Ref. [5.48] for a recent review of experimental advances, or [5.49] for a very recent realization in Si quantum dots.

The qubit (and a bit of quantum information):

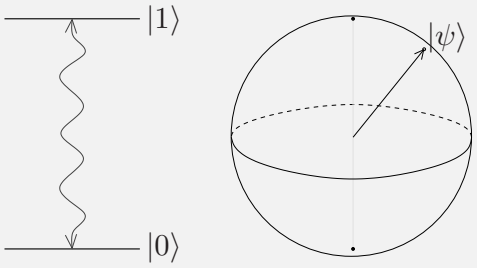

As usual bits, a qubit can be formed by any system with two states, $|0\rangle$ and $|1\rangle$.[a] The essential difference with usual bits is that quantum mechanics allows superpositions of the two states:

$$|\psi\rangle = \alpha|0\rangle + \beta|1\rangle,$$

where $|\alpha|^2 + |\beta|^2 = 1$. Ignoring the irrelevant global phase, the state can be described by only two parameters (e.g., polar and azimuthal angles). For this reason, the state can be represented as a point in the surface of a sphere (the Bloch sphere) whose poles are $|0\rangle$ and $|1\rangle$. Unitary operations acting on $|\psi\rangle$ that define the logical gates can then be seen as rotations on the Bloch sphere.

A different way to write the state of the system is by its density operator (or matrix)

$$\hat{\rho} = |\psi\rangle\langle\psi|.$$

In this case, $\hat{\rho}$ corresponds to a pure state. It then satisfies $\mathrm{tr}(\hat{\rho}^2) = \mathrm{tr}(\hat{\rho}) = 1$.[b] Note this is not always the case. A density matrix might represent a state of which we have only probabilistic information: these are called mixed states. They have purity $\mathrm{tr}(\hat{\rho}^2) < \mathrm{tr}(\hat{\rho}) = 1$ and are therefore buried in the sphere.[c]

[a] It can be a purely two-level system (e.g., the spin of an electron), or be defined with the ground and first excited states of a system with multiple states.

[b] Can you proof this?

[c] Which are the states on the polar axis?

Let us see how the single qubit rotations can be done using an electron spin in a quantum dot. For this, we need a way to couple coherently the two spin states, in this case via time dependent magnetic fields. Other physical realizations are possible using for instance superconducting circuits or trapped ions (among others). Even in quantum dot systems, singlet and triple states can be used. For each configuration, the way the two qubit states are coupled will require different mechanisms.

5.7.1. Coherent dynamics in a closed system

Consider a single-level quantum dot that is occupied by one electron (doubly occupancy is avoided by strong Coulomb interactions). The spin of the electron defines a two level system that will serve as the qubit: $|+\rangle = |\uparrow\rangle$ and $|-\rangle = |\downarrow\rangle$. The energy of the level is not important, so we will set it to $\varepsilon = 0$, for simplicity. The splitting of the two levels is tuned with a Zeeman field, $\mathbf{B}_z = (0, 0, B_0)$. The resulting hamiltonian $\propto B_0 \hat{S}_z$ is diagonal. In order to be able to perform qubit operations, a time dependent magnetic field perpendicular to it, $\mathbf{B}_\perp(t) = (B_x(t), B_y(t), 0)$, is applied that couple the two spin states, so the hamiltonian of the system becomes:

$$\hat{H} = g\mu_B \mathbf{B}(t)\hat{\mathbf{S}}, \tag{5.52}$$

with $\mathbf{B}(t) = \mathbf{B}_z + \mathbf{B}_\perp(t)$, and the spin operators are

$$\hat{\mathbf{S}} = \frac{\hbar}{2} \sum_{\sigma\sigma'} \langle \sigma' | \hat{\tau} | \sigma \rangle \, \hat{c}^\dagger_{\sigma'} \hat{c}_\sigma, \tag{5.53}$$

written in terms of the Pauli matrices τ_i, see Eq. (A.1). The simplest case[48] is to consider a circularly polarized field[49], with $B_x(t) = B_\perp \cos(\omega t)$ and $B_y(t) = B_\perp \sin(\omega t)$. We can then express $\hat{H}(t)$ in matrix form:

$$\hat{H}(t) = \begin{pmatrix} \Delta/2 & \hbar\Omega e^{-i\omega t} \\ \hbar\Omega e^{i\omega t} & -\Delta/2 \end{pmatrix}, \quad \text{with} \quad |\uparrow\rangle = \begin{pmatrix} 1 \\ 0 \end{pmatrix}, \quad \text{and} \quad |\downarrow\rangle = \begin{pmatrix} 0 \\ 1 \end{pmatrix}, \tag{5.54}$$

and with the Zeeman splitting $\Delta = \hbar g \mu_B B_0$ and the Rabi frequency $\Omega = g\mu_B B_\perp$.[50] It is helpful to get rid of the explicit time dependence of the hamiltonian by performing a unitary transformation

$$\hat{\mathcal{U}}(t) = \begin{pmatrix} e^{-i\hbar\omega t/2} & 0 \\ 0 & e^{i\hbar\omega t/2} \end{pmatrix}, \tag{5.55}$$

that expresses the hamiltonian in the rotating frame:

$$\hat{H}' = \hat{\mathcal{U}}^\dagger(t) \left[\hat{H}(t) - i\hbar\partial_t \right] \hat{\mathcal{U}}(t) = \begin{pmatrix} (\Delta - \hbar\omega)/2 & \hbar\Omega \\ \hbar\Omega & -(\Delta - \hbar\omega)/2 \end{pmatrix}. \tag{5.56}$$

Note that the time dependence has disappeared[51]. In this frame, the interpretation is clear: the time-dependent field provides energy quanta $\hbar\omega$ which enable the spin to flip despite the energy difference Δ. In the case $\omega = \Delta/\hbar \equiv \omega_0$, the transition is resonant (the process is called electron-spin resonance).

[48] Theoretically, at least. In an experiment, circularly polarized fields are much harder to realize than linear ones.

[49] Circularly polarized fields are difficult to implement experimentally, though. Typically, linearly polarized ones are employed, which can be treated analytically only under appropriate (rotating wave) approximations, see footnote 51 below.

[50] Why we call *frequency* to the amplitude of the ac field should become clear later.

[51] For linearly polarized fields, counter-rotating terms survive. They can be neglected close to resonance if the field is weak, $\Omega < \omega_0$. This is the rotating wave approximation.

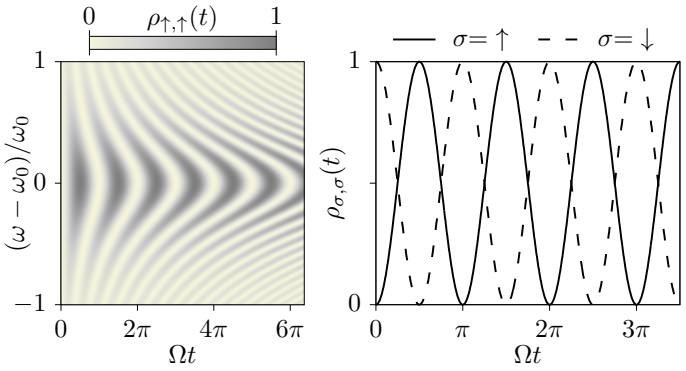

Figure 5.9.:
Coherent spin rotations by applying a time-dependent magnetic field with amplitude $\hbar\Omega$ and frequency ω perpendicular to a constant field that induces a Zeeman splitting $\hbar\omega_0$. The spin of the electron oscillates in time. For ω=ω_0, the oscillations are periodic (right panel). Here, $\omega_0 = 5\Omega$.

The evolution of the system is given by the Heisenberg equation of motion for the density matrix:

$$\dot{\hat{\rho}}' = -\frac{i}{\hbar}[\hat{H}', \hat{\rho}']. \tag{5.57}$$

Remember we are now in the rotating frame. The density matrix in the lab frame will need to be transformed back as $\hat{\rho} = \hat{\mathcal{U}}(t)\hat{\rho}'\hat{\mathcal{U}}^{\dagger}(t)$. The matrix elements read:

$$\begin{aligned} \dot{\rho}'_{\uparrow,\uparrow} &= i\Omega\left(\rho'_{\uparrow,\downarrow} - \rho'_{\downarrow,\uparrow}\right) \\ \dot{\rho}'_{\downarrow,\uparrow} &= -i\left[\Omega\left(\rho'_{\uparrow,\uparrow} - \rho'_{\downarrow,\downarrow}\right) - (\omega_0 - \omega)\rho'_{\downarrow,\uparrow}\right]. \end{aligned} \tag{5.58}$$

with $\dot{\rho}'_{\downarrow,\downarrow} = -\dot{\rho}'_{\uparrow,\uparrow}$ and $\dot{\rho}'_{\uparrow,\downarrow} = \dot{\rho}'^{*}_{\downarrow,\uparrow}$ due to the properties of the density matrix[52]. The oscillating terms hence couple the population of the two states via the off-diagonal elements (known as coherences), resulting in a system of coupled differential equations.

Let us now assume the system is initially at the lowest energy level: $\rho'_{\downarrow,\downarrow}(0) = 1$. We can then take the Laplace transform $\mathcal{L}\{\rho'\}$ and use the property $\mathcal{L}\{\dot{\rho}'\} = z\rho' - \rho'(0)$. The system of equations is then algebraic and can be solved easily, resulting in

$$\rho'_{\downarrow,\downarrow}(z) = \frac{z^2 + 2\Omega^2 + (\omega_0 - \omega)^2}{z\left[z^2 + 4\Omega^2 + (\omega_0 - \omega)^2\right]} \qquad \text{and} \qquad \rho'_{\uparrow,\uparrow}(z) = \frac{2\Omega^2}{z\left[z^2 + 4\Omega^2 + (\omega_0 - \omega)^2\right]}, \tag{5.59}$$

which we will need to inverse-Laplace-transform, rendering:

$$\rho_{\uparrow,\uparrow}(t) = \frac{4\Omega^2}{4\Omega^2 + (\omega_0 - \omega)^2} \sin^2\left(\frac{t}{2}\sqrt{4\Omega^2 + (\omega_0 - \omega)^2}\right), \tag{5.60}$$

and $\rho_{\downarrow,\downarrow}(t) = 1 - \rho_{\uparrow,\uparrow}(t)$, as plotted in the left panel of Fig. 5.9. Note that the occupations are the same in the lab and in the rotating frames.

One typically wants to operate at resonance, $\omega = \omega_0$, in which case we get:

$$\rho_{\downarrow,\downarrow}(t) = \cos^2(\Omega t) \quad \text{and} \quad \rho_{\uparrow,\uparrow}(t) = \sin^2(\Omega t), \tag{5.61}$$

i.e., the state of the qubit oscillates periodically with a frequency $f = 2\Omega$ (see right panel of Fig. 5.9). The frequency of the oscillations is given by the amplitude of the applied field!

Single spin rotations where demonstrated in quantum dot systems by adding a micromagnet that generates the Zeeman field, and driving a rf current through a wire situated nearby on top of the metal gates (and separated by a 100 nm thick dielectric) that generates the perpendicular and time-dpenendent magnetic field on the electron [5.50].

[52] Its trace is 1 and it is hermitian.

5.7.2. The qubit as an open quantum system. Decoherence

In real life, quantum systems are not perfectly isolated, but are physical systems immersed in a larger environment or bath. The hamiltonian is then decomposed as $\hat{H} = \hat{H}_S + \hat{H}_B + \hat{H}_{S-B}$, where $\hat{H}_S$ describes the system of interest, $\hat{H}_B$, the bath, and $\hat{H}_{S-B}$, their coupling. One could in principle write a Heisenberg equation of the form of Eq. (5.57) for the density matrix of the whole system+environment problem, $\hat{\rho}_{S+B}$, but this is not something that one can really due in practice as soon as the environment has many degrees of freedom[53]. In the best case, they system-environment coupling is weak and it can be considered as a perturbation on the system dynamics. However, the effect of the environment cannot be totally disregarded. For instance, it affects the system conservation laws by means of e.g., the exchange of energy or particles. A partial description of the open quantum system is possible if one ignores what happens in the environment [5.51]. This is done by *tracing out* (i.e., summing) all the environmental degrees of freedom in the total density operator. This results in a reduced density operator of the system $\hat{\rho}_s = \mathrm{Tr}_B \hat{\rho}_{S+B}$ that only contains the information of the quantum system one is interested in. The price to pay is that the system evolution stops being unitary i.e., not any more described by a Heisenberg equation (this is also said to correspond to a non-hermitian system).

In some cases, one can try to get advantage from the action of the environment on the system. For instance, the system can be a quantum engine that is powered by exploiting some form of energy exchanged with the environment as a resource. This is the field of quantum thermodynamics [5.52, 5.53]. On the contrary in some other cases, like for systems of interest in quantum information processing, these effects need to be minimized because they harm the system coherent properties by introducing uncontrollable dynamics: the environment causes decoherence.

Master equation

In the case of a system weakly coupled to an environment (represented by e.g., a thermal bath at temperature T), the system coherent dynamics is affected by transitions induced by the environment. Importantly, the absence of information of what happens in the environment upon the occurrence of these transitions imposes a statistical treatment that perturbs the coherent evolution. Performing a time-dependent perturbation expansion on the system-bath coupling, these transitions are described by the rates at which they happen to occur: W_{km} for the transition between states $|m\rangle \rightarrow |k\rangle$ in the system. At lowest order in the expansion, these are given by the Fermi golden rule. The equation of motion for the *reduced* density matrix of the system takes the form [5.54]

$$\dot{\hat{\rho}}_s = \mathcal{L}(\hat{\rho}_s) = -\frac{i}{\hbar}[\hat{H}_S, \hat{\rho}_s] + \mathcal{D}(\hat{\rho}_s), \tag{5.62}$$

where $\mathcal{L}(\bullet)$ is the *Liouvillian superoperator* acting on the density operator[54]. The commutator in (5.62) describes the coherent dynamics *in* the quantum system, recovering the evolution of the closed system when the coupling vanishes. Dissipation due to coupling to the environment is contained in $\mathcal{D}(\bullet)$, with elements: [55].

$$\langle m'|\mathcal{D}[\hat{\rho}(t)]|m\rangle = \sum_{k\neq m} W_{mk} \langle k|\hat{\rho}(t)|k\rangle \delta_{m'm} - \frac{1}{2}\left(\sum_{k\neq m'} W_{km'} + \sum_{k\neq m} W_{km}\right)\langle m'|\hat{\rho}(t)|m\rangle, \tag{5.63}$$

[53] Also that is something one does not want to do, if one is only interested in the system properties.

[54] In the same way as operators act on states. A more intuitive way of seeing this is thinking on operators as matrices and states as vectors. One can always write the elements of a matrix as a vector, and then the superoperator is a matrix.

[55] Note that you have already seen an example in section 5.6.1: the rate equations (5.43) (due to electron tunneling) are the simplest case where only diagonal elements of the density matrix contribute (coherence play no role at the lowest order in the perturbation expansion).

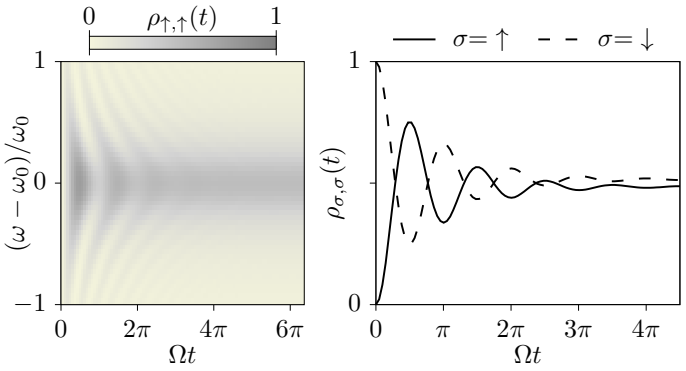

Figure 5.10.:
Effect of decoherence on the electron spin rotation. The time-dependent oscillations caused by the driving field are damped by relaxation and excitation processes due to a thermal bath. All parameters are as in Fig. 5.9, with $k_BT = \hbar\Omega$ and relaxation rate $\gamma = \Omega/2$.

in terms of the transition rates W_{mn}. If the environment is in local equilibrium (described by a chemical potential μ and a temperature T), they satisfy a detailed balance property:

$$W_{nm} = W_{mn}e^{(\mu-\hbar\omega_{nm})/k_BT} \tag{5.64}$$

imposed by the thermodynamics of the bath, where $\hbar\omega_{nm} = \langle n|\hat{H}_S|n\rangle - \langle m|\hat{H}_S|m\rangle$.

Decay of Rabi oscillations

Let us apply this to the two-level system treated in Sec. 5.7.1. If the qubit is made by the spin of an electron in a quantum dot, we find different possible sources of decoherence: e.g., charge fluctuations from the 2DEG, spin fluctuations due to exchange interactions with the nuclear spins of the lattice, or vibrations of the material [5.41]. These are large environments that can be represented by reservoirs of different nature (be them systems of fermions, bosons or spins). This will affect the details of the transition rates. However, they are in general dominated by thermal fluctuations. We can them assume a simple description where the spin is immersed in a thermal bath and relaxes with a rate $W_{\downarrow\uparrow} = \gamma$. Thermally induced excitations occur with a rate $W_{\uparrow\downarrow} = \gamma e^{-\Delta/k_BT}$ (note the verification of the detailed balance condition)[56]. Thus we get the evolution of the density matrix elements[57]:

$$\begin{aligned}\dot{\rho}'_{\uparrow,\uparrow} &= i\Omega\left(\rho'_{\uparrow,\downarrow} - \rho'_{\downarrow,\uparrow}\right) + \gamma e^{-\Delta/k_BT}\rho'_{\downarrow,\downarrow} - \gamma\rho'_{\uparrow,\uparrow}\\ \dot{\rho}'_{\downarrow,\uparrow} &= -i\Omega\left(\rho'_{\uparrow,\uparrow} - \rho'_{\downarrow,\downarrow}\right) + i\left(\omega_0 - \omega + i\frac{\gamma_{tot}}{2}\right)\rho'_{\downarrow,\uparrow},\end{aligned} \tag{5.65}$$

with $\gamma_{tot} = \gamma\left(1 + e^{-\Delta/k_BT}\right)$. We can follow the same procedure as we did to solve the master equation in Sec. 5.7.1. The first we note is that the term $i\gamma_{tot}/2$ in the off-diagonal elements leads to an exponential damping of the oscillations, as shown in Fig. 5.10.

In order to better understand what happens, let us first consider the undriven case, with $\Omega = 0$. Then, the diagonal and off-diagonal elements are decoupled. The populations follow a rate equation of the form of Eq. (5.43). Solving the system of equations[58], we find that the coherences acquire a decaying mode, so:

$$\rho'_{\downarrow,\uparrow}(t) = \rho_{\downarrow,\uparrow}(0)e^{[i(\omega_0-\omega)-\gamma_{tot}/2]t}. \tag{5.66}$$

[56] What happens in the limit where the bath is at zero temperature?
[57] Why do we only need two?
[58] Remember your ordinary differential equations courses.

As a consequence, any initial coherence (due to the system being in a coherent superposition[59]) is lost at long times[60]. At the same time, the system populations evolve towards a Boltzmann (or Gibbs) distribution, with:

$$\rho_{\downarrow,\downarrow}(t\to\infty) = \left(1+\mathrm{e}^{-\Delta/k_\mathrm{B}T}\right)^{-1} \qquad \text{and} \qquad \rho_{\uparrow,\uparrow}(t\to\infty) = \mathrm{e}^{-\Delta/k_\mathrm{B}T}\left(1+\mathrm{e}^{-\Delta/k_\mathrm{B}T}\right)^{-1}, \tag{5.67}$$

i.e., the system thermalizes due to the coupling to the bath[61]. The system is then in a *mixed* state, where all information about it is merely probabilistic[62].

Back to the case with finite driving, Ω, and close to the resonance condition $\omega \approx \omega_0$, the populations are no longer Boltzmann-distributed: the periodic modulation of the magnetic field is a source of non-equilibrium to the system[63]. Also, the coherences are not totally washed out in the long time limit, as they are fed by the driven oscillations. Indeed, it can be shown that $\rho'_{\downarrow,\uparrow}(t\to\infty) \propto \Omega$.[64] Nevertheless, the system reaches a mixed steady state where the density matrix of the system cannot be described by a single wave function, but one can only get a probabilistic description of the population of the different states. This constitutes a serious problem for quantum information processing and limits the time at which coherent spin rotations are effective.

Bibliography

[5.1] H. Bruus and K. Flensberg. *Many-Body Quantum Theory in Condensed Matter Physics*. Oxford University Press, Sep 2004.

[5.2] T. Ihn. *Semiconductor Nanostructures: Quantum states and electronic transport*. Oxford University Press, Oxford, 2009.

[5.3] K. v. Klitzing, G. Dorda, and M. Pepper. New Method for High-Accuracy Determination of the Fine-Structure Constant Based on Quantized Hall Resistance. *Phys. Rev. Lett.*, 45(6):494–497, Aug 1980.

[5.4] D. B. Newell. A more fundamental International System of Units. *Phys. Today*, 67(7):35, Jun 2014.

[5.5] P. W. Anderson. Absence of Diffusion in Certain Random Lattices. *Phys. Rev.*, 109(5):1492–1505, Mar 1958.

[5.6] B. I. Halperin. Quantized Hall conductance, current-carrying edge states, and the existence of extended states in a two-dimensional disordered potential. *Phys. Rev. B*, 25(4):2185–2190, Feb 1982.

[5.7] B. I. Halperin. The quantized Hall effect. *Sci. Am.*, 254:52–60, Apr 1986.

[5.8] K. von Klitzing. The quantized Hall effect. *Rev. Mod. Phys.*, 58(3):519–531, Jul 1986.

[59] What famous superpositions of two states do you know?

[60] If this solution corresponds to the undriven case ($\Omega = 0$), how come it depends on the driving frequency, ω? (Hint: look the frame you are in!).

[61] This is closely related to the detailed balance condition.

[62] Mixed states are typically put in contrast with *pure* states, for which the system state is precisely determined by a density matrix $\hat{\rho} = |\psi\rangle\langle\psi|$, for a given wavefunction ψ.

[63] What happens if the driving is far from resonance?

[64] Left as an exercise.

[5.9] M. Büttiker. Absence of backscattering in the quantum Hall effect in multiprobe conductors. *Phys. Rev. B*, 38(14):9375–9389, Nov 1988.

[5.10] E. Bocquillon, V. Freulon, F. D. Parmentier, J.-M. Berroir, B. Plaçais, C. Wahl, J. Rech, T. Jonckheere, T. Martin, C. Grenier, D. Ferraro, P. Degiovanni, and G. Fève. Electron quantum optics in ballistic chiral conductors. *Ann. Phys.*, 526(1-2):1–30, Jan 2014.

[5.11] M. Büttiker. Chapter 4: The Quantum Hall Effect in Open Conductors. In *Semiconductors and Semimetals*, volume 35, pages 191–277. Elsevier, Walthm, MA, USA, Jan 1992.

[5.12] C.-X. Liu, S.-C. Zhang, and X.-L. Qi. The Quantum Anomalous Hall Effect: Theory and Experiment. *Annu. Rev. Condens. Matter Phys.*, 7(1):301–321, Mar 2016.

[5.13] M. König, S. Wiedmann, C. Brüne, A. Roth, H. Buhmann, L. W. Molenkamp, X.-L. Qi, and S.-C. Zhang. Quantum Spin Hall Insulator State in HgTe Quantum Wells. *Science*, Nov 2007.

[5.14] J. Maciejko, T. L. Hughes, and S.-C. Zhang. The Quantum Spin Hall Effect. *Annu. Rev. Condens. Matter Phys.*, 2(1):31–53, Feb 2011.

[5.15] G. M. Ferguson, R. Xiao, A. R. Richardella, D. Low, N. Samarth, and K. C. Nowack. Direct visualization of electronic transport in a quantum anomalous Hall insulator. *arXiv:2112.13122*, Dec 2021.

[5.16] I. T. Rosen, M. P. Andersen, L. K. Rodenbach, L. Tai, P. Zhang, K. L. Wang, M. A. Kastner, and D. Goldhaber-Gordon. Measured potential profile in a quantum anomalous Hall system suggests bulk-dominated current flow. *arXiv:2112.13123*, Dec 2021.

[5.17] N. Agraït, A. Levy Yeyati, and J. M. van Ruitenbeek. Quantum properties of atomic-sized conductors. *Phys. Rep.*, 377(2):81–279, Apr 2003.

[5.18] G. Binnig and H. Rohrer. Scanning tunneling microscopy—from birth to adolescence. *Rev. Mod. Phys.*, 59(3):615–625, Jul 1987.

[5.19] J. C. Cuevas and E. Scheer. *Molecular Electronics | World Scientific Series in Nanoscience and Nanotechnology*. World Scientific Publishing Company, Singapore, Jun 2017.

[5.20] M. Sundaram, S. A. Chalmers, P. F. Hopkins, and A. C. Gossard. New Quantum Structures. *Science*, Nov 1991.

[5.21] M. Büttiker. Quantized transmission of a saddle-point constriction. *Phys. Rev. B*, 41(11):7906–7909(R), Apr 1990.

[5.22] H. van Houten, C. W. J. Beenakker, and B. J. van Wees. Chapter 2: Quantum Point Contacts. In *Semiconductors and Semimetals*, volume 35, pages 9–112. Elsevier, Walthm, MA, USA, Jan 1992.

[5.23] R. Landauer. Electrical transport in open and closed systems. *Z. Phys. B: Condens. Matter*, 68(2):217–228, Jun 1987.

[5.24] G. B. Lesovik and I. A. Sadovskyy. Scattering matrix approach to the description of quantum electron transport. *Phys.-Usp.*, 54(10):1007–1059, Oct 2011.

[5.25] G. Benenti, G. Casati, K. Saito, and R. S. Whitney. Fundamental aspects of steady-state conversion of heat to work at the nanoscale. *Phys. Rep.*, 694:1–124, Jun 2017.

[5.26] Yu. V. Nazarov and Ya. M. Blanter. *Quantum Transport: Introduction to Nanoscience*. Cambridge University Press, May 2009.

[5.27] S. Datta. *Electronic Transport in Mesoscopic Systems*. Cambridge University Press, May 1997.

[5.28] M. V. Moskalets. *Scattering Matrix Approach to Non-Stationary Quantum Transport*. World Scientific Publishing Company, Sep 2011.

[5.29] B. J. van Wees, H. van Houten, C. W. J. Beenakker, J. G. Williamson, L. P. Kouwenhoven, D. van der Marel, and C. T. Foxon. Quantized conductance of point contacts in a two-dimensional electron gas. *Phys. Rev. Lett.*, 60(9):848–850, Feb 1988.

[5.30] D. A. Wharam, T. J. Thornton, R. Newbury, M. Pepper, H. Ahmed, J. E. F. Frost, D. G. Hasko, D. C. Peacock, D. A. Ritchie, and G. A. C. Jones. One-dimensional transport and the quantisation of the ballistic resistance. *J. Phys. C: Solid State Phys.*, 21(8):L209, Mar 1988.

[5.31] U. Sivan and Y. Imry. Multichannel Landauer formula for thermoelectric transport with application to thermopower near the mobility edge. *Phys. Rev. B*, 33(1):551–558, Jan 1986.

[5.32] J. B. Pendry. Quantum limits to the flow of information and entropy. *J. Phys. A: Math. Gen.*, 16(10):2161, 1983.

[5.33] S. Jezouin, F. D. Parmentier, A. Anthore, U. Gennser, A. Cavanna, Y. Jin, and F. Pierre. Quantum Limit of Heat Flow Across a Single Electronic Channel. *Science*, 342(6158):601–604, Nov 2013.

[5.34] L. Cui, W. Jeong, S. Hur, M. Matt, J. C. Klöckner, F. Pauly, P. Nielaba, J. C. Cuevas, E. Meyhofer, and P. Reddy. Quantized thermal transport in single-atom junctions. *Science*, 355(6330):1192–1195, 2017.

[5.35] H. W. Kroto, J. R. Heath, S. C. O'Brien, R. F. Curl, and R. E. Smalley. C60: Buckminsterfullerene. *Nature*, 318:162–163, Nov 1985.

[5.36] M. F. Crommie, C. P. Lutz, and D. M. Eigler. Confinement of Electrons to Quantum Corrals on a Metal Surface. *Science*, Oct 1993.

[5.37] J. Clarke and F. K. Wilhelm. Superconducting quantum bits - Nature. *Nature*, 453:1031–1042, Jun 2008.

[5.38] A. Cottet, M. C. Dartiailh, M. M. Desjardins, T. Cubaynes, L. C. Contamin, M. Delbecq, J. J. Viennot, L. E. Bruhat, B. Douçot, and T. Kontos. Cavity QED with hybrid nanocircuits: from atomic-like physics to condensed matter phenomena. *J. Phys.: Condens. Matter*, 29(43):433002, Sep 2017.

[5.39] A. Blais, A. L. Grimsmo, S. M. Girvin, and A. Wallraff. Circuit quantum electrodynamics. *Rev. Mod. Phys.*, 93:025005, May 2021.

[5.40] Y. Wen, N. Ares, F. J. Schupp, T. Pei, G. A. D. Briggs, and E. A. Laird. A coherent nanomechanical oscillator driven by single-electron tunnelling - Nature Physics. *Nat. Phys.*, 16:75–82, Jan 2020.

[5.41] R. Hanson, L. P. Kouwenhoven, J. R. Petta, S. Tarucha, and L. M. K. Vandersypen. Spins in few-electron quantum dots. *Rev. Mod. Phys.*, 79(4):1217–1265, Oct 2007.

[5.42] W. G. van der Wiel, S. De Franceschi, J. M. Elzerman, T. Fujisawa, S. Tarucha, and L. P. Kouwenhoven. Electron transport through double quantum dots. *Rev. Mod. Phys.*, 75(1):1–22, Dec 2002.

[5.43] P. Barthelemy and L. M. K. Vandersypen. Quantum Dot Systems: a versatile platform for quantum simulations. *Ann. Phys.*, 525(10-11):808–826, Nov 2013.

[5.44] L. Onsager. Reciprocal Relations in Irreversible Processes. I. *Phys. Rev.*, 37(4):405–426, Feb 1931.

[5.45] H. B. G. Casimir. On Onsager's Principle of Microscopic Reversibility. *Rev. Mod. Phys.*, 17(2-3):343–350, Apr 1945.

[5.46] P. Jacquod, R. S. Whitney, J. Meair, and M. Büttiker. Onsager relations in coupled electric, thermoelectric, and spin transport: The tenfold way. *Phys. Rev. B*, 86(15):155118, Oct 2012.

[5.47] D. Loss and D. P. DiVincenzo. Quantum computation with quantum dots. *Phys. Rev. A*, 57(1):120–126, Jan 1998.

[5.48] G. Burkard, T. D. Ladd, J. M. Nichol, A. Pan, and J. R. Petta. Semiconductor Spin Qubits. *arXiv:2112.08863*, Dec 2021.

[5.49] A. R. Mills, C. R. Guinn, M. J. Gullans, A. J. Sigillito, M. M. Feldman, E. Nielsen, and J. R. Petta. Two-qubit silicon quantum processor with operation fidelity exceeding 99%. *arXiv:2111.11937*, Nov 2021.

[5.50] F. H. L. Koppens, C. Buizert, K. J. Tielrooij, I. T. Vink, K. C. Nowack, T. Meunier, L. P. Kouwenhoven, and L. M. K. Vandersypen. Driven coherent oscillations of a single electron spin in a quantum dot. *Nature*, 442:766–771, Aug 2006.

[5.51] H.-P. Breuer and F. Petruccione. *The Theory of Open Quantum Systems*. Oxford University Press, Oxford, England, UK.

[5.52] F. Binder, L. A. Correa, Ch. Gogolin, J. Anders, and G. Adesso. *Thermodynamics in the Quantum Regime*. Springer, Cham, Switzerland, 2018.

[5.53] P. P. Potts. Introduction to Quantum Thermodynamics (Lecture Notes). *arXiv:1906.07439*, Jun 2019.

[5.54] K. Blum. *Density Matrix Theory and Applications*. Springer-Verlag, Berlin, Germany, 2012.

Further reading

- ☞ T. Ihn, *Semiconductor Nanostructures: Quantum states and electronic transport* (Oxford Univ. Press, Oxford, 2009)
- ☞ H. Bruus and K. Flensberg, *Many-Body Quantum Theory in Condensed Matter Physics* (Oxford Univ. Press, Oxford, 2004)

☞ Yu. V. Nazarov, Ya. M. Blanter, *Quantum Transport: Introduction to Nanoscience* (Cambridge Univ. Press, Cambridge, 2009)
☞ S. M. Girvin and K. Yang, *Modern Condensed Matter Physics* (Cambridge Univ. Press, Cambridge, 2019)
☞ D. Tong, *The Quantum Hall Effect,* lecture notes

A. Other things

Useful constants and units

$\hbar = 6.582 \times 10^{-13}$ meV s	$k_B = 8.617 \times 10^{-2}$ meV K^{-1}
$e = 1.602 \times 10^{-19}$ C	$m_e = 0.510 \times 10^{9}$ meV$/c^2$

1 K $= 8.6175 \times 10^{-2}$ meV	$\frac{e}{\hbar} = 0.243\ \mu$A meV^{-1}	$a_0 = \hbar^2/e^2 m_e \approx 0.5292$ Å

Pauli matrices

$$\tau_x = \begin{pmatrix} 0 & 1 \\ 1 & 0 \end{pmatrix}, \qquad \tau_y = \begin{pmatrix} 0 & -i \\ i & 0 \end{pmatrix}, \qquad \tau_z = \begin{pmatrix} 1 & 0 \\ 0 & -1 \end{pmatrix} \tag{A.1}$$

Limits to the Dirac delta

The Dirac delta can be obtained as the limit of some functions,

$$\delta(x) = \lim_{\eta \to 0} f_i(x, \eta), \tag{A.2}$$

for instance:

$$f_1 = \frac{1}{\pi} \frac{\eta}{x^2 + \eta^2}, \qquad f_2 = \eta \left(\frac{1}{x} \right)^{1-\eta}, \qquad f_3 = \frac{1}{s\sqrt{\pi\eta}} \mathrm{e}^{-\frac{x^2}{4\eta}}. \tag{A.3}$$